# Identification and Functional Studies of *Arabidopsis thaliana* Ubc13-interacting E3 Ubiquitin Ligases

A Thesis Submitted to the College of

Graduate Studies and Research

In Partial Fulfillment of the Requirements

For the Degree of Master of Science

In the Department of Biochemistry

University of Saskatchewan

Saskatoon

By

**Shifeng Qian**

© Copyright Shifeng Qian, March 2012. All rights reserved.

## PERMISSION TO USE

In presenting this thesis in partial fulfillment for Master of Science degree from the University of Saskatchewan, I agree that the Libraries of this University may make it freely available for inspection. I further agree that permission for copying of this thesis in any manner, in whole or in part, for scholarly purposes may be granted by the professor or professors who supervised my thesis work, or in their absence, by the Head of the Department of Biochemistry or the Dean of the College in which my thesis work was done. It is understood that any copying, publication, or use of this thesis or parts thereof for financial gain shall not be allowed without my written permission. It is also understood that due recognition shall be given to me and to the University of Saskatchewan in any way scholarly use which may be made of any material in my thesis.

Requests for permission to copy or to make other use of material in this thesis in whole or in part should be addressed to:

Head of the Department of Biochemistry
University of Saskatchewan
Saskatoon, Saskatchewan
S7N 5E5 Canada

**ABSTRACT**

In eukaryotic organisms, polyubiquitination is the modification of a protein with polymerized ubiquitin (Ub) chain. This process is well known for its function in targeting proteins for degradation by the 26S proteasome. However, a polyUb chain assembled through the lysine 63 residue of the Ub moiety (Lys63-linked polyubiquitination) has been shown to play a signaling role rather than targeting proteins for degradation. In plants, the functions of Lys63-linked polyubiquitination are currently not well understood.

Ub-protein ligase (E3) catalyzes the last step in the ubiquitination reactions, and to a large extent it also determines the substrate specificity of protein ubiquitination. In order to study the roles of Lys63-linked polyubiquitination in plants, two E3s of *Arabidopsis thaliana*, proteins encoded by *AtCHIP* and *At1g74370* (tentatively named *E3-A1*), were chosen for functional studies, since they interacted with AtUbc13A protein. Sequence analysis showed that AtCHIP is the only member in the family. A T-DNA insertion mutant line (*Atchip-1*) was obtained to study the *AtCHIP* gene knock-out effect. The mutant line was grown in normal conditions and further tested in a variety of conditions: hormonal treatments, osmotic stress, seed deterioration, high temperature stress, high-intensity light stress, oxidative stress and DNA damaging stress. However, no clear difference was observed between the mutant and wild type plants based on the several parameters measured. Sequence analysis of E3-A1 indicated two closely related proteins, tentatively named E3-A2 and E3-A3. As E3-A1 and E3-A2 appeared to share more sequence similarity, RNA interference (RNAi) transformants, with the level of transcripts for either of the two *E3-A* genes reduced by over 90% were generated. Selected RNAi mutant lines for *E3-A1* and *E3-A2* were crossed with each other, and double RNAi mutants were obtained. However, no distinct phenotype was detected under normal, high-sucrose or hormonal conditions for either single or double RNAi lines.

Although various assays did not reveal a significant phenotype in the mutants in this study,

the materials generated and the assays used will benefit a wider range of phenotypic survey in the future.

**ACKNOWLEDGEMENTS**

First of all, I would like to express my sincerest gratitude to my supervisor Dr. Hong Wang, for offering me this invaluable opportunity to study and research on this project, for his patience and persistence throughout my entire M.Sc. program, especially his guidance in every single experiment, on data handling, and more importantly, his instruction on scientific thinking. He encouraged and challenged me to become a better researcher for which I am forever grateful. I am also thankful for the guidance received from my co-supervisor Dr. Wei Xiao, and for reviewing my project and providing me with important comments and advice.

I would like to thank my advisory committee, past and present, Dr. Stanley Moore, Dr. Michele Loewen, Dr. Ramji Khandelwal, Dr. William Roesler for their advice and evaluation on my thesis project. And I also would like to thank Dr. Peta Bonham-Smith for being my external examiner.

I would like to especially thank Dr. Xianzong Shi from Dr. Hong Wang's laboratory for helping with the preparation of bacteria constructs and plant transformation. With gratitude I also thank Dr. Rui Wen from Dr. Wei Xiao's laboratory for the preliminary work on AtUbc13A-AtCHIP protein interaction assays. I also appreciate the countless times of help and encouragement from Mr. Yan Cheng, a former member in Dr. Wang's laboratory, and Mr. Sheng Wang from Dr. Xiao's laboratory.

I also gratefully acknowledge the monetary support from the College of Graduate Studies and Research, the College of Medicine, and the Department of Biochemistry at the University of Saskatchewan.

In conclusion, I would like to give a special thanks to my beloved parents and friends: to my parents, Guiming and Liya Qian, for their immeasurable love and care during my studies overseas, and to my friends Cameron and Josephine Janzen, Gerald and Shirley Falk, Ning Cao and many other friends from my Christain fellowship who always built me up, especially as I encountered obstacles in my studies and in other parts of my life.

**TABLE OF CONTENTS**

**PERMISSION TO USE** ..... **i**

**ABSTRACT** ..... **ii**

**ACKNOWLEDGEMENTS** ..... **iv**

**TABLE OF CONTENTS** ..... **v**

**LIST OF TABLES** ..... **ix**

**LIST OF FIGURES** ..... **x**

**LIST OF ABBREVIATIONS** ..... **xii**

**1 INTRODUCTION** ..... **1**

1.1 Ubiquitin System ..... 1

1.1.1 The Ubiquitin Protein ..... 1

1.1.2 Ubiquitination Reaction ..... 2

1.1.3 Different Types of Ubiquitination ..... 4

1.1.4 The Ubiquitin-Proteasome System (UPS) ..... 7

1.2 Major Classes of E3 Ligases ..... 9

1.2.1 RING-Type E3s ..... 10

1.2.2 U-Box-Type E3s ..... 13

1.2.3 HECT-Type E3s ..... 14

1.3 Lys63-Linked Polyubiquitination ..... 16

1.3.1 General Features of Lys63-Linked Polyubiquitination ..... 16

1.3.2 E2 and E3 Enzymes in Lys63-Linked Polyubiquitination ..... 17

1.3.3 Involvement of Lys63-Linked Polyubiquitination in Cellular Functions ..... 18

1.3.3.1 DNA Repair ..... 18

1.3.3.2 Endocytosis and Intracellular Protein Trafficking ..... 21

1.3.3.3 Kinase Activation ..... 23

1.4 The Ubiquitin System in *Arabidopsis thaliana* ..... 25

1.4.1 *Arabidopsis thaliana* as a Model Species ..... 25

1.4.2 Characterization of the Ubiquitin System in Arabidopsis ..... 26

1.4.3 Ubc13-Uev E2 Conjugating Enzyme in Arabidopsis ..... 28

1.4.4 Significance of Studying E3 ligases in Arabidopsis ..... 29

1.5 Functional Roles of Example E3 Ligases in Arabidopsis ..... 29

1.5.1 Co-Chaperone AtCHIP ..... 29

1.5.2 RGLG in Regulating Apical Dominance ..... 31

1.5.3 $SCF^{TIR1}$ and Auxin Signalling ..... 32

1.6 Objectives ..... 33

**2 MATERIALS AND METHODS ..... 35**

2.1 Plant Materials and Growth Conditions ..... 35

2.2 Sequence Analysis and Domain Prediction ..... 35

2.3 Plant Genomic DNA Extraction ..... 36

2.4 Polymerase Chain Reaction and DNA Gel Electrophoresis ..... 36

2.5 Total RNA Isolation and RT-PCR ..... 37

2.6 Plant Transformation ..... 38

2.7 Plant Phenotypic Surveys ..... 39

2.7.1 Parameter Measurements ..... 39

2.7.2 Hormonal Treatments and Osmotic Stress Tolerance ..... 40

2.7.3 Seed Longevity ..... 41

2.7.4 Thermal Tolerance ..... 41

2.7.5 High-intensity Light Treatment ..... 42

2.7.6 Oxidative Stress ..... 42

2.7.7 DNA Damage Tolerance ..... 42

**3 RESULTS ..... 43**

3.1 Functional Characterization of AtCHIP ..... 43

3.1.1 AtCHIP Protein Sequence Analysis ..... 43

3.1.2 Confirmation of T-DNA Insertion of *Atchip-1* Mutant ..... 45

3.1.3 Phenotypic Characterization of *Atchip-1* Mutant ..... 46

3.1.3.1 Hormonal Treatments and Osmotic Stress Tolerance ..... 47

3.1.3.2 Seed Longevity ..... 54

3.1.3.3 Thermal Tolerance ..... 59

3.1.3.4 Light Intensity Treatment ..... 61

3.1.3.5 Oxidative Stress ..... 63

3.1.3.6 DNA Damage Tolerance ..... 65

3.2 Characterization of At1g74370 (*E3-A1*) and At1g69330 (*E3-A2*) Genes ..... 67

3.2.1 Sequence Analysis of Putative E3-A Proteins ..... 67

3.2.2 Screen for RNAi Down-Regulation Lines of *E3-A1* and *E3-A2* Genes ..... 69

3.2.3 Obtaining Double RNAi Lines of *E3-A1* and *E3-A2* Genes ..... 71

3.2.4 Phenotypic Characterization of *E3-A1 and E3-A2* RNAi lines ..... 72

3.2.5 Identification of "Stem-Fusion" Phenotype on *E3-A2* RNAi Transformants ..... 75

3.3 Summary of Phenotypic Surveys ..... 76

**4 DISCUSSION ..... 79**

4.1 AtCHIP and Protein Quality Control ..... 79

4.2 AtCHIP and Homeostasis of Chloroplast Protein Turnover ..... 82

4.3 Other Potential Functions of AtCHIP ..... 83

4.4 E3-A Family ..... 84

4.5 Phenotypic Analyses of *A. thaliana* ..... 85

4.6 General Discussion and Future Work ..... 87

**APPENDICES ..... 90**

## LIST OF TABLES


| | | |
|---|---|---|
| **Table 1.1** | An overview of major protein domains carrying E3 catalytic activity | 10 |
| **Table 2.1** | Oligonucleotide primers for PCR | 37 |
| **Table 3.1** | Predicted domains within sequences of E3-A proteins | 69 |
| **Table 3.2** | Phenotypic surveys for *Atchip-1* mutant line | 77 |
| **Table 3.3** | Phenotypic analysis of *E3-A1* and *E3-A2* RNAi transformants | 78 |

## LIST OF FIGURES


| | | |
|---|---|---|
| **Figure 1.1** | Ubiquitination reaction | 3 |
| **Figure 1.2** | Roles of Lys-63 linked polyubiquitination in DNA damage response | 19 |
| **Figure 1.3** | Lys63-linked polyubiquitination is involved in kinase activation in NF-κB signalling pathways | 24 |
| **Figure 3.1** | Domain information and sequence analysis of AtCHIP protein | 43 |
| **Figure 3.2** | Insertion site and gene expression analysis of a *AtCHIP* T-DNA mutant *Atchip-1* | 46 |
| **Figure 3.3** | Phenotypic survey of *Atchip-1* mutant plants in response to hormonal and sucrose treatments | 48 |
| **Figure 3.4** | Phenotype of *Atchip-1* mutant | 49 |
| **Figure 3.5** | Analysis of **s**eed germination and cotyledon greening | 50 |
| **Figure 3.6** | ABA treatment analysis of *Atchip-1* and control lines grown under identical conditions | 52 |
| **Figure 3.7** | Seed longevity analysis of *Atchip-1* mutant and wild type lines | 55 |
| **Figure 3.8** | Comparison of seed longevity of two pairs of seed lots between *Atchip-1* and the wild type | 56 |
| **Figure 3.9** | Comparison of seed longevity of three pairs of seed lots between *Atchip-1* and the wild type | 58 |
| **Figure 3.10** | Analysis of basal thermal tolerance | 60 |
| **Figure 3.11** | Analysis of acquired thermal tolerance | 61 |
| **Figure 3.12** | Plant morphologies under normal and high-intensity light conditions | 62 |
| **Figure 3.13** | Phenotypic survey of *Atchip-1* under oxidative stress | 64 |

**Figure 3.14** Phenotypic survey of *Atchip-1* following DNA damaging treatments 66

**Figure 3.15** Sequence analysis of E3s that are closely related to At1g74370 (*E3-A1*) 68

**Figure 3.16** Transcripts of *E3-A* genes in RNAi transformants analyzed by RT-PCR 71

**Figure 3.17** Down-regulation of *E3-A1* and *E3-A2* in hybrid RNAi plants (F1 generation) 72

**Figure 3.18** Phenotypic survey of E3-A1 and E3-A2 RNAi lines in response to hormonal treatments and osmotic stress. 73

**Figure 3.19** Analysis of seed germination of RNAi lines, wild type line and unrelated T-DNA mutant line as control 74

**Figure 3.20** Morphology of “stem fusion” plants 76

## LIST OF ABBREVIATIONS

| | |
|---|---|
| ABA | abscisic acid |
| ABRC | Arabidopsis Biological Resource Center |
| AD | activation domain |
| AFB | auxin signaling F-box protein |
| APC | anaphase-promoting complex |
| ARF | auxin response factor |
| At | *Arabidopsis thaliana* |
| ATM | ataxia telangiectasia mutated |
| BARD1 | BRCA1-associated RING domain protein 1 |
| BD | DNA binding domain |
| BRCA1 | breast and ovarian cancer type 1 susceptibility protein |
| BRCC | BRCA1/2-containing complex |
| CHIP | carboxyl terminus of Hsc70-interacting protein |
| CP | core particle of 26S proteasome |
| DSB | DNA double strand break |
| DUB | deubiquitinating enzyme |
| E1 | ubiquitin activating enzyme |
| E2 | ubiquitin conjugating enzyme |
| E3 | ubiquitin-protein ligase |
| E6-AP | human papilloma virus E6-associated protein |
| EGFR | epidermal growth factor receptor |
| ESCRT | endosomal sorting complex required for transport complex |
| F1 | First filial generation plants from the cross |
| FBP | F-box protein |

| | |
|---|---|
| GAP | general amino acid permease |
| GST | glutathione S-transferase |
| HECT | homology to E6AP C-terminus |
| HPV | human papilloma virus |
| Hsc70 | heat shock protein cognate 70 |
| Hsp70 | heat-shock protein 70 |
| Hsp90 | heat-shock protein 90 |
| IAA | indole-3-acetic acid |
| IBR | in-between ring-finger |
| IKK | IκB kinase |
| KN | kinetin |
| LRR | leucine-rich-repeat |
| MDC1 | mediator of DNA damage checkpoint protein 1 |
| MeJA | methyl jasmonate |
| MMS | methylmethane sulfonate |
| MRN | MRE11–RAD50–NBS1 |
| MS | Murashige and Skoog basal salt |
| MVB | multivesicular body |
| NAA | naphthaleneacetic acid |
| NASC | Nottingham Arabidopsis Stock Centre |
| NEDD8 | neural precursor cell expressed, developmentally downregulated 8 |
| NEMO | NF-κB essential modulator |
| NF-κB | nuclear factor κB |
| PCNA | proliferating cell nuclear antigen |
| PCR | polymerase chain reaction |
| PP2A | protein phosphatase 2A |

| | |
|---|---|
| RAD | radiation (repair genes) |
| RAP80 | RAP80, receptor-associated protein 80 |
| RBR | RING-IBR-RING |
| RGLG1 | RING domain Ligase 1 |
| RGLG2 | RING domain Ligase 2 |
| RING | really interesting new gene |
| RIP | receptor interacting protein |
| RLD | regulator of chromosome condensation 1-like domain |
| RNF | RING finger protein |
| RNAi | RNA interference |
| RP | regulatory particle of 26S proteasome |
| RTK | receptor tyrosine kinase |
| RT-PCR | reverse transcriptase mediated polymerase chain reaction |
| SA | salicylic acid |
| SCF | skp1-cullin-F-box protein |
| Skp1 | S-phase-kinase-associated protein-1 |
| SRS | suppressor of RAD6 |
| SUMO | small ubiquitin-like modifier |
| TAB2 | TAK1-binding protein 2 |
| TAIR | The Arabidopsis Information Resource |
| TAK1 | transforming growth factor $\beta$-activated kinase 1 |
| TIR1 | transport inhibitor response 1 |
| TLS | translesion synthesis |
| TPR | tetratricopeptide repeat |
| TRAF | TNF receptor-associated factor |
| Ub | ubiquitin |

| | |
|---|---|
| UBA | ubiquitin-associated domain |
| UBC | ubiquitin conjugating domain |
| UBD | ubiquitin-binding domain |
| UBE1 | ubiquitin-activating enzyme E1 |
| UBL | ubiquitin-like protein |
| UEV | Ubc enzyme variant |
| UFD | ubiquitin fusion degradation |
| UIM | ubiquitin-interacting motif |
| UPS | ubiquitin-proteasome system |
| UV | ultraviolet |
| WT | wild type |
| WW | tryptophan-tryptophan domain |

# 1 INTRODUCTION

## 1.1 Ubiquitin System

Ubiquitin (Ub), a 76-amino-acid-residue protein, is ubiquitously present in all examined eukaryotic species (Jentsch, 1992; Smalle and Vierstra, 2004). It functions as a posttranslational tag on another protein in a form of monomer or polymer (polyUb chain), and thereby directs the tagged protein to certain cellular processes. This covalent attachment of Ub monomer or polymer to the target protein is a well-known process called ubiquitination (ubiquitylation). The initial discoverers of Ub as an inducing signal for protein degradation were awarded the Nobel Prize in Chemistry 2004, and this pathway has been well studied for over three decades (Hershko and Ciechanover, 1998; Jackson, 2006). However, eukaryotes employ protein ubiquitination to function more than directing the proteasome-mediated protein degradation, and increasing attention has been paid to the proteasome-independent pathways in recent years (Haglund and Dikic, 2005; Komander, 2009). In addition, through a process called deubiquitination Ub modification can also be removed and a polyUb chain can be disassembled (Hershko and Ciechanover, 1998). Therefore, protein ubiquitination can be more widely considered as a reversible signaling system that regulates various cellular signaling networks.

### 1.1.1 The Ubiquitin Protein

Ub is translated from a gene family that codes for fusion precursors. These genes can be divided into two categories: polyUb genes in which multiple Ub-coding units are connected head-to-tail, or Ub-fusion genes in which a single Ub-coding region is next to the 5' end of a different coding region (Callis *et al.*, 1995). The number of Ub-coding units in polyUb genes varies (in the case of the plant *Arabidopsis thaliana* 3, 4, 5 and 6 repeating units were found)

(Callis *et al.*, 1995), and in Ub-fusion genes the region connected to 3' end of Ub-coding unit encodes ribosomal proteins or the Related to Ub (RUB)-1 protein (Callis *et al.*, 1990). From Ub genes, the precursor proteins are rapidly processed by deubiquitinating enzymes (DUBs), a protease family which cleaves the carboxy (C-) terminus of Ub moieties (Wing, 2003; Wu *et al.*, 2003). Thus, the processed Ub monomers are released and attached to target proteins through a three-step conjugation cascade (see below).

The primary sequence of the Ub protein is highly conserved, with only three amino acid differences between yeast and human (Ozkaynak *et al.*, 1984). All higher plants share an identical Ub sequence, with only two amino acid differences comparing to yeast Ub (Smalle and Vierstra, 2004). Such extent of sequence conservation is remarkable, considering Ub is encoded by multiple genes in some organisms. In Arabidopsis, for example, there are 28 coding genes distributed among 11 loci (Goettsch and Bayer, 2002).

The small Ub protein (about 8.5 kDa) folds into a compact globular structure, with a mixed parallel-anti-parallel β sheet around an α-helix. The abundance of intracellular hydrogen bonds possibly keeps Ub stable at a wide range of different denaturation conditions (Jackson, 2006). This structural stability seems crucial as Ub is recycled during protein conjugation-degradation cycles, and may also implicate a reason for the high conservation of Ub sequences.

### 1.1.2 Ubiquitination Reaction

Through the ubiquitination reaction the C-terminus of Ub is attached to the side chain of a Lys residue in the substrate protein by forming an isopeptide bond (Figure 1.1A). Usually this reaction consists of three enzymatic steps (Hershko and Ciechanover, 1998; Jentsch, 1992) (Figure 1.1B). Firstly, with ATP, the C-terminal Gly residue of a Ub is activated by the Ub activating enzyme (E1 or UBA). Following the formation of an intermediate Ub adenylate, the Ub is transferred to a conserved Cys residue of E1 via a thioester bond, with the release of

AMP. Secondly, the Ub thioester is passed on to the Cys residue in the active site of a Ub conjugating enzyme (E2 or UBC). Thirdly, catalyzed by a Ub-protein ligase (E3), the C-terminal Gly is linked to the ε-amino group of a Lys residue in the target protein. The E3 ligases either receive an E2-linked Ub by thioester linkage before Ub-substrate ligation, or directly transfer Ub from E2 to the substrate by binding to the Ub-carrying E2.

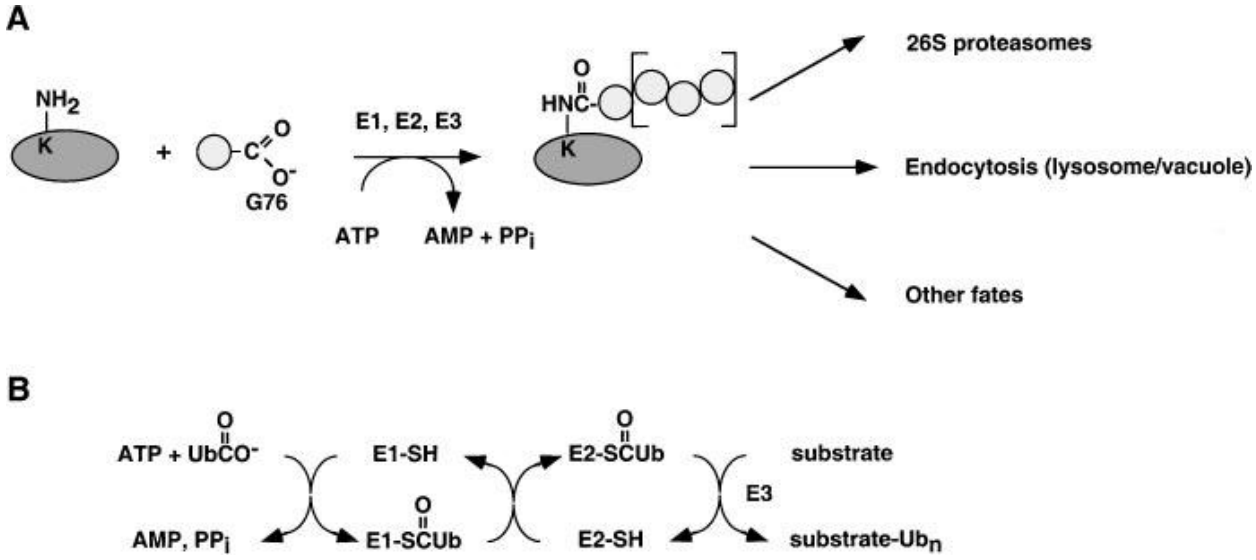


**Figure 1.1** Ubiquitination reaction, (taken from Pickart, 2001). **(A)** An overview of ubiquitination and its related signalling pathways. K: lysine residue; G: glycine residue. **(B)** The process of three-step enzymatic ubiquitination reaction.

For any of the studied eukaryotic organisms, only one or very few E1s have been found for Ub activation, yet there are usually a number of E2s and numerous families of E3s. The first E1 was originally identified and purified from rabbit reticulocytes (Ciechanover *et al.*, 1981; Ciechanover *et al.*, 1982; Haas *et al.*, 1982). The first identified E1 genes in both yeast (Mcgrath *et al.*, 1991) and plants (Hatfield *et al.*, 1990) were named *UBA1*, and in mammals the first E1 gene was named *UBE1* (ubiquitin-activating enzyme E1) (Disteche *et al.*, 1992). Since then, structurally related homologues of UBA1 and UBE1 enzymes have been discovered.

In Arabidopsis, two E1 genes (*AtUBA1* and *AtUBA2*) have been reported and their products share 81% sequence identity (Hatfield *et al.*, 1997). In mice (Kay *et al.*, 1991) and marsupials (Mitchell *et al.*, 1992), a second *UBE1*-like gene was found in the Y chromosome, with about 90% identity to the *UBE1* gene identified initially in the X chromosome. However, it seems that UBE1 and structurally related UBE1-like proteins are not the only E1s for Ub activation, since a novel mammalian E1 enzyme UBA6 (also known as UBE1L2), which has only about 40% identity to UBE1, was found to be capable of activating Ub (Groettrup *et al.*, 2008). All known E2 enzymes for Ub conjugation have a catalytic Cys site in a conserved UBC domain of approximately 140-150 amino acids functioning to receive an activated Ub from E1. The E2 UBC domains usually interact with the corresponding E3s during the ubiquitination reaction, with a few exceptions that interact with substrates directly (Wu *et al.*, 2003). Based on the presence of the distinct UBC domain putative E2s have been identified in different model species. In *Saccharomyces cerevisiae*, there are 11 ubiquitin E2 proteins (Hochstrasser, 1996), and in Arabidopsis, 37 putative E2 proteins were found (Smalle and Vierstra, 2004). The human genome was predicted to encode approximately 50 E2 proteins (Markson *et al.*, 2009). Compared to the limited variety of E1s and E2s, E3s are more abundant in both number and structural diversity. There are about 80 putative E3 genes in *S. cerevisiae* and 617 putative E3 genes in human genome (Li *et al.*, 2008). More than 1300 genes in Arabidopsis have been predicted to encode E3s or components of E3s (Smalle and Vierstra, 2004). As E3 ligases are the components that recruit substrates into the Ub system; they are considered most responsible for the specificity in substrate recognition. Therefore, given the abundance and diversity of substrates recognized specifically by numerous E3s in the Ub system, Ub modification can be involved in a broad range of cellular signalling pathways.

### 1.1.3 Different Types of Ubiquitination

Target proteins can be modified by a single Ub (monoubiquitination) or by a poly-Ub chain

(polyubiquitination). For multiubiquitination, two or more lysine residues of a target protein are ubiquitinated. The Ub protein itself has seven Lys residues (Lys6, Lys11, Lys27, Lys29, Lys33, Lys48 and Lys63), and these Lys residues can also be linked to the C-terminus of another Ub through an isopeptide bond. Therefore, by connecting one after another, Ub molecules can be polymerized. All the seven Lys residues can be potentially ubiquitinated, resulting in poly-Ub chains (Komander, 2009).

To date, studies of monoubiquitination have implicated its important roles in membrane associated functions such as endocytosis, endosomal protein sorting and in other regulatory functions such as virus budding, histone regulation and DNA repair in the cell (Hicke, 2001). For eukaryotic cells, internalization of plasma membrane proteins through the endocytic pathway is a common mechanism for down-regulation. For the majority of membrane proteins in *S. cerevisiae*, ubiquitination of the cytoplasmic domains is required for the internalization (Hicke, 1999; Rotin *et al.*, 2000). Some signal-transducing receptors and ion channels on mammalian cell membrane were found to be ubiquitinated for them to be internalized upon the ligand stimulations (Hicke, 1999; Sun *et al.*, 2011). These ubiquitinated proteins are usually targeted to the lysosome for degradation, through the functions of Ub-binding proteins that possess specific Ub-binding domains (UBD). Endocytic transport seems also to be regulated by ubiquitination. It is clear that monoubiquitination is essential for sorting many internalized receptors from the early endosome into vesicles inside the nascent multivesicular bodies (MVBs), and cargo-containing vesicles eventually will fuse into lysosomes to be degraded (Haglund *et al.*, 2003). Studies on epidermal growth factor receptor (EGFR) and platelet-derived growth factor receptor (PDGFR) have shown the involvement of ligand-induced multiubiquitination in receptor endocytosis, and such multiple mono-Ubs might lead to stronger and more specific interactions with UBDs, which in this case may be required for the endocytic pathway (Haglund *et al.*, 2003). Monoubiquitination is found in other cellular processes. For example, Cag is a common retrovirus protein that pinches off membrane particles containing enveloped virus, and the mono-Ub modification of Cag is found

to be essential for its function during virus budding (Garoff *et al.*, 1998). Histones have also been found to be monoubiquitinated. For example, histone H2B were found to be monoubiquitinated in *S. cerevisiae*, Arabidopsis and mammals (Weake and Workman, 2008). Yeast cells that lack the monoUb modification on H2B do not sporulate, which is usually caused by dysfunctions in meiosis (Robzyk *et al.*, 2000). Knocking out a specific E2 that catalyzes H2B ubiquitination in mice leads to male infertility (Roest *et al.*, 1996). Impaired H2B monoubiquitination causes defects in seed dormancy and flowering time in Arabidopsis (Cao *et al.*, 2008; Liu *et al.*, 2007). In addition, histone H1 was found to be monoubiquitinated in *Drosophila melanogaster*, and lack of this monoUb modification leads to defects in the activation of gene transcription (Pham and Sauer, 2000).

The polyUb chain assembled through Lys48 linkage between Ubs was the first discovered homotypic chain, and is also the most abundant type in different organisms. This Lys48-linked polyUb chain serves as a specific tag recognized by a multi-subunit protease called the 26S proteasome, which degrades the tagged substrate proteins. The Ub/26S proteasome pathway has been extensively studied, and Lys48-linked polyubiquitination is considered the most classical type of polyUb modification (Komander, 2009). However, a different type of polyUb chain assembled through Lys63 linkage has also been discovered (Deng *et al.*, 2000; Hofmann and Pickart, 1999). This Lys63-linked polyubiquitination has been found to be involved in various cellular processes such as DNA repair and kinase activation in all eukaryotic organisms (Komander, 2009). So far, the Lys63-linked polyUb chain is the best studied atypical polyUb chain. Besides Lys48-linked and Lys63-linked polyUb chains, homotypic Ub chains can be linked through any of the remaining five Lys residues (*i.e.* a chain linked through Lys6, Lys11, Lys27, Lys29 or Lys33 only), and there is an increasing interest in these atypical polyUb chains (Behrends and Harper, 2011; Ikeda and Dikic, 2008). All the chain types above have been found to target substrate proteins for degradation via UPS, although the majority of studied substrates polyubiquitinated by Lys63-linked polyUb chains have a non-degradative fate. Moreover, polyUb chains formed

through mixed-linkage have also been found (Mukhopadhyay and Riezman, 2007), as a result of mixed-linkage, bifurcations may occur in polyUb chains composing two types of Lys linkages (*i.e.* Lys 6/11, Lys 27/29, Lys 29/48 or Lys 29/33).

Eukaryotic cells also have ubiquitin-like proteins (UBLs), such as small Ub-like modifier (SUMO), interferonstimulated gene 15 (ISG15), autophagy 8 (ATG8) and neural precursor cell expressed, developmentally downregulated 8 (NEDD8). In total about 16 types of UBLs in addition to Ub have been identified (Komander, 2009). These UBL proteins all resemble Ub in structural fold and in enzymatic conjugation machinery, although SUMO and NEDD8 are so far the only ones capable of chain formation (Ikeda and Dikic, 2008). Making the ubiquitination system even more complex, SUMO and NEDD8 have been found in polyUb chains (Ikeda and Dikic, 2008). So far little is known about the functions of these heterologous Ub chains.

### 1.1.4 The Ubiquitin-Proteasome System (UPS)

Since the first discovery of ubiquitin (Lys48-linked polyubiquitination) dependent proteolysis, the involvement of the ubiquitin-proteasome system (UPS) has been found in almost every aspect of cellular functions (Hershko and Ciechanover, 1998; Pickart and Fushman, 2004). Such diverse roles are also implied by the large population of genes encoding UPS related factors among eukaryotes. Although the number varies among different species, in Arabidopsis, the number of UPS-related genes amounts to over 6% of the entire genome (Downes and Vierstra, 2005).

The 26S proteasome is a major component of the UPS where substrates with a polyUb tag are finally degraded. The process at the 26S proteasome consists of signal recognition, protein unfolding, substrate translocation and deubiquitination (Finley, 2009). The structure of this large protein complex (over 2.5 MDa) contains two subcomplexes, the 20S core particle (CP) and 19S regulatory particle (RP). The CP possesses ATP independent protease activity. It

has a barrel-like structure consisting of four stacked rings, and each ring is composed of seven related subunits. In each of the two outer rings are α1-7 subunits and in each inner ring are β1-7 subunits. The α-subunits form a narrow channel in both outer rings so that the access to the inner proteolytic region is restricted to unfolded polypeptides. X-ray crystallography indicated a proteolytic chamber which harbors three catalytic sites in subunits β1, β2 and β5 (Unno *et al.*, 2002). These three subunits all belong to the amino (N-) terminal nucleophile (Ntn) hydrolase family and use an N-terminal threonine as the catalytic nucleophile (Voges *et al.*, 1999). Although β1, β2 and β5 subunits are classified as caspase-like, trypsin-like and chymotrypsin-like, respectively, according to their preferences in cleaving specific sites in polypeptides, they also have certain flexibility in hydrolyzing a wide range of peptide sequences. To sum up, these structural features of the CP together ensure efficient digestion of imported proteins. The 19 subunits of the RP can be divided into the lid and base subcomplexes (Glickman *et al.*, 1998). The base of the RP directly associates with the α-subunit ring of the CP. Among the ten subunits there are six related AAA-ATPases namely Rpt1-6 and non-ATPase subunits (Rpn1, 2, 10 and 13). Rpn1 and Rpn2 are scaffolding proteins, and Rpn10 and Rpn13 are Ub binding proteins. Protein degradation at the 26S proteasome is ATP dependent. Therefore, the Rpn subunits seem to be essential for steps such as substrate unfolding and the entry of unfolded polypeptides through the α-subunit ring (Finley, 2009). The lid subcomplex of the RP consists of nine subunits (Rpn3, 5-9, and 11-12). However, the functions of these subunits are largely unknown, except Rpn11 which has been identified with a DUB function (Verma *et al.*, 2002; Yao and Cohen, 2002).

When a substrate is being processed by the 26S proteasome the polyUb label has to be removed. Eukaryotic cells have a family of DUBs, which break down the polyUb chain into single free Ubs so that the free Ubs can be recycled or sometimes the fate of the substrates controlled by ubiquitination can be reversed (Smalle and Vierstra, 2004). The 26S proteasome disassembles the polyUb chain through the activity of DUBs. Rpn11 is an ATP-dependent DUB in the lid of the RP. Its deubiquitination activity is coupled with substrate degradation,

and the absence of its activity greatly impairs proteasome function (Finley, 2009). Two ATP-independent DUBs Ubp6 and Uch37 also cooperate with Rpn11 to process the polyUb chain effectively (Hanna *et al.*, 2006). However, the mechanism of their cooperation still remains unclear.

The polyUb chain is the key signal recognized by the 26S proteasome. It had been assumed that Lys48-linkage solely serves as the proteolytic signal, as most *in vivo* studies of Lys63-linked polyubiqutination showed nonproteolytic destinies of substrates, and Lys48 was found to be the only essential lysine residue within the Ub protein in yeast (Finley *et al.*, 1994). However, more recent studies indicated that Lys63- and Lys11-linked polyUb chains also possibly target substrates to the proteasomes *in vivo* (Saeki *et al.*, 2009; Xu *et al.*, 2009). It seems that the selectivity of polyUb chain type by 26S proteasome is still not well understood. In addition, there were possibly many earlier cases of proteins degraded through UPS that were assumed to be due to substrates being modified with Lys48-linked polyUb chain, but could have been due to modification with atypical forms of polyUb chains (Komander, 2009).

UPS plays important roles in a vast range of intracellular signaling pathways. Through its selective proteolytic activities the UPS balances the removal of abnormal proteins and the recycle of amino acids, and regulates cellular activities through rapid proteolysis of particular regulatory factors. For instance, in control of the cell cycle certain regulatory proteins such as cyclins, inhibitors of cyclin-dependent kinases, and anaphase inhibitors are degraded to promote cell-cycle progression (Hershko and Ciechanover, 1998). There are numerous pathways that are regulated similarly by UPS, such as the control of cell proliferation, apoptosis, gene transcription, metabolic control, and embryogenesis (Hochstrasser, 1996; Lecker *et al.*, 2006; Smalle and Vierstra, 2004).

## 1.2 Major Classes of E3 Ligases

As introduced above, Ub E3 ligases mediate the attachment of the Ub moieties onto substrates

and are considered the main determinants that recognize specific substrates. E3 enzymes can be monomers, with E2 interacting, substrate recognizing and catalytic activities all in a single polypeptide, or multi-subunit protein complexes with different functional components (Glickman and Ciechanover, 2002). Due to the diversity of catalytic mechanisms and structural arrangement of E3s, they are often categorized into three major classes according to the characteristic E2-interacting domains that they possess, namely, homology to E6AP C-terminus (HECT) domain, Really Interesting New Gene (RING) domain and U-Box domain E3s (Komander, 2009) (Table 1.1). In most cases E3s promote Ub-substrate ligation by bringing the E2 and substrate together to facilitate direct transfer of activated Ub from E2 to the substrate (Glickman and Ciechanover, 2002). However, HECT E3s uniquely break down the E2-Ub thioester bond and link the Ub moiety to the active Cys residue of E3s before Ub modification of the substrates (Kee and Huibregtse, 2007).

**Table 1.1** List of three E3 ubiquitin ligase families in three model species.

| **Family** | **Number of predicted encoding genes** | | | **Examples of associated subunits/domains** |
|---|---|---|---|---|
| | ***S. cerevisiae*** | ***H. sapiens*** | ***A. thaliana*** | |
| RING | 47 | 300 | 469 | SCF, APC, RING |
| U-box | 2 | 21 | 64 | TPR |
| HECT | 2 | 28 | 7 | C2-WW, RLD |

### 1.2.1 RING-Type E3s

The RING-type E3s that contain the zinc-binding RING finger domain constitute the majority of E3 ligases. RING E3s are conserved among eukaryotes, with 47 *RING* genes in *S. cerevisiae*, 469 in plant Arabidopsis and 300 predicted in human (Li *et al.*, 2008; Stone *et al.*, 2005). This largest E3 class can be further divided into two subgroups: the simple RING E3s

having both a substrate-interacting domain and an E2-binding RING finger domain in a single protein, and the complex RING E3s composed of multiple subunits as different functional components. A simple RING E3 ligase may also associate with another RING finger protein to form a homodimer or a heterocomplex (Stone *et al.*, 2005). Complex RING E3s include Skp1-cullin-F-box-protein (SCF) E3 complexes and anaphase-promoting complex (APC)-type E3s.

The RING finger domain has conserved Cys and/or His residues (metal ligand residues) coordinating two zinc ions, similar to DNA-binding zinc fingers. However, instead of binding nucleic acid sequences as zinc fingers do, the RING domain mediates protein-protein interactions. RING domains share the consensus sequence $CX_2CX_{(9–39)}CX_{(1–3)}HX_{(2–3)}C/HX_2CX_{(4–48)}CX_2C$ (X represents any amino acid), with either a Cys or a His at the fifth zinc-binding site (Kraft *et al.*, 2005). Based on the type of fifth metal ligand residue, RING domains can be C3HC4 type (RING-HC) or C3H2C3 type (RING-H2) (Freemont, 1993; Lovering *et al.*, 1993). The eight metal ligand residues stabilized by zinc ions form a cross-brace structure, which differs from zinc fingers where metal ligands coordinate two zinc ions in tandem (Deshaies and Joazeiro, 2009).

The RING domain mediates a ligation between an Ub and the substrate by its association with an E2 enzyme. Since the initial suggestion made based on the studies of RING finger containing proteins Rbx1/Roc1, c-Cbl and AO7 (Zheng *et al.*, 2000), there have been increasing data from structural studies and mutational analyses that illustrate the structural basis of E2-RING finger interface (Deshaies and Joazeiro, 2009). According to X-ray crystallography and NMR data (Zheng *et al.*, 2000), the two zinc coordination regions of the RING domain together with the helix between the two regions provide the binding surface for the E2 UbcH7, with Ile383 and Trp408 of c-Cbl and equivalent residues in other RING E3s implicated in interaction with E2s. Systematic two-hybrid and NMR studies on Brca1 have also provided insight into a set of residues that constantly contact multiple E2s (Deshaies and Joazeiro, 2009). However, the residues in the E2-RING domain interface still vary among different E2-E3

matches. Moreover, although most RING domains have intrinsic ligase activity, there are also proteins that possess RING domains without ligase activity. In these cases usually the non-catalytic RING finger protein associates with another one that has ligase activity within a RING domain (Deshaies and Joazeiro, 2009).

A SCF E3 complex contains at least four core components: Skp1 (S-phase-kinase-associated protein-1), cullin, F-box protein (FBP) and a RING finger protein RBX. CUL1, a canonical example of cullins, serves as the scaffold associating with both Skp1 and RBX. Skp1 is an adaptor protein interacting with the substrate-receptor F-box, and it binds the N-terminal region of CUL1 that is composed of three repeats of a five-helix bundle called cullin repeats (CR) (Petroski and Deshaies, 2005). RBX contains a RING-H2 domain that interacts with the C-terminal globular domain of CUL1 (Petroski and Deshaies, 2005). The Skp1-binding F-box domain is the signature domain of FBPs, while the C-terminal substrate-binding domain determines the substrate specificity. Therefore FBPs are normally categorized into different classes according to the types of substrate-binding domains. For instance, the FBW ('FB' for F-box and 'W' for WD-40 repeat domain) class of FBPs recognizes a β-propeller structure; another class is the FBL ('L' for leucine-rich repeat or LRR) where the LRR domain is an arc-shaped α-β-repeat structure. In most cases they involve substrate phosphorylation for their interactions; other FBPs that resembling neither FBL nor FBW domain architecture are grouped as class FBX (Cardozo and Pagano, 2004).

The APC is the largest type of E3, with one or more copies of at least 13 different subunits (Thornton and Toczyski, 2006). The large size of the APC makes this protein complex difficult to study. The subunits of APC sometimes are divided into four parts: structural complex (Apc1/Apc4/Apc5), catalytic complex having the E2-binding affinity (Apc2/Apc11/Doc1), tetratricopeptide repeat (TPR) arm that functions primarily in adaptor association (Cdc23/Cdc16/Cdc27/Cdc26/Swm1), and the adaptors responsible for the interaction with substrates (Cdc20/Cdh1/Ama1) (Thornton and Toczyski, 2006). The catalytic core of APC appears to function in a similar manner to its counterpart in SCF E3s. Apc2 and

Apc11 in APC were found structurally related to cullin and RBX of the SCF complex, respectively, and these two subunits together were shown to possess a Ub ligase activity *in vitro* (Thornton and Toczyski, 2006). The APC has been considered a key element in the rapid degradation of cell cycle regulators, and therefore research on the APC targets has primarily focused on proteins involved in growth control and cell cycle regulation (Skaar and Pagano, 2009).

### 1.2.2 U-Box-Type E3s

The class of U-box E3s was identified more recently than other E3 types. U-box E3s contain a signature domain called U-box domain consisting of about 75 amino-acid residues and related to the RING finger domain. Sequence alignment of U-box domains and RING fingers showed the absence of metal ligand Cys and His residues in U-boxes, yet both types of domains share a similar pattern of hydrophobic and polar residues (Aravind and Koonin, 2000). Therefore, the U-box is predicted to fold similarly to the RING finger domain, and is presumably stabilized by intramolecular interactions such as salt bridges and hydrogen bonds, instead of the zinc ions coordinated by Cys and His residues in the RING finger domain (Ohi *et al.*, 2003).

Interestingly, the first U-box protein was initially discovered in the UFD (ubiquitin fusion degradation) pathway, where the U-box-containing Ufd2 functions in elongation of polyUb chain (Hatakeyama and Nakayama, 2003). In this case, Ufd2 together with HECT E3 Ufd4 extends the polyUb chain to enable proteasomal degradation. This specialized ligase activity of Ufd2 was termed as “E4” activity (Hatakeyama and Nakayama, 2003). Although only a handful of U-box E3s have been thoroughly studied, this elongation activity was also discovered in a well-known U-box protein CHIP (carboxyl terminus of Hsc70-interacting protein) in addition to its E3 ligase activity (Ohi *et al.*, 2003), which leads to a speculation that U-box proteins may commonly share the E4 characteristic. As the assembly of atypical polyUb chains (other than Lys48-linkage) requires the switch of E3 ligases, the U-box type E3s may have their significant roles in attaching a Ub moiety to previously formed monoUb or

oligoUb chain at different Lys positions (Hatakeyama and Nakayama, 2003).

Compared to the large number of RING finger E3s in different species, U-box proteins comprise a much smaller portion of the entire E3 population. For example, only 2 and 21 U-box genes have been identified in the yeast *S. cerevisiae* and the human genome, respectively (Yee and Goring, 2009). However, in plants, there are much larger numbers of U-box proteins, with 64 U-box genes found in the Arabidopsis genome (Wiborg *et al.*, 2008), and 77 in the rice genome (Zeng *et al.*, 2008). Hence, plants seem to employ a greater diversity of U-box proteins for a broader range of functions.

### 1.2.3 HECT-Type E3s

There are five HECT domain containing E3s in *S. cerevisiae*, seven in Arabidopsis and 28 in human (Li *et al.*, 2008; Smalle and Vierstra, 2004). HECT E3s have been found in diverse functions in yeast and human cells (Rotin and Kumar, 2009). However, not much is known about plant HECT E3s; in Arabidopsis the only two of them that have been characterized are involved in the trichome development and leaf senescence respectively (Downes *et al.*, 2003; Miao and Zentgraf, 2010). The HECT E3s are usually large proteins (smallest ones are about 90 kDa and largest can be over 500 kDa) (Kee and Huibregtse, 2007). The HECT domain is an approximately 350-amino-acid long region located in the C-terminus of the E3 ligase. It was originally identified in human papilloma virus (HPV) E6-associated protein (E6-AP) (Huibregtse *et al.*, 1995). This domain serves as the E2-binding site with a smaller C-terminal lobe possessing ligase activity, and a flexible linker region connecting the two lobes. The HECT E3-catalyzed reaction starts with the binding of E2, proceeding with the formation of an E3-Ub intermediate by transferring the Ub-linked thioester bond from E2 to the catalytic Cys site in the C-terminal lobe of the HECT domain, and ends with the attachment of Ub to the substrate (Bernassola *et al.*, 2008).

The substrate-binding region is at the N-terminal region of the HECT domain. Based on

the substrate recognition domains HECT E3s are usually divided into three subgroups: C2-WW-HECT E3s, HERC E3s, and other HECT ligases.

Compared to other types, members of the C2-WW-HECT subgroup are the best characterized HECT E3s so far. They all share several domains in the following order: an N-terminal protein kinase C (PKC)-related C2 domain, two to four tryptophan-tryptophan (WW) protein-interacting domains, and a C-terminal HECT domain (Schwarz *et al.*, 1998). The C2 domains usually bind to $Ca^{2+}$ and phospholipids and mediate intracellular trafficking of E3s to the plasma membrane, endosomes or MVBs (Dunn *et al.*, 2004). The WW domains recognize and selectively bind to proline-rich phosphoserine/phosphothreonine sequences in substrate proteins, and thus they are the domains responsible for E3-substrate interactions (Bernassola *et al.*, 2008). WW domains usually contain the consensus sequence PPXY (PY), nevertheless, atypical interactions with domains other than the PY sequence have also been reported (Bernassola *et al.*, 2008).

The HERC subgroup of HECT E3s contains regulator of chromosome condensation 1 (RCC1)-like domains (RLDs) and a HECT domain (Rotin and Kumar, 2009). Larger HERC E3s possess multiple RLD domains, whereas smaller HERC E3s contain only a single RLD domain. The RLD domain forms a seven-bladed β-propeller fold, and has chromatin -interacting activity and might function as a guanine nucleotide-exchanging factor (GEF) (Renault *et al.*, 2001).

Other HECT E3s contain a variety of protein-interacting domains such as WWE, Ub-associated (UBA) domain, zinc fingers, and poly(A)-binding protein (PABP) C terminus (PABC) domains (Rotin and Kumar, 2009). These different E3s do not belong to either of the two large subgroups described above, and therefore they together can be categorized as a new subgroup. These HECT E3s also play important roles in diverse functions. For example, E6-AP is involved in HPV-induced cervical cancers, and mutations in its coding gene contribute to the pathogenesis of Angelman syndrome (Scheffner and Staub, 2007).

## 1.3 Lys63-Linked Polyubiquitination

### 1.3.1 General Features of Lys63-Linked Polyubiquitination

Apart from canonical Lys48-linked polyubiquitination, the Lys63-linked polyUb chain is the best understood chain type. According to quantitative studies on the relative abundance of different types of Ub-Ub linkages in yeast, Lys63 linkage accounts for 17% of total linkages, which is the third most (29% for Lys48-linkage and 28% for Lys11-linkage, both of them target the substrates for degradation via UPS) (Xu *et al.*, 2009). The significant amount of Lys63 linkage implies a wide range of roles that it may have in eukaryotic cells. Indeed, this type of polyubiquitination has been demonstrated to participate in several vital cellular pathways, such as DNA-damage tolerance, kinase activation and protein trafficking (Pickart and Fushman, 2004). To date, almost all the functions played by Lys63-linked polyubiquitination are UPS independent functions. Nevertheless, a Lys63-linked polyUb signal still appears to be capable of conferring substrate degradation *in vivo* (Saeki *et al.*, 2009), and it remains a mystery regarding the possible machinery that determines the non-proteolytic fates of Lys63-linked-polyUb-tagged substrates.

Structural studies have shown that a Lys63-linked polyUb chain has a different conformation to that of a Lys48-linked chain (Komander, 2009). The globular Ub protein contains a flexible C-terminal Leu-Arg-Gly-Gly tail and a prominent hydrophobic surface around Ile44 (Komander, 2009). In a Lys48-linked polyUb chain both Ile44-centered hydrophobic surfaces from the two adjacent Ub moieties contact each other. Therefore, the Lys48-linked chain folds into a closed structure where the C-terminal tail is packed within Ub moieties (Varadan *et al.*, 2002). This chain conformation is not rigid (Ikeda and Dikic, 2008), so that it may be partially unfolded to facilitate the binding of DUBs. In contrast, the Lys63-linked chain has an open conformation where the neighbouring Ub moieties do not contact each other through hydrophobic surfaces (Komander *et al.*, 2009; Tenno *et al.*, 2004). Such an open conformation enables free access to the hydrophobic Ile44 region. Besides,

since the Ubs in a Lys63-linked polyUb chain can rotate with little restraint, the Ile44 region can be associated with certain UBDs (Sato *et al.*, 2009). On the other hand, a Lys63-linked chain may not always be in a completely extended conformation, as the non-adjacent Ubs can still interact with each other (Tenno *et al.*, 2004).

The differences between conformations of Lys63- and Lys48-linked polyUb chains lead to a proposed mechanism through which different chain types may be distinguished, as some UBDs preferentially bind to a particular type of Ub chain linkage. For instance, a study on over 30 UBA domains characterized one group that preferentially recognizes Lys48-linked polyUb chains and another group that instead recognizes Lys63-linked polyUb chains (Raasi *et al.*, 2005). Other domains were also reported to bind a Lys63-linked chain specifically, such as the Ub-interacting motif (UIM) domain of RAP80 (Sato *et al.*, 2009) and SH3 (Src homology 3) domain of STAM (Sato *et al.*, 2008). However, little is known concerning how certain UBDs selectively recognize a particular type of polyUb chain whereas others can bind different polyUb chains regardless of the types of Ub-Ub linkages.

### 1.3.2 E2 and E3 Enzymes in Lys63-Linked Polyubiquitination

To date, the only known E2 responsible for Lys63-linked polyubiquitination is a heterodimer consisting of a Ubc13 and Ubc-like protein called Uev (Ubc enzyme variant) (Broomfield *et al.*, 1998; Sancho *et al.*, 1998). Although the majority of E2 enzymes do not selectively target any particular Lys residues in Ub, the Ubc13-Uev E2 is a special case for it specifically catalyzes the Ub chain elongation on the Lys63 site. In yeast *S. cerevisiae*, the only Uev protein is called Mms2; in human there are two Uev homologs named Mms2 and Uev1a which form heterodimers with Ubc13 (Andersen *et al.*, 2005). Orthologs of both Ubc13 and Uev proteins have been found in plants including Arabidopsis (Wen *et al.*, 2006; Wen *et al.*, 2008).

Previous crystallographic analyses of the Ubc13-Uev complexes from human and yeast cells have revealed a more detailed picture about how specific polyUb chain linkage is

determined (Eddins *et al.*, 2006; McKenna *et al.*, 2003; Pastushok *et al.*, 2005; VanDemark *et al.*, 2001). Structural studies and mutational analyses indicated that Uev proteins in both yeast and human are required for the Ubc13-Uev complex to catalyze polyUb chain assembly (VanDemark *et al.*, 2001). Therefore, Uev proteins seem to have non-catalytic roles that are crucial for the E2 function. In the currently accepted model based on the crystal structure of yeast Ubc13-Mms2 binding a human Ub (Eddins *et al.*, 2006), after Ubc13 of the Ubc13-Uev E2 complex receives an (donor) Ub moiety from E1, the Ubc13-Uev complex binds the substrate Ub at its acceptor site on Mms2, where the side chain of Lys63 from the acceptor Ub is oriented toward the C-terminus of the donor Ub which is anchored by a thioester bond. The positioning of the Lys63 residue in the acceptor Ub is mainly determined by Mms2, and specific residues at the Mms2-Ub interface are critical for the binding and positioning of the donor Ub (Eddins *et al.*, 2006).

Considering the large number of characterized E3s, the number of E3s that have been demonstrated to catalyze Lys63-linked polyUb chain is still relatively small. In addition, individual E3s often can interact with more than one E2s to catalyze different forms of ubiquitination. For example, E3 ligase BRCA1 produces Lys63-linked polyUb chain together with Ubc13-Mms2, whereas it produces a Lys48-linked chain with UBE2K and catalyzes monoubiquitination with multiple E2s (Sun and Chen, 2004). CHIP ligase catalyzes a Lys63-linked chain in the presence of human Ubc13-Uev1a complex and induces a Lys48-linked chain with UBCH1, while it catalyzes all possible linkages with the help of E2 UBCH5 and E3 MDM2 (Kim *et al.*, 2007). Therefore, the Ubc13-Uev heterodimer seems to be determinant for the formation of Lys63-linked polyUb chains.

### 1.3.3 Involvement of Lys63-Linked Polyubiquitination in Cellular Functions

#### 1.3.3.1 DNA Repair

One highly conserved function of the Lys63-linked polyUb chain involves DNA damage

tolerance (Figure 1.2). The *RAD6* (RAD was named after a number of radiation sensitive mutants) pathway, named after one prominent member of a group of DNA repair genes, is responsible for DNA postreplication repair in budding yeast *S. cerevisiae* (Ulrich, 2005). There are conceptually three branches (subpathways) in the *RAD6* pathway: two translesion synthesis (TLS) branches are mediated by different damage-tolerant DNA polymerases, and one is an error-free DNA damage avoidance subpathway (Ulrich, 2005). The proliferating cell nuclear antigen (PCNA) is a target for the RAD6 pathway. It forms a 'sliding clamp' structure encircling DNA double strands, and functions to upload DNA polymerases during DNA

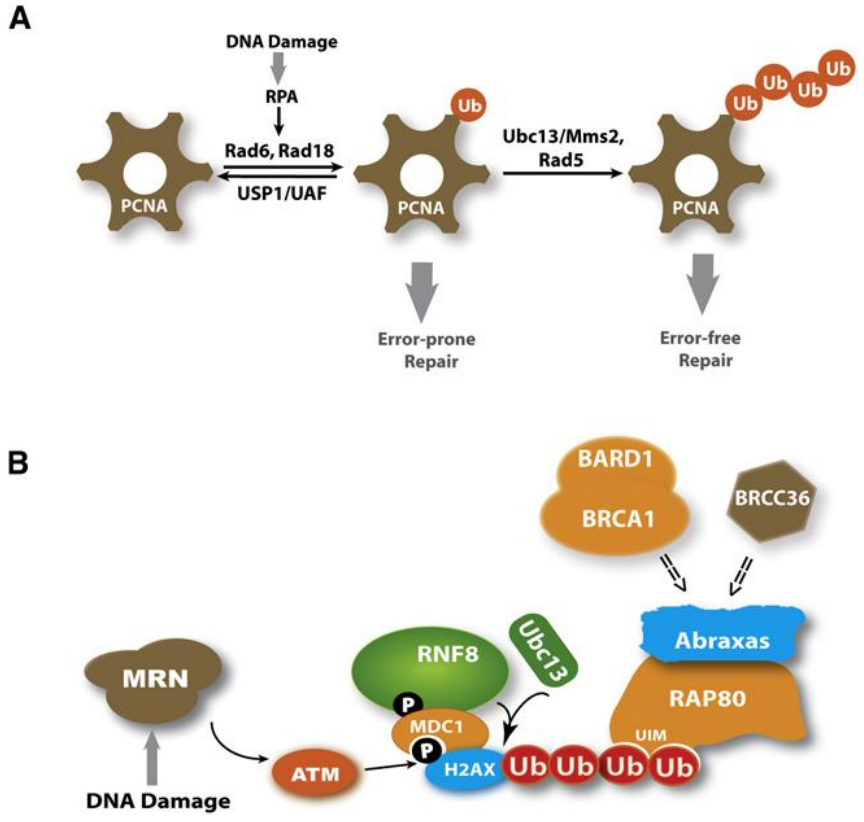


**Figure 1.2** Roles of Lys63-linked polyubiquitination in the DNA damage response (taken from Chen and Sun, 2009). **(A)** Yeast PCNA ubiquitination is involved in DNA damage tolerance. **(B)** DSBs induce histone H2AX modifications including Lys63-linked polyubiquitination, which recruits large protein complexes including BRCA1 and other components involved in DNA damage repair.

replication and also DNA repair. PCNA can be modified at its conserved Lys164 residue with the attachment of Ub or Ub-like modifier SUMO and as a result can exist in several different states: unmodified, monoubiquitinated, polyubiquitinated and sumoylated. Intriguingly, different states of PCNA modifications alter its functionality (Figure 1.2A). The unmodified PCNA functions to anchor DNA polymerases for normal DNA replication, monoubiquitinated PCNA recruits DNA damage tolerance polymerase for TLS, and PCNA polyubiquitinated through Lys63-linkages activates the error-free damage-avoidance pathway (Stelter and Ulrich, 2003). In yeast, the sumoylated PCNA recruits the Srs2 (Srs for suppressor of Rad6) helicase, in order for recombination factors to accumulate at replication forks (Papouli *et al.*, 2005; Pfander *et al.*, 2005). The DNA-damage induced monoubiquitination and polyubiquitination on PCNA both have been observed in all eukaryotic organisms examined to date (Ulrich and Walden, 2010). In neither of these two cases the modified PCNA is targeted to UPS for degradation. In the *RAD6* pathway, Rad6 and Rad18 are a pair of E2 and E3 enzymes responsible for monoubiquitinating PCNA. The ubiquitination can be extended by the Ubc13-Mms2 heterodimer together with an E3 Rad5.

Recent studies in cancer research have led to a new understanding about the essential role of Lys63-linked polyUb modification in DNA double-strand break (DSB) response in human cells (Figure 1.2B). Histones H2A and H2AX were shown to be polyubiquitinated with Lys63-linked chains after a DSB to initiate specific DNA repair processes (Bennett and Harper, 2008; Ulrich and Walden, 2010). The occurrence of DSB events can be recognized by the Mre1-Rad5-Nbs1 (MRN) sensor complex, which activates ATM protein kinase. Thereafter, the variant histone H2AX is phosphorylated by the activated ATM and consequently recruits ATM substrate MDC1. The phosphorylated MDC1 is recognized by the FHA domain of RNF8, a RING finger E3 that interacts with Ubc13 to assemble Lys63-linked polyUb chain. As a result, H2AX and H2A, two critical substrates of RNF8 and Ubc13, are modified with Lys63-linked polyUb chains. Interestingly, a second E3 ligase RNF168 possesses two UIM domains that bind polyUb chains on H2AX and H2A, and also collaborates with Ubc13 to

catalyze more Lys63-linked polyubiquitination reactions on those two histones (Doil *et al.*, 2009). The function of RNF168 in this case was proposed to amplify Lys63-linked polyUb signals. These polyUb signals on H2AX and H2A are recognized by RAP80 through its UIM domain, which in turn recruits a complex including breast and ovarian cancer type 1 susceptibility protein (BRCA1) and other proteins (Wang and Elledge, 2007). BRCA1 was initially found in the cancer patients and provided the initial hint of involvement of Ub modifications in the DSB response (Ruffner *et al.*, 2001). BRCA1 associates with BRCA1-associated RING domain protein 1 (BARD1) and forms a heterodimer with an E3 ligase activity (Wu *et al.*, 1996). The BRCA1-BARD1 heterodimer is involved in homologous recombination-induced DNA repair which is an important error-free process in repairing DSBs. Mediated by PALB2, BRCA1 is associated with BRCA2, a protein responsible for loading an essential recombinase RAD51 on single-strand DNA at DSB sites to initiate the homologous recombination process (Sy *et al.*, 2009). In addition, by associating with different groups of proteins the BRCA1-BARD1 E3 ligase also participates in other processes related to the DNA-damage response such as G2-M checkpoint control, response to stalled replication folks during S phase, and resection of DSBs (Huen *et al.*, 2010). However, since multiple E2s can cooperate with the BRCA1-BARD1 complex to catalyze different types of Ub modifications, it has been a challenge with regard to clarifying how BRCA1-BARD1 E3 ligase regulates each of those DNA repair-related processes through its ubiquitination activity (Christensen *et al.*, 2007).

#### 1.3.3.2 Endocytosis and Intracellular Protein Trafficking

Lys63-linked polyubiqutination has also been found to be important in inducing endocytosis of membrane associated proteins and intracellular protein trafficking. Ligand-induced receptor endocytosis is a strategy for cells to down-regulate signalling by reducing the receptor density on the cell surface. The role of Ub in the endocytic pathway was first identified in yeast cells (Hicke and Riezman, 1996). A monoUb signal on plasma membrane proteins in yeast is

sufficient to initiate their internalization (Terrell *et al.*, 1998), while Lys63-linked polyUb chains appear to increase the efficiency of the process and facilitate endocytosis (Galan and HaguenauerTsapis, 1997). Although in mammalian cells the details of Ub induced endocytosis is much less clear, a considerable amount of work has been done on effects of Ub modification of receptor tyrosine kinases (RTKs) following extracellular stimuli (Bache *et al.*, 2004). The epidermal growth factor receptor (EGFR) is a well-known example of a RTK regulated by Ub. Quantitative analyses showed that EGFRs were modified by both monoUbs and Lys63-linked polyUb chains (Huang *et al.*, 2006). The ubiquitination of EGFR seems to depend on the ligand concentrations. At a low EGFR ligand level, the receptors are internalized through a clathrin-dependent pathway only, whereas at a high ligand level when ubiquitination takes place both clathrin-dependent and independent pathways occur. Ubquitination appears to be required in clathrin-independent internalization of receptors while not essential for the clathrin-dependent route (Sigismund *et al.*, 2005). Some membrane proteins have been shown to require Lys63-linked polyubiquitination for their internalization. For example, the yeast protein general amino acid permease (Gap)1p requires modification with a Lys63-linked poly-Ub chain for its efficient internalization in order to adapt to the change of nitrogen source in the medium (Springael *et al.*, 1999). A nerve growth factor (NGF) receptor tyrosine receptor kinase A (TrkA) also requires Lys63-linked polyubiquitination for its internalization and involvement in signal transduction (Geetha *et al.*, 2005).

Following the Ub-induced endocytosis of membrane-associated proteins, ubiquitination (both monoUb and Lys63 polyUb modification) is also a key signal at endosomes to sort its substrates into intraluminal vesicles (ILVs), generating multivesicular bodies (MVBs) that transport proteins to lysosomes (Komada and Kitamura, 2005). Ub-induced sorting of endosomal proteins into MVBs is performed by the endosomal sorting complex required for transport (ESCRT) complexes (Hurley and Emr, 2006). Four components of an ESCRT complex have been characterized to date: ESCRT-0, -I, -II and -III; they are able to recognize a Ub signal through their UBDs. It is clear that short Lys63-linked polyUb chains are critical for

MVB sorting *in vivo*, as cells harboring the Ub-K63R mutation and incapable of assembling Lys63-linked polyUb chains showed severe deficiencies during MVB sorting of protein cargos (Lauwers *et al.*, 2009; Paiva *et al.*, 2009). ESCRTs showed preference in binding to a polyUb signal over a monoUb modification (Barriere *et al.*, 2007). Interestingly, by disabling the function of a DUB, Lys63-linked polyUb chains were extended further than usual, which negatively affected MVB sorting (Kee *et al.*, 2006). Therefore, proper length of the Lys63-linked polyUb signals may ensure an efficient processing of MVB sorting, while long polyUb chains may reduce the efficiency, implying potential regulatory roles of DUBs during intracellular trafficking of ubiquitinated proteins.

#### 1.3.3.3 Kinase Activation

The best-understood role of a Ub cellular signaling pathway is in the nuclear factor κB (NF-κB) signaling pathways. The sensing of cytokines such as tumor necrosis factor a (TNFa) and interleukin-1b (IL-1b) triggers sequential intracellular signal transduction which eventually activates TGF*β* (transforming growth factor *β*)-activated kinase 1 (TAK1) and IκB kinase (IKK), two kinase complexes that lead to the release and activation of NF-κB which in turn activates transcription of target genes (Haglund and Dikic, 2005) (Figure 1.3). During this process, IKK is activated by TAK1, and in turn phosphorylates IκB, which triggers Lys48-linked polyubiquitination on IκB so that it will be degraded by UPS and enable the release of active NF-κB. It is clear that both IKK and TAK1 require Lys63-linked polyubiquitination for their activation (Krappmann and Scheidereit, 2005), and the polyUb chain assembly at these two kinases is catalyzed by TNF receptor-associated factor 6 (TRAF6) (Deng *et al.*, 2000). Many components in the receptor complex were also found to be modified with Lys63-linked polyUb chains, including TRAF proteins (Deng *et al.*, 2000), receptor interacting protein 1 (RIP1) (Ea *et al.*, 2006), interleukin-1 receptor-associated kinase (IRAK) (Ordureau *et al.*, 2008), and components of the TAK1 complex (Reiley *et al.*, 2007). The assembly of a TAK1 complex is

mediated through the interaction between Lys63-linked polyUb chains and UBDs within its subunits TAK1-binding protein 2 (TAB2) and TAB3 (Kanayama *et al.*, 2004; Wang *et al.*, 2001). The UBDs in TAB2 and TAB3 both belong to a type of Ub-binding zinc-finger domain with preferential binding to Lys63-linked chains, and they are essential for TAB2 and TAB3 to activate TAK1 (Kanayama *et al.*, 2004). Moreover, Lys63-linked polyubiquitination of the regulatory subunit NEMO (NF-κB essential modulator) of IKK triggers its kinase activity (Zhou *et al.*, 2004). It is proposed that upon binding of TABs to Lys63-linked polyubiquitinated NEMO, TAK1 is brought in proximity of IKK to facilitate IKK activation (Haglund and Dikic, 2005).

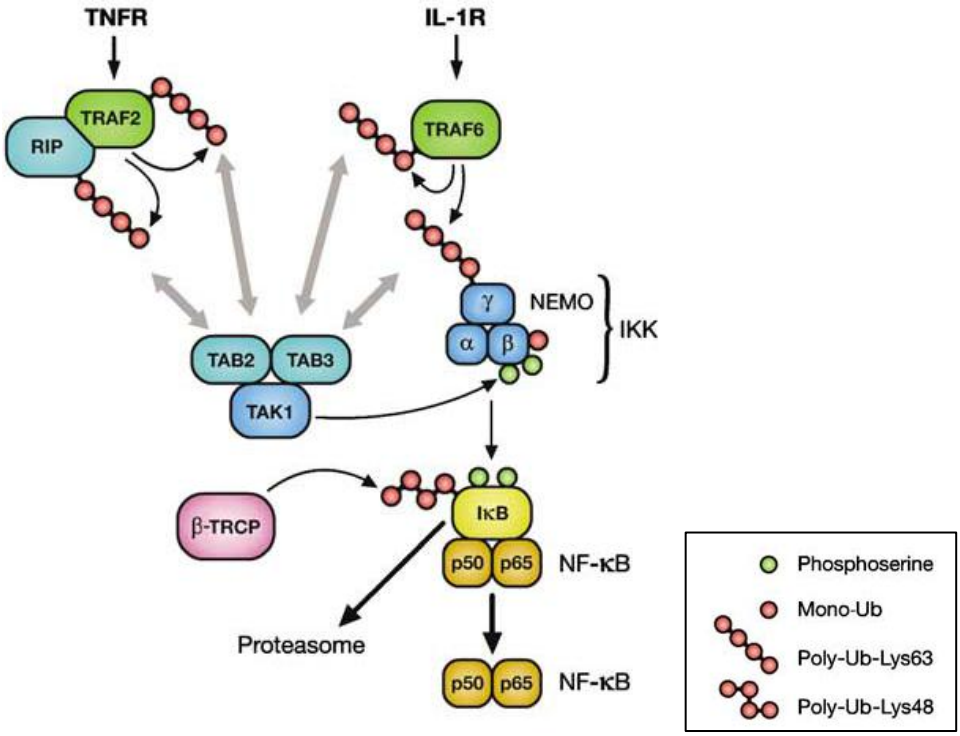


**Figure 1.3** Lys63-linked polyubiquitination is involved in kinase activation in NF-κB signalling pathways (taken from Haglund and Dikic, 2005). Lys63-linked polyubiquitination of NEMO, a component of kinase IKK, triggers the activation of IKK and thereby induces the release of active transcription factor NF-κB.

In addition, the Lys63-linked polyUb chain-specific DUBs appear to have important roles in counteracting effects induced by Lys-63-linked polyubiquitination. A20, a zinc finger protein that inhibits NF-κB activity in the cytoplasm, may serve as a negative feedback regulator of NF-κB signaling by both of its DUB function and E3 ligase activity (Wertz *et al.*, 2004). A20 selectively removes Lys63-linked polyUb chains on RIP and catalyzes Lys48-linked polyubiquitination to induce degradation of RIP. Another DUB called tumor suppressor cylindromatosis (CYLD) removes Lys63-linked polyUb chains from TRAF2, TRAF6 and NEMO and can also down-regulate NF-κB signaling (Brummelkamp *et al.*, 2003).

In conclusion, Lys63-linked polyubiquitination is found in a variety of key components in regulating NF-κB activity, which is essential for the activation of kinase activities and also can induce Lys48-linked polyubiquitination on IκB to activate NF-κB. Since the activation of target proteins by Lys63-linked polyubiquitination has also been observed in other signaling pathways (for example, Lys63-linked polyUb modifications on H2AX and H2A consequently lead to the E3 ligase activity of the BRCA1-BARD1 heterodimer), it is possible that Lys63-linked polyubiquitination has a broad range of involvement in activating enzymatic activities of its target proteins.

## 1.4 The Ubiquitin System in *Arabidopsis thaliana*

### 1.4.1 *Arabidopsis thaliana* as a Model Species

*Arabidopsis thaliana*, a small flowering plant belonging to the mustard (*Cruciferae* or *Brassicaceae*) family has already become the most-widely used model organism of plant sciences. It has a wide range of distribution across the world and a short reproductive cycle (Meinke *et al.*, 1998). The entire life cycle, from seed germination to maturation of first seeds, takes 5-6 weeks under optimal growth conditions. Other advantages for Arabidopsis as a model species include small size (mature plants reach 15 to 20 cm in height), self-pollinated

flower (crossed by applying pollen to the stigma) and a small diploid genome (Meinke *et al.*, 1998).

The sequencing of the entire genome of Arabidopsis was completed in 2000 (The Arabidopsis Genome Initiative, 2000). Since then, considerable efforts have been made to characterize the functions of the over 25,000 predicted genes and the 11,000 families of proteins they encode. The majority of gene families are similar to those of other eukaryotic species, and studies on these genes have been providing a new perspective and better understanding of diverse essential cellular functions (Bennetzen, 2001). For example, 70% of cancer genes have close orthologs in Arabidopsis, which implies a potential value in understanding molecular bases in human diseases (Jones *et al.*, 2008). Several hundred gene families are unique to the plant kingdom (The Arabidopsis Genome Initiative, 2000), and are of great value for studying cellular activities unique in plants such as photosynthesis.

The most critical methods and materials for genetic and molecular research have also been well-established for Arabidopsis as a model organism, such as protocols of chemical and insertional mutagenesis, plant transformation methods for introducing exogenous DNA and collections of mutants with various phenotypes (Meinke *et al.*, 1998). Plant transformation with T-DNA using *Agrobacterium tumefaciens* has become routine due to the development of whole-plant transformation procedures (Clough and Bent, 1998), which also has enabled the generation of thousands of transgenic lines with random T-DNA insertions covering almost the entire genome (Alonso *et al.*, 2003). The Arabidopsis Information Resource (TAIR) and Nottingham Arabidopsis Stock Centre (NASC) curate genetic and molecular biological information of Arabidopsis, and seed and DNA stocks are available from the Arabidopsis Biological Resource Center (ABRC) and NASC.

### 1.4.2 Characterization of the Ubiquitin System in Arabidopsis

As in other eukaryotes, the Ub system is also involved in a broad range of functions in plants.

Its components are highly conserved with other well-studied eukaryotic species (e.g. budding yeast and human). For example, Arabidopsis Ub proteins are also all encoded by fusion genes and require specific proteases to separate the Ub monomers from fusion polypeptides (Bachmair *et al.*, 2001). For ten of the 11 E2 consensus enzymes in yeast, at least one orthologous protein can be found in Arabidopsis (Bachmair *et al.*, 2001). All three classes of E3 ligases (RING, U-box and HECT) play diverse roles in plants (Smalle and Vierstra, 2004). Although most of the pioneering studies of Ub, such as polyUb chain topology and atypical Ub-Ub linkage, have been performed on yeast and human cells, it should not be surprising that some fundamental aspects of the Ub system are conserved in plants, considering the extensive conservation of the Ub system among different eukaryotes.

On the other hand, the plant Ub system has some unique features as well. Taking Arabidopsis as an example, more than 1400 genes have been found to encode UPS-related components (Vierstra, 2003), and the gene products were estimated to represent over 5% of the entire Arabidopsis proteome, which at least doubles the percentage of those in yeast, Drosophila, mice, and human (Semple *et al.*, 2003). Since it has been estimated that each week plants replace up to 50% of the total protein through a protein hydrolysis-synthesis cycle (Vierstra, 2003), UPS should have a significant role in such massive protein turnover. Over 1300 genes that are predicted to encode putative E3 components (Smalle and Vierstra, 2004) may give rise to greater diversity of substrates in plants than in other eukaryotes. Similarly, Arabidopsis possesses a large number of SCF E3 complexes. Its genome contains almost 700 F-box encoding genes, while there are merely 14 and 74 F-box genes in budding yeast and human, respectively (Smalle and Vierstra, 2004). These features of plant Ub system may be explained by various environmental conditions and stresses due to the sessile lifestyle, which requires UPS and perhaps other Ub-dependent machineries to function more actively. In addition, the Ub system may also play vital roles in many processes unique to plants including photosynthesis, plant hormone metabolism and response, plant development (Smalle and Vierstra, 2004; Vierstra, 2003).

### 1.4.3 Ubc13-Uev E2 Conjugating Enzyme in Arabidopsis

Homologs of both Ubc13 and Uev have been identified in *Arabidopsis thaliana* (Wen *et al.*, 2006; Wen *et al.*, 2008). There are two Arabidopsis *UBC13* genes named *AtUBC13A* and *AtUBC13B* (At abbreviates for *A. thaliana*), respectively (Wen et al, 2006). Yeast two-hybrid and protein pull-down assays showed that both AtUBC13 proteins could interact with yeast Mms2 or human Uev1. Furthermore, *AtUBC13*s could functionally complement the yeast *ubc13* null mutant for spontaneous mutagenesis and sensitivity to DNA-damaging agents. These data suggest that the AtUbc13 protein may function similarly to the yeast Ubc13 in the Lys63-linked polyubiquitination reaction.

In catalyzing Lys63-linked polyubiquitination, the Ubc13 protein requires a Uev, Four Arabidopsis genes orthologous to human Mms2 (Uev1) have been identified and named *UEV1A*, *UEV1B*, *UEV1C* and *UEV1D* (Wen et al, 2008). Based on sequence similarity, the four Arabidopsis *UEV1* genes can be grouped into two pairs, *UEV1A/UEV1B* and *UEV1C/UEV1D*, which likely arose from gene duplication. All four *AtUEV1* genes could complement the yeast *mms2* null mutant (Wen et al, 2008). Interestingly, in complementing the yeast *mms2 ubc13* double mutant together with *AtUBC13A*, *UEV1C* and *UEV1D* were more effective than *UEV1A* and *UEV1B*, suggesting possible functional differences between the two pairs of *AtUEV1* genes.

The four *AtUEV1* genes have different expression patterns, *UEV1D* expressed most strongly in germinating seeds and pollen (Wen et al, 2008). Two *UEV1D* null mutants created by T-DNA insertion mutagenesis were identified. Seeds of *Atuev1d* null plants germinated poorly in the presence of DNA-damaging agent compared to wild type seeds. In addition, pollen germination of *UEV1D* plants was also affected in the presence of DNA damage although the effect was more moderate compared to the effect on seed germination (Wen et al, 2008). These results demonstrate that the Ubc13-Uev1 complex functions in DNA-damage

response in plants. Possible functions in other processes of plants remain to be explored.

### 1.4.4 Significance of Studying E3 ligases in Arabidopsis

A current understanding about E3 ligases is that they are most responsible for determining the substrate specificity in the ubiquitination reaction. Since there are about 37 E2s and more than 1,300 genes encoding E3 components in Arabidopsis (Smalle and Vierstra, 2004), it is important to gain a better insight on protein ubiquitination by characterizing individual E3 families. Some E3s may participate in processes conserved among eukaryotic species, while others may play signalling or regulatory roles in processes more specific to plants. Considering the remarkable abundance of different SCF E3 complexes in plants compared to other organisms [700 F-box encoding genes in Arabidopsis, yet only 14 and 74 in yeast and human, respectively (Smalle and Vierstra, 2004)], the diversity of E3 ligases in plants implies a broad involvement in numerous aspects of plant growth. In the case of Lys63-linked polyubiquitination, the specific E2 enzyme Ubc13-Uev complex has been found to be conserved throughout eukaryotic organisms, yet to understand more specific mechanisms requires the functional illustration of those E3s that interact with AtUbc13-AtUev. Therefore, characterization of E3s in Arabidopsis will provide a clearer picture on how the Ub system regulates different aspects of plant physiology and development.

## 1.5 Functional Roles of Example E3 Ligases in Arabidopsis

### 1.5.1 Co-Chaperone AtCHIP

Arabidopsis protein AtCHIP was named after its animal close sequence ortholog CHIP (Yan *et al.*, 2003). CHIP was initially identified in mice. It binds to the C-terminus of heat shock protein cognate 70 (Hsc70), a member of heat-shock protein 70 (Hsp70) family (Ballinger *et al.*, 1999). Since then orthologs of CHIP have been found in *Homo sapiens*, *Drosophila*

*melanogaster*, and *Caenorhabditis elegans* (Patterson, 2002).

AtCHIP has the same domain architecture as its animal orthologs: three N-terminal tetratricopeptide repeats (TPRs) and a C-terminal U-box domain. TPRs in AtCHIP share at least 54% identity with animal CHIPs. The TPR domains mediate interactions between CHIP and Hsp70 and Hsp90 in animals (Connell *et al.*, 2001), and in Arabidopsis AtCHIP was also found to bind cytosolic Hsp70 (Lee *et al.*, 2009; Shen *et al.*, 2007a). The U-box domain of AtCHIP shares over 75% identity with that of animal CHIPs. Like the animal CHIPs, the U-box domain of AtCHIP is also capable of performing E3 ligase activity in catalyzing polyubiquitination on substrate proteins (Yan *et al.*, 2003).

The molecular chaperones Hsp70 and Hsp90 play important roles in response to protein misfolding, either through catalyzing substrate refolding or causing protein degradation through UPS (Wang *et al.*, 2004). In this protein quality control pathway, CHIP plays an important role through its association with chaperones. CHIP is considered to be responsible for targeting misfolded polypeptides into UPS for destruction, as it was found to catalyze polyubiquitination on a number of substrates of Hsp70 and Hsp90 (McDonough and Patterson, 2003). Eukaryotic cells usually have an increasing amount of misfolded proteins under stress conditions. In transgenic Arabidopsis plants, overexpression of *AtCHIP* was shown to lead to defects in low and high temperature tolerance (Yan *et al.*, 2003). Therefore, in Arabidopsis AtCHIP might have a similar role in protein quality control as animal CHIPs.

On the other hand, AtCHIP also has its unique roles in plants, *e.g.* plastid-destined precursor proteins that remain unfolded before being imported into plastids. Cytosolic Hsp70 remains associated with these precursor proteins to assist the process of transportation and possibly to regulate precursor level as well (Agne and Kessler, 2009). In association with Hsc70, AtCHIP has been demonstrated to regulate the level of chloroplast-destined precursor proteins in the cytosol by targeting precursors into UPS through polyUb modification (Lee *et al.*, 2009; Shen *et al.*, 2007a).

Interestingly, in animals CHIP has the capability to catalyze polyubiquitination via different

types of Ub-Ub linkages (Hatakeyama *et al.*, 2001; Jiang *et al.*, 2001). CHIP was demonstrated to associate with the Ubc13-Uev E2 complex, and X-ray crystallographic analyses have even revealed the interface of the mouse CHIP with the human Ubc13-Uev1a complex (Xu *et al.*, 2008; Zhang *et al.*, 2005). Therefore, CHIP can possibly catalyze Lys63-linked polyubiquitination in animals. It remains to be determined whether these nonconventional features of AtCHIP ligase activity are also conserved in plants, except for a report showing that AtCHIP monoubiquitinates an A subunit of protein phosphatase 2A (PP2A) (Luo *et al.*, 2006). In this case AtCHIP did not seem to cause degradation, as overexpressing of *AtCHIP* in Arabidopsis increased PP2A activity.

### 1.5.2 RGLG in Regulating Apical Dominance

To date, the only characterized E3 ligases that specifically catalyze Lys63-linked polyubiquitination in Arabidopsis are two RING finger proteins RGLG1 and RGLG2 (for RING domain Ligase 1 and 2, respectively) (Yin *et al.*, 2007). RGLG1 and RGLG2 are sequence homologs and their coding genes *RGLG1* (At3g01650) and *RGLG2* (At5g14420) belong to a putative five-member family (Stone *et al.*, 2005).

RGLG2, with a higher level than RGLG1 *in vivo*, was demonstrated by Yin *et al.* (2007) to interact with AtUbc13A (or Ubc35) which forms an E2 complex with AtUev1A to facilitate Lys63-linked polyUb chains. RGLG2 together with the AtUbc13A-AtUev1A complex failed to assemble polyUb chains from the Ub-K63R mutants which lack the Lys63 residues, and it did not show a substantial catalytic activity with another E2 UBC9 and wild type Ubs. Therefore, RGLG2 specifically catalyzes *in vitro* Lys63-linkage between Ub moieties instead of Lys48-linkage. The plants showed no observable defects by down-regulating either one of the two RGLG proteins. However, *rglg1 rglg2* double mutant plants lost apical dominance and had altered phyllotaxy. Both of these phenotypic characteristics are regulated by the plant hormone auxin, and indeed those mutant plants also showed altered auxin and cytokinin levels

and a decreased sensitivity to exogenous auxin as well. The RGLG ligase activity may be required for the regulation of directional flow of auxin, as in *rglg1 rglg2* double mutants, the abundance of certain auxin transport proteins was altered, and a mutation in the auxin transport regulator BIG led to synthetic lethality (Yin *et al.*, 2007). Therefore, the current understanding of RGLG E3 ligases implicates an involvement of Lys63-linked polyubiquitination in hormone regulation. However, many details concerning the substrates and regulatory pathways remain to be uncovered.

### 1.5.3 $SCF^{TIR1}$ and Auxin Signalling

Auxin is an essential plant hormone regulating plant growth in various environmental conditions and developmental processes. For instance, the predominant auxin indole-3-acetic acid (IAA) modulates expression of genes that lead to cell expansion and division (Mockaitis and Estelle, 2008). The increasing understanding of the intracellular auxin signalling pathway has revealed a key role for UPS in transducing the auxin signal to activate transcription of target genes (Mockaitis and Estelle, 2008). The core component in this signal transduction is a SCF E3 complex in which the F-box subunit is transport inhibitor response 1 (TIR1). The substrates of $SCF^{TIR1}$ consist of a family of transcriptional repressors called Aux/IAAs which inhibit the activity of a family of transcription factors known as auxin response factors (ARFs). Thus, once Aux/IAAs are polyubiquitinated by $SCF^{TIR1}$ the suppression on ARFs will be alleviated or removed via a UPS dependent substrate degradation, leading to the transcription of auxin responsive genes. The discovery that TIR1 functions as a novel auxin receptor has largely uncovered the details about the link between auxin signal perception and the downstream signaling pathway (Dharmasiri *et al.*, 2005; Kepinski and Leyser, 2005). Arabidopsis Aux/IAAs share a conserved degron sequence (domain II), which serves as a binding surface for the leucine-rich-repeat (LRR) domains of TIR1 (Tan *et al.*, 2007). However, the binding affinity between Aux/IAA and TIR1 is low in the absence of auxin.

Auxin fits into a hydrophobic cavity within TIR1, and provides an extra binding surface for Aux/IAA degrons (Tan *et al.*, 2007). Therefore, the binding of auxin within the TIR subunit is required for the interactions between $SCF^{TIR1}$ and its substrates.

The auxin induced $SCF^{TIR1}$-substrate interaction provides new insight into molecular mechanisms that integrate hormone response and ubiquitination. In addition, TIR1 has at least five close paralogs in Arabidopsis, namely, auxin signaling F-box protein 1 to 5 (AFB1-5) (Dharmasiri *et al.*, 2005). AFB1-3 showed functional redundancy with TIR1, as impairment of the *TIR1* gene or any one of the three *AFB* genes did not cause observable defects in plant growth, yet a combination of *TIR1* and *AFB1-3* mutations decreased auxin response (Dharmasiri *et al.*, 2005). It seems plausible that AFBs have the same functions in forming SCF E3 complexes and transducing the auxin signal as TIR1.

## 1.6 Objectives

Results from studies in mammals and yeast suggest that Lys63-linked polyubiquitination is a fundamental process of protein modification that plays a role in several diverse pathways. The identification and studies of the Ubc13 and Uev1 homologs in Arabidopsis indicates that the fundamental function of the Ubc13-Uev complex in catalyzing the Lys63-linked polyubiquitination is conserved throughout eukaryotic species. Lys63-linked polyubiquitination targets substrate proteins and modulates their activities and functions. Substrate specificity is likely conferred by E3 ubiquitin ligases in the Ubc13-mediated ubiquitination. Thus, identification and functional characterization of E3 ligases that interact with the Ubc13-Uev complex would provide means to further understand the biological functions of Ubc13-mediated ubiquitination.

The primary objective for this project is to identify the functions of E3 ligases that interact with the Ubc13-Uev complex. The specific aims of this project are as follow:

1. Initial survey of E3s and selection of 2-3 E3 genes (families) for further studies

2. Down-regulation of selected E3 genes
3. Phenotyping *Arabidopsis* lines with down-regulation of the selected E3s

Arabidopsis plants (lines) with the respective genes down-regulated will be analyzed for:

(1) Plant growth and morphology
(2) Response to some hormonal treatments
(3) Tolerance to some abiotic stress treatments

# 2 MATERIALS AND METHODS

## 2.1 Plant Materials and Growth Conditions

Plants used for this study were all *Arabidopsis thaliana* ecotype ‘‘Columbia’’. T-DNA insertion lines *Atchip-1* (SALK_059253c) and SALK_058353c were obtained from ABRC.

Arabidopsis plants were grown on soil (Sunshine Mix #4) in 10-cm square pots or on half-strength (w/v) Murashige and Skoog basal salt (1/2 MS, Sigma-Aldrich M5524, 4.3 g/L) medium (with 0.7% (w/v) agar, 1% (w/v) sucrose, and pH 5.8) at 20 ℃ and with a 16/8-hour-day/night photoperiod. Plants grown in pots were placed on a shelf, exposed to florescent light with daylight intensity of 80 μmol/$m^2$/sec. Plants grown on 1/2 MS agar medium were under 60 μmol/$m^2$/sec in a tissue culture chamber. Seeds to be plated onto 1/2 MS agar medium were surface-sterilized with 20% bleach and 0.5% Triton X-100 three times within 20 min, followed by three rinses in sterile water. After sterilization, seeds were stratified in sterile water at 4 ℃ in the dark for three days to synchronize germination. Three days later, the seeds were suspended in 0.1% agarose (w/v, sterile) and sown on 1/2 MS agar medium (containing 1% sucrose), with or without one of specific ingredients as indicated.

## 2.2 Sequence Analysis and Domain Prediction

Protein sequence alignment was performed in ClustalX program, with Gonnet250 protein matrix. As described by Stone *et al.*, (2005), in pairwise alignment the gap opening and gap extend parameters were set at 10 and 0.1, respectively; in multiple alignment the gap opening and gap extend parameters were 10 and 0.2, respectively.

Potential functional domains within each protein were analyzed in PROSITE (http://prosite.expasy.org) and SMART (http://smart.embl-heidelberg.de) databases with full-length protein sequences.

To search for closely related proteins of E3 ligases, the full-length protein sequences of

AtCHIP and At1g74370 (E3-A1) were analyzed by BLASTP program (http://www.arabidopsis.org/Blast). T-DNA insertion lines and insertion site of T-DNA sequences were obtained from TAIR web site (http://www.arabidopsis.org).

### 2.3 Plant Genomic DNA Extraction

Genomic DNA was extracted as described by (Edwards *et al.*, 1991). A piece of Arabidopsis plant leaf tissue (50 mg) was pinched out into a 1.5 mL Eppendorf tube. Then, 400 µl of extraction buffer (200 mM tris-HCl, pH7.5; 250 mM NaCl; 25 mM EDTA; 0.5% SDS) was added and the tissue was ground with a disposable pestle against the tube wall. The mixture was left at room temperature until all samples were extracted. The tubes were centrifuged at 12,000 g for 5 min and 350 µL of supernatant was transferred to a new Eppendorf tube. This supernatant was mixed with 350 µl isopropanol and left at room temperature for at least 20 min, followed by centrifugation at 12,000 g for 5 min. The supernatant was discarded and the pellet dried for about 20 min at room temperature. The pellet was dissolved in 100 µL TE buffer (100 mM Tris-HCl with pH 7.5 and 10 mM EDTA, pH 8.0).

### 2.4 Polymerase Chain Reaction and DNA Gel Electrophoresis

In a 20 µL polymerase chain reaction (PCR), two microliters of the genomic DNA sample extracted from plant tissues or the cDNA sample reverse transcribed from the mRNA was used as the template in a 96-well plate. All the primers used in this study are listed in Table 2.1. The PCR thermal cycle was: denaturing at 94 ℃ for 1 min, annealing at 55 ℃ for 1 min, and primer extension at 72 ℃ for 1 min per kilobase of sequence. Usually 28 to 30 cycles were performed for amplification of genomic DNA or cDNA sequences of E3s.

PCR products were analyzed by agarose gel electrophoresis. An 1% agarose gel was made by dissolving a corresponding amount of agarose in 1 × TAE buffer (40 mM Tris-acetate,

2 mM $Na_2EDTA$, pH 8.0). Ethidium bromide was added into the gel to the final concentration of 0.5 μg/mL. Electrophoresis was run in 1 × TAE buffer at 100 V until nucleic acid samples migrated for 15 - 30 minutes depending on the fragment size. DNA samples in the gel were visualized under UV light using a BioDoc gel imager.

**Table 2.1** Oligonucleotide primers for PCRs. The start and stop codons are underlined.

| Name | Sequence | Used for |
|---|---|---|
| **LB1** | 5'-GCGTGGACCGCTTGCTGCAACT-3' | Left border of T-DNA sequence |
| **HW599** | 5'-CAGTGTCGACAATGGTTACAGGCGTGGCTTC-3' | 5' end of full-length *AtCHIP* genomic DNA or cDNA |
| **HW560** | 5'-CAGTGCGGCCGCTCAACAACCCATCTTGTAAGC-3' | 3' end of full-length *AtCHIP* genomic DNA or cDNA |
| **HW601** | 5'-CAGTGTCGACAATGTGGAATTTAGCTTCAAAAT-3' | 5' end of full-length *E3-A1* cDNA |
| **HW602** | 5'-CAGTGCGGCCGCTCAGGTTGCAATCTCTCTG-3' | 3' end of full-length *E3-A1* cDNA |
| **HW621** | 5'-ACTGGGATCCAGAGTATGGGGTTAAAGAAGTC-3' | 5' end of *E3-A2* cDNA fragment |
| **HW622** | 5'-ACTGGTCGACGAGACATGCTACACCTC-3' | 3' end of *E3-A2* cDNA fragment |
| **HW797** | 5'-CAGTGTCGACAATGGCCAACAGTAATTTGCC-3' | 5' end of full-length *AtUBC13A* cDNA |
| **HW798** | 5'-CAGTGCGGCCGCTCATGCGCCGCTTGCATA-3' | 3' end of full-length *AtUBC13A* cDNA |

## 2.5 Total RNA Isolation and RT-PCR

To perform a reverse transcriptase mediated polymerase chain reaction (RT-PCR) analysis, total RNA was isolated from leaf or floral tissue with TRIzol reagent (Invitrogen). Arabidopsis tissue was added into 500 μL of TRIzol reagent (less than 100 mg tissue per mL TRIzol) in a 1.5 mL Eppendorf tube. The tissue was ground with a disposable pestle against the tube wall. Another 500 μL of TRIzol reagent was added to the homogenized tissue, and the mixture in the tube was left on ice until all samples were extracted. Then 200 μL of chloroform was added to

each sample, and all samples were shaken vigorously by hand for 15 sec. The samples were incubated at room temperature for 10 min before being centrifuged at 12,000 g for 10 min at 4 ℃. The aqueous phase on the top (300 μL) was transferred into a fresh tube, and 300 μL isopropanol was added. The sample was incubated at 4 ℃ for at least 10 min and centrifuged at 12,000 g for 10 min at 4 ℃. The supernatant was discarded, and the pellet was washed with 1 mL 70% ethanol. The RNA sample was centrifuged again at 12,000 g for 5 min at 4 ℃. The supernatant was discarded, and the pellet was air dried for 5-10 min. The isolated RNA samples were stored at -80 ℃. RNA concentration was determined by a spectrophotometer (Pharmacia Biotech, Ultrospec 3000).

Reverse transcription was performed using a ThermoScript RT-PCR system (Invitrogen) following the manufacturer's instructions. For each cDNA synthesis reaction, 1 μg of total RNA was used. After reverse transcription the cDNA reaction mixture was diluted by ten times using diethylpyrocarbonate (DEPC) treated water, and 2 μL was used for PCR amplification. A primer pair specific to the particular full-length cDNA was used in the reaction, and a primer pair specific to *AtUBC13A* cDNA was also used as a control. See Table 2.1 for primers used for RT-PCR.

## 2.6 Plant Transformation

With the help of Dr. Xianzong Shi in our laboratory, RNA interference (RNAi) constructs were prepared for down-regulating *E3-A1* (At1g74370) or *E3-A2* (at1g69330) and plant transformation was performed. For preparing the RNAi constructs, sense and antisense fragments of *E3-A1* cDNA (covering the nucleotide sequence of 213-619 from the translational start ATG) or *E3-A2* (covering the nucleotide sequence of 168-597 from ATG) cDNA were cloned into the plant expression vector pWS855 which was modified from pBI121 (Clontec). Each of the RNAi constructs was fused to the native promoter of the target gene so that the expression profile of the RNAi transcript matched that of the wild type gene. The constructs

were then introduced into the *Agrobacterium tumefaciens* strain GV3101 (Vanlareb *et al.*, 1974) and the *Agrobacterium* transformants were used to infiltrate wild type Arabidopsis plants as described (Wang *et al.*, 2000). The seeds (T1) were harvested from initially infiltrated plants. After surface-sterilization, the T1 seeds were plated on 1/2 MS agar medium containing 50 mg/L kanamycin and 300 mg/L timentin (referred as ½ MSTK). Transformants were able to grow on the plates due to their resistance to kanamycin while non-transformants would die after germination. The transformants were transferred into soil in pots and grown on the shelf.

## 2.7 Plant Phenotypic Surveys

### 2.7.1 Parameter Measurements

To perform phenotypic surveys on Arabidopsis plants, surface-sterilized seeds were germinated on ½ MS agar medium in Petri plates, and five repeats of plates were used for each treatment. For each plate, half was used for control (reference) plants and half for test plants. The growth-related values such as primary root length, fresh weight and dry weight of mutant plants were expressed relative to the values of wild type plants grown in the same plate, so that the impact of variation among plates could be minimized.

To assess growth, the seedlings were grown on 1/2 MS agar medium in 150 mm Petri dishes, which were placed vertically. For each plate, half was used for control plants and the other half test plants. For each half, 12 seeds were planted in a straight row (with equal distance between two neighboring seeds). Several growth parameters such as primary root length, fresh weight and dry weight were measured. Seedlings were also grown on 1/2 MS agar medium in 100 mm Petri dishes. For each plate, half was for the control seedlings and the other half for the test seedlings. For each half, 16 seeds were planted. Several phenotypic parameters such as seed germination rate, cotyledon green rate, fresh weight, dry weight and survival rate were measured.

To determine primary root length, photographs of each plate were taken with a digital camera. A ruler was placed next to the plate so that both plate and ruler would be included in the photograph. The photographs were all analyzed by ImageJ, and the root lengths of individual seedlings could be determined using the ruler as the reference. The germination rate was determined by counting seeds with the emerging radical longer than the length of the seed. The cotyledon greening rate was determined by counting the number of seedlings with green cotyledons. The survival rate of seedlings after treatments was calculated from seedlings with the centers of shoots remaining green, while the shoot centers of non-surviving seedlings turned white or pale. To obtain weight measurements, Petri dishes were opened and the shoot part of each seedling was cut off (to avoid variation due to agarose being carried by the roots) and seedlings for the same type from one plate were weighed together on plastic weighing dishes. The average weight of individual seedlings (shoot portion) for each plate could be calculated. To obtain dry weight, the plant tissues were left in the weighing dishes to be air dried for one week, before being weighed.

The statistical significance of the data was determined by Student's *t*-test, with two-tailed distribution, two-sample assuming equal variance.

### 2.7.2 Hormonal Treatments and Osmotic Stress Tolerance

To determine the response of Arabidopsis plants to hormones and osmotic stress, seeds were plated to germinate and further grow on ½ MS agar medium (containing 1% sucrose) supplemented with a test ingredient. Following concentrations of ingredients were used: 5% (w/v) sucrose (total concentration in the medium), 150 mM NaCl, 0.10 μM naphthaleneacetic acid (NAA), 2.5 μM kinetin (KN), 25 μM methyl jasmonate (MeJA), 50 μM salicylic acid (SA) or 0.75 μM abscisic acid (ABA). These concentrations were based on tests that were done previously in Dr. Wang's laboratory to assess conditions for various assays. Absolute and relative primary root length, fresh weight and dry weight were measured on vertical plates, as

described above. Germination and cotyledon greening rates were measured on horizontal plates.

### 2.7.3 Seed Longevity

Seed longevity assay was performed as described (Sugliani *et al.*, 2009) to determine the deterioration of seed viability of mutant seeds compared to wild type. High temperature (37˚C) and high humidity conditions were used to accelerate seed deterioration. Mutant and wild type seeds harvested from plants grown under identical conditions were incubated at 37˚C. The high humidity condition was created by placing seeds around an open bottle containing saturated KCl solution inside a sealed container (which maintains about 83% relative humidity at 37˚C). After seeds being treated for particular days, they were taken out and air dried for three days. Seeds were then plated on ½ MS agar medium with or without 0.75 μM ABA in 100 mm Petri dishes. Seed germination and cotyledon greening were analyzed.

### 2.7.4 Thermal Tolerance

Arabidopsis seeds were plated on ½ MS agar medium in 100 mm Petri dishes and seedlings were grown under standard condition. Ten-day old seedlings were treated with elevated temperatures by incubating in metal trays inside an incubator, with aluminum foils placed between the surface of Petri dishes and the metal plates to facilitate efficient and even heat transfer. For basal thermal tolerance, plants were incubated at 42˚C for the specified period of time. For acquired thermal tolerance, plants were first incubated at 37 ˚C for 90 min and then placed under normal conditions for 2 hours, followed by incubation at 45˚C for 2-8 hours. After high temperature treatments, seedlings were grown under normal conditions for seven days before measurements were taken on survival rate, fresh weight and dry weight.

### 2.7.5 High-intensity Light Treatment

To treat plants growing on soil with high-intensity light, Arabidopsis seeds were germinated under normal conditions (with light intensity at 90 μmol/$m^2$/sec). Starting from the seventh day after seed germination, light intensity was increased to 170 μmol/$m^2$/sec by adding light panels and lowering the light source above the pots. The morphology of mutant and wild type plants were observed during plant growth under increased light intensity. To determine the growth of seedlings on plates, seeds were germinated and seedlings grown vertically in 150 mm Petri dishes under increased light-intensity.

### 2.7.6 Oxidative Stress

To determine the tolerance to oxidative stress, 0, 0.05, 0.10 or 0.20 μM Paraquat (*N*,*N*′-dimethyl-4,4′-bipyridinium dichloride, also called methyl viologen) was included in ½ MS agar medium. Arabidopsis seeds were grown on ½ MS plates in 150 mm Petri dishes. Plates were put vertically and exposed under either normal (60 μmol/$m^2$/sec) or high-intensity light (150 μmol/$m^2$/sec) conditions. On the 11$^{th}$ day after seed plating, primary root length was measured.

### 2.7.7 DNA Damage Tolerance

DNA-damage tolerance of Arabidopsis plants was determined using the DNA-damaging agent MMS (methylmethane sulfonate). Arabidopsis seeds were grown on ½ MS plates containing 0, 25, 50 or 75 ppm MMS in 150 mm Petri dishes. The plates were placed vertically for plant growth. Primary root length was measured on the 11$^{th}$ day after seed plating.

# 3 RESULTS

## 3.1 Functional Characterization of AtCHIP

*AtCHIP* (At3g07370) was identified as an E3 ligase gene involved in protein degradation and its over-expression has a clear phenotype (Yan *et al.*, 2003). Interestingly a yeast two-hybrid screen using AtUbc13A as the bait identified AtCHIP protein and the interaction between AtUbc13A and AtCHIP was further confirmed by the yeast two-hybrid analysis and protein pull-down (Appendices). These observations suggest that AtCHIP may be a potential E3 ligase associated with Ubc13 in catalyzing Lys63-linked polyubiquitination. However, there is no report regarding the effect of its down-regulation in plants. Thus, one focus of my thesis is to obtain *AtCHIP* T-DNA knockout mutant and to explore the function of *AtCHIP* based on whether the mutant has any phenotype.

### 3.1.1 AtCHIP Protein Sequence Analysis

Based on information obtained from PROSITE (http://prosite.expasy.org) and SMART (http://smart.embl-heidelberg.de) databases, the AtCHIP protein has a three-motif TPR domain near the N-terminus and a U-box domain near the C-terminus (Figure 3.1A).

Close paralogous genes can often have redundant functions. In order to search for potential paralogs of AtCHIP in the Arabidopsis proteome, the full-length protein sequence of AtCHIP was used as a query in the BLASTP program to search the TAIR 10 protein database (http://www.arabidopsis.org/Blast). However, this sequence analysis did not reveal any closely related proteins. According to the BLAST result, the most related sequence (At2g42810) showed 31% identity in a region of 132 amino acid residues when compared with AtCHIP (Figure 3.1). And alignment of the full-length sequences of AtCHIP and At2g42810 by EMBOSS Needle program (http://www.ebi.ac.uk/Tools/psa/emboss_needle) showed only 9.5% sequence identity. Therefore, AtCHIP seems to be a distinct protein in Arabidopsis.

Indeed, among the 64 putative Arabidopsis U-box containing proteins identified so far, only AtCHIP has a TPR domain (Wiborg *et al.*, 2008). Bioinformatics studies on TPR proteins in Arabidopsis did not reveal any candidates closely related to AtCHIP, and in the phylogenetic analysis no other TPR proteins were found to contain a U-box domain (Prasad *et al.*, 2010).

**A**

**B**

```
>AT2G42810.1 | Symbols: PAPP5, PP5 | protein phosphatase 5.2 |
           chr2:17812336-17815896 REVERSE LENGTH=484 Length = 484

 Score = 72.0 bits (175), Expect = 4e-13,   Method:
Composition-based stats.
 Identities = 39/123 (31%), Positives = 61/123 (49%)

Query: 10  AERLKEDGNNCFKKERFGAAIDAYTEAIALSPNVPAYWTNRALCHMKRKDWTKVEEDCRK 69
           AE  K   N  FK  ++ +AID YT+AI L+ N   YW NRA  H K +++    +D  K
Sbjct: 13  AEEFKSQANEAFKGHKYSSAIDLYTKAIELNSNNAVYWANRAFAHTKLEEYGSAIQDASK 72

Query: 70  AIQLVHNSVKAHYMLGLALLQKKEFTNGVKELQRALDLGRCSNPTGYMVEEIWEELSKAK 129
           AI++     K +Y  G A L   +F + +K+ Q+   L          ++E  + + K K
Sbjct: 73  AIEVDSRYSKGYYRRGAAYLAMGKFKDALKDFQQVKRLSPNDPDATRKLKECEKAVMKLK 132

Query: 130 YME 132
           + E
Sbjct: 133 FEE 135
```

**Figure 3.1** Domain information and sequence analysis of the AtCHIP protein. (**A**) Domain architecture of AtCHIP protein. (**B**) Sequence identity and alignment between AtCHIP (Query) and At2g42810 (Sbjct). The result was obtained from http://www.arabidopsis.org/Blast using BLASTP program with AtCHIP as the query sequence to search TAIR10 protein database. According to the BLAST result At2g24810 (protein phosphatase 5) showed the highest degree of similarity with AtCHIP in Arabidopsis.

### 3.1.2 Confirmation of T-DNA Insertion of *Atchip-1* Mutant

Since sequence analysis did not reveal any closely related paralogs in the Arabidopsis genome, it was reasoned that there is less of a chance that the function of AtCHIP could be performed by other related proteins, thus making it a good candidate for functional studies by down-regulation. Accordingly, a T-DNA insertional mutagenesis line (SALK_059253c) of *AtCHIP* was obtained from ABRC. This mutant line is named *Atchip-1* for the convenience of illustration. The T-DNA insertion was shown by ABRC to interrupt exon 6 and before the U-box coding region of the gene. Therefore, the insertion is expected to abolish the E3 ligase activity of AtCHIP in *Atchip-1*. The homozygosity of the mutant line was confirmed by genomic PCR. As shown in Figure 3.2A, a primer (LB1) specific to left-border region of T-DNA paired with a primer specific for the gene (HW599) would identify the T-DNA insertion in the genome. While using a pair of primers (HW599 and HW560) specific to the target gene and spanning the T-DNA insertion site would identify the wild type allele. Therefore, presence of the T-DNA band and absence of genomic DNA band in agarose gel electrophoresis should indicate that the plant is homozygous for the T-DNA insertion (excluding any experimental error). Genomic PCR showed that all plants from the line were homozygous in terms of T-DNA insertion (Figure 3.2B). Subsequently, total RNA was isolated from the *Atchip-1* mutant plants and analyzed by RT-PCR. No transcript of *AtCHIP* was detected (Figure 3.2C).

Since the *Atchip-1* line was confirmed to be homozygous and the insertion was shown to efficiently interrupt *AtCHIP* gene transcription, this line was used for further studies to identify possible effects from the down-regulation of *AtCHIP*.

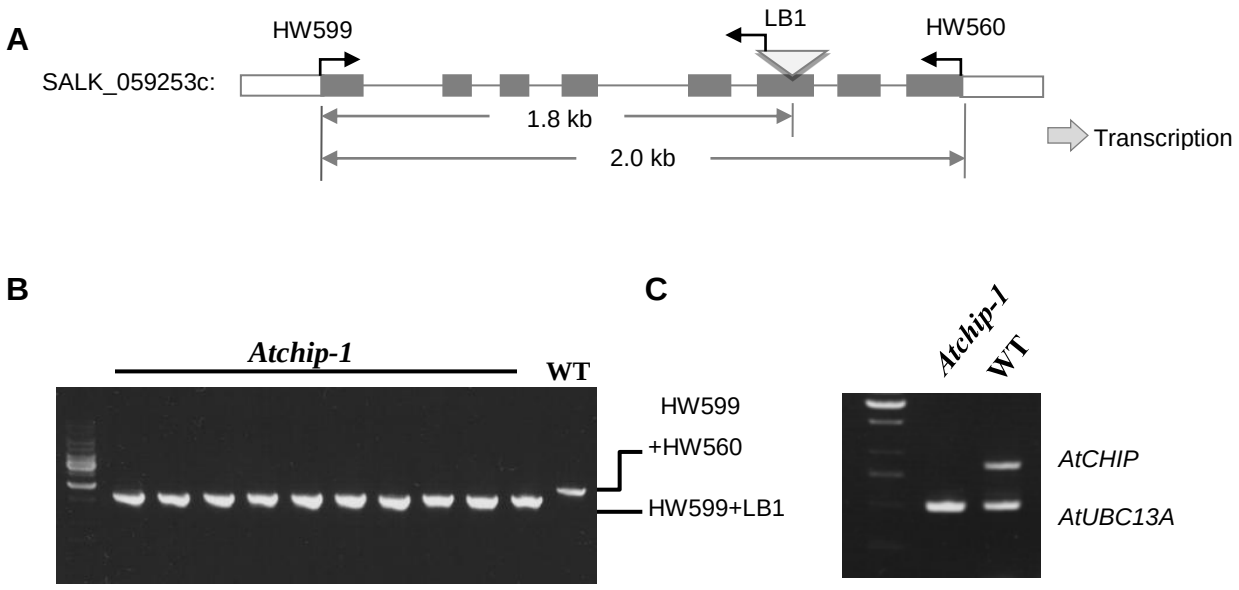


**Figure 3.2** Insertion site and gene expression analysis of an *AtCHIP* T-DNA mutant *Atchip-1*. **(A)** Genomic structure showing T-DNA insertion site of *Atchip-1* mutant. Filled boxes represent exons, while lines in between represent introns. T-DNA is inserted in the sixth exon. LB1: T-DNA left border primer; HW599, 5' gene specific primer; HW560: 3' gene specific primer. **(B)** Genomic DNA PCR result. The WT fragment was amplified by using primers HW599 and HW560, and the T-DNA fragment was amplified by primers HW599 and LB1. **(C)** RT-PCR confirmed the complete interruption of *AtCHIP* transcription in *Atchip-1* mutant line. *AtUBC13A* cDNA was used as a reference. The primer pair for *AtCHIP* cDNA is HW599 and HW560, and for *AtUBC13A* is HW797 and HW798. From both wild type and *Atchip-1* mutant plants, *AtUBC13A* cDNA template was amplified, while *AtCHIP* cDNA template was amplified only from wild type plant. The wild type line was segregated from a T-DNA line SALK_112098 and used as the control.

### 3.1.3 Phenotypic Characterization of *Atchip-1* Mutant

In order to determine the possible functions of candidate genes in plants, a common approach is to use a knockout or knockdown mutant, and observe whether there is any phenotypic alteration associated with the mutant. There was no apparent morphological difference between *Atchip-1* and wild type plants. Still, AtCHIP may play a more prominent role under a specific condition. A series of conditions were thus used to determine whether the mutant has a phenotype.

#### 3.1.3.1 Hormonal Treatments and Osmotic Stress Tolerance

Since plant hormones play crucial roles in plant growth and development as well as the adaptation to environmental changes, initially the *Atchip-1* mutant plants were tested for their response to hormonal and sucrose treatments. Seeds were germinated and seedlings grown on 1/2 MS agar medium (containing 1% sucrose) supplemented with one of the following ingredients: high sucrose (5% total concentration), 0.10 μM naphthaleneacetic acid (NAA, a synthetic auxin), 2.5 μM kinetin (KN, one of the cytokinins), 25 μM methyl jasmonate (MeJA), 50 μM salicylic acid (SA) or 0.75 μM abscisic acid (ABA). These concentrations were based on the tests that were previously done in Dr. Wang's laboratory, to ensure the significant effects on the growth of wild type plants (for instance 50% difference in root length compared with plain ½ MS agar medium). The seedlings were grown in Petri plates. There was some variation in plant growth among different plates. Thus, control plants (wild type, segregated from a T-DNA line SALK_112098) were grown side-by-side with the mutant plants in the same plate (half for control plants and half for mutant plants). Several phenotypic parameters such as primary root length, fresh weight and dry weight were measured. The values of *Atchip-1* plants were expressed relatively to the values of the wild type plants grown in the same plate, so that the impact of variation among plates could be minimized.

As shown in Figure 3.3 and Figure 3.4, there was a difference between the *Atchip-1* mutant and wild type plants in the presence of 0.75 μM ABA by *t*-test ($P < 0.01$), whereas no difference was observed for any other treatments. Relative primary root length, relative fresh and dry weight data (compared with wild type plants) all showed a decrease for *Atchip-1* mutant compared to the control in the presence of 0.75 μM ABA. To confirm this observation, the ABA treatment was repeated using the same seed lots. It was observed that the *Atchip-1* mutant plants were slower to germinate and in cotyledon greening (Figure 3.5). Since ABA treatment can delay seedling growth and development (see Figure 3.4), these data indicate over-sensitivity of mutant plants to ABA.

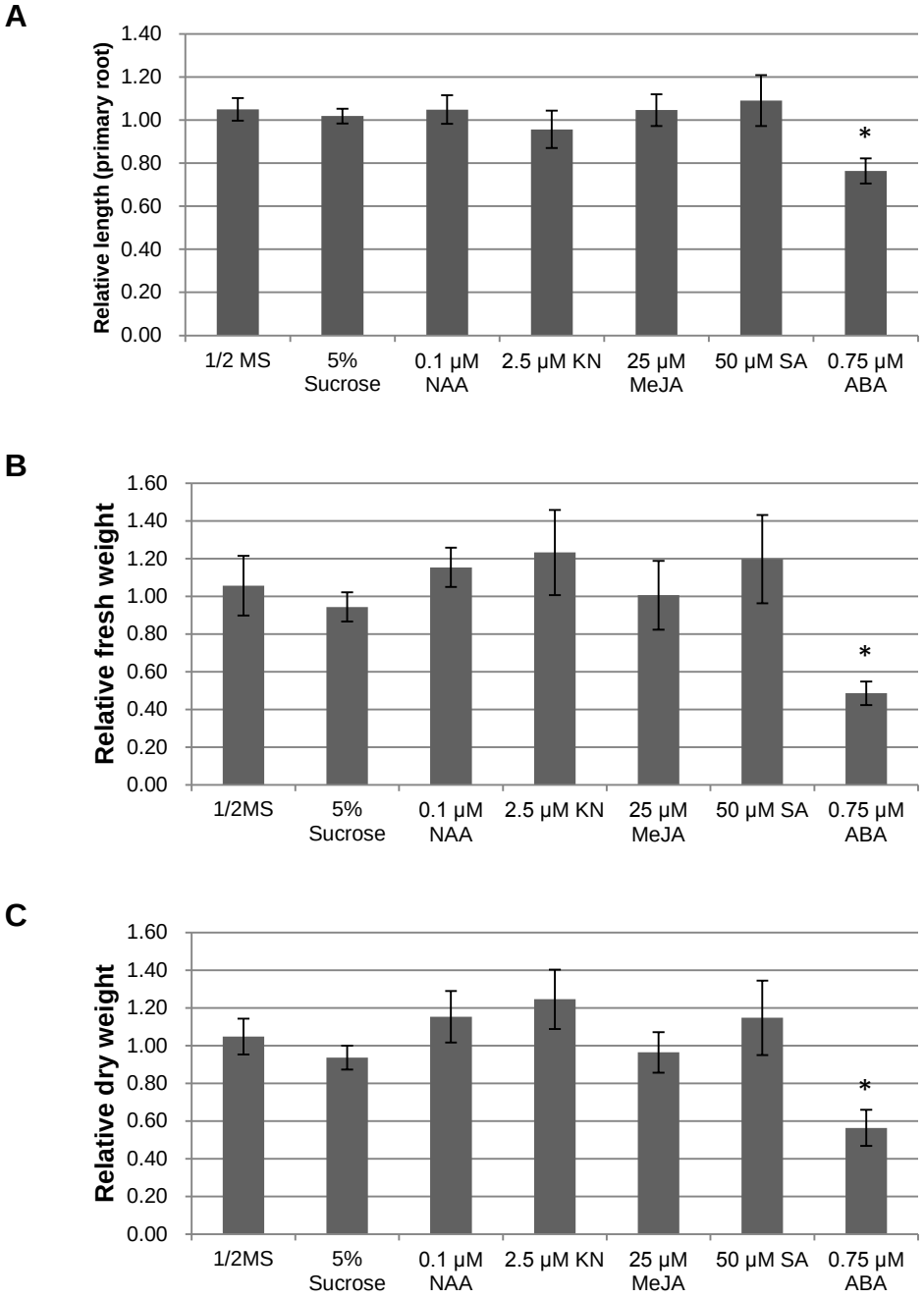


**Figure 3.3** Phenotypic survey of *Atchip-1* mutant plants in response to hormonal and sucrose treatments. The average values of the *Atchip-1* plants were expressed relative to those of wild type plants being assigned the value of one. **(A)** Relative primary root length of 11-day old *Atchip-1* plants (to wild type, 11-day old plants). After plates were photographed, primary root lengths were measured using the software ImageJ. **(B)** Relative fresh weight of 15-day old plants. **(C)** Relative dry weight of 15-day old plants. Seedlings from plates were allowed to

air-dry for three days and then were weighed. The data for each treatment represents the average of five plates and on each plate 12 mutants and 12 control plants were measured. Error bars represent standard deviations. * indicates $P < 0.01$ by *t*-test.

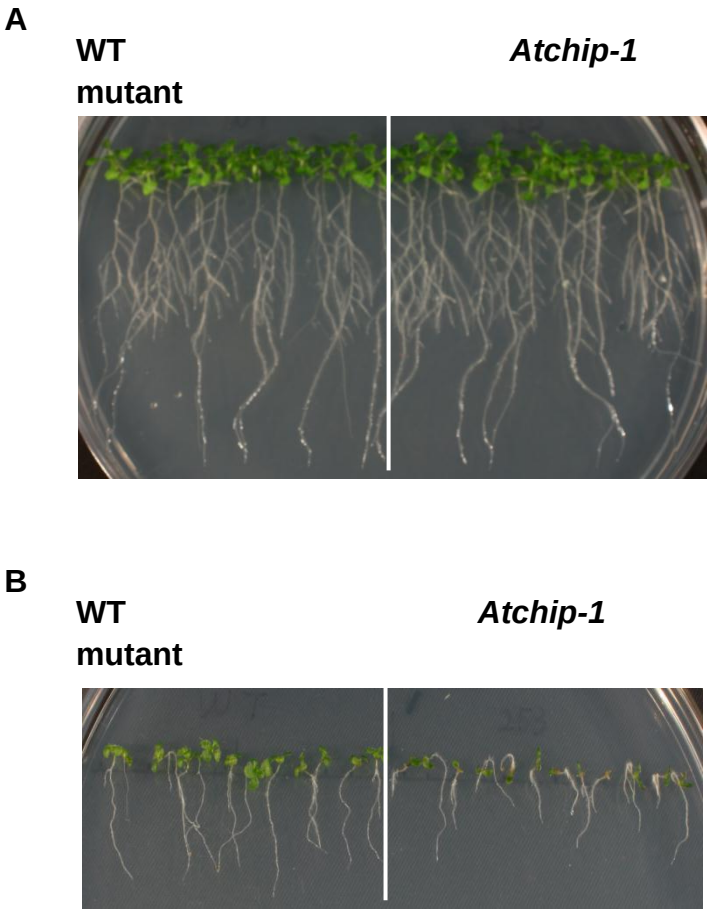


**Figure 3.4** Root phenotype of *Atchip-1* mutant plants. **(A)** Wild type (left) and *Atchip-1* mutant (right) plants growing on ½ MS agar medium (containing 1% sucrose). **(B)** Wild type (left) and *Atchip-1* mutant (right) plants growing in the presence of 0.75 μM ABA. All plants were 15-day old.

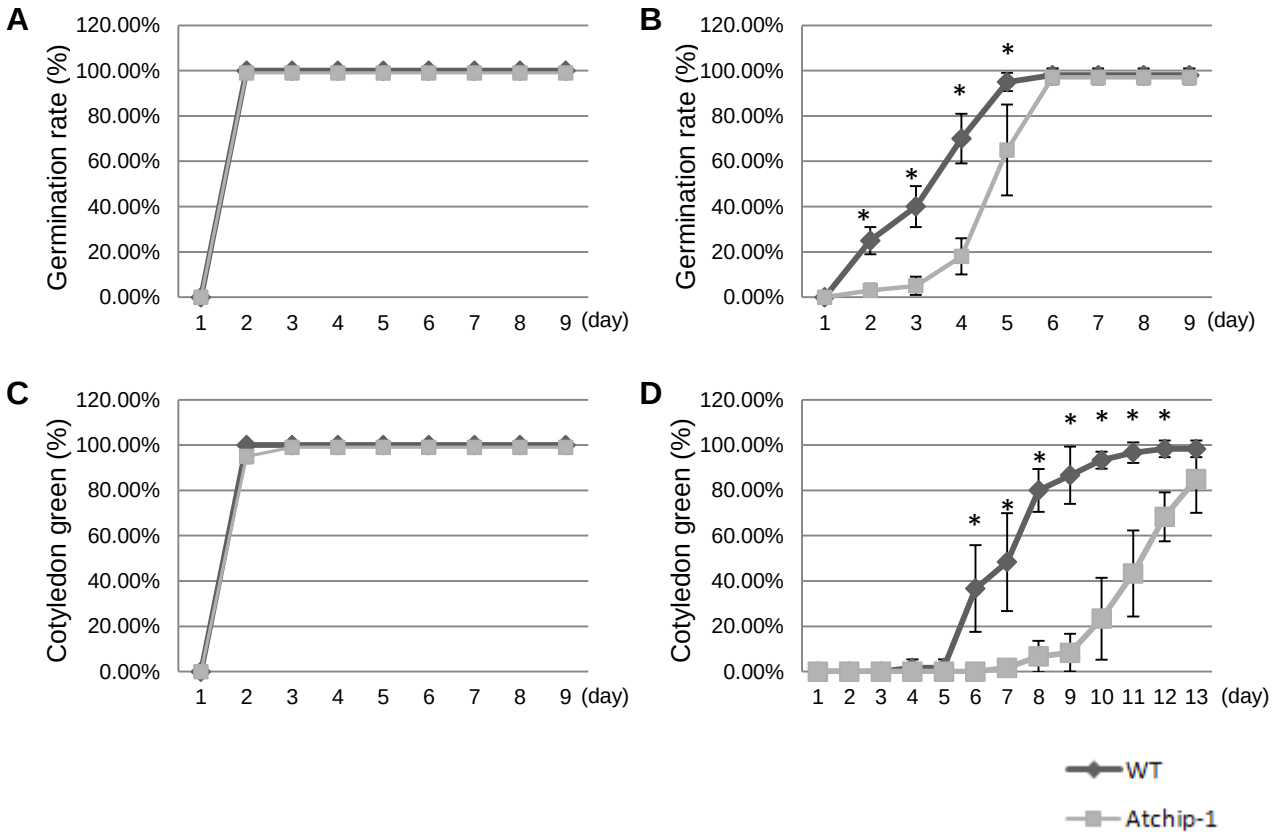


**Figure 3.5** Analysis of seed germination and cotyledon greening. **(A, B)** Average of germination rate (%) of *Atchip-1* and wild type plants on ½ MS agar medium **(A)** and on ½ MS agar medium containing 0.75 μM ABA **(B)** between day 1 and day 9 after seeds were plated. **(C, D)** Average of cotyledon green rate (%) of *Atchip-1* and wild type plants on ½ MS agar medium **(C)** and on ½ MS agar medium containing 0.75 μM ABA **(D)** between day 1 and day 14 after plating seeds. The data for each treatment represents the average of five plates and on each plate 16 mutants and 16 control plants were measured. Error bars represent standard deviations. * indicates $P < 0.01$ by *t*-test.

The above results were obtained using one pair of seed lots (wild type and *Atchip-1* seeds were collected at similar times). To exclude the possibility that the difference in ABA sensitivity might be due to minor difference in seed quality and viability, the same mutant and wild type lines were grown side by side in the same tray (to keep the conditions as identical as possible). Seeds were subsequently harvested at the same time and in the same way. Then these harvested seeds (mutant seed lots with corresponding control seed lots) were used in a repeat of ABA treatment. Surprisingly, in this new round of ABA experiment the *Atchip-1* mutant did not show an increase in ABA sensitivity compared to wild type plants (Figure 3.6).

Since the results from the newly collected seed lots did not show the difference, it was hypothesized that the decrease observed with the earlier seed lots might be due to a difference in seed quality between the mutant and wild type plants. Considering that the seeds of mutant and wild type lines used in the initial experiments were stored for a similar length of time, there are two possibilities concerning seed quality: the *AtCHIP* null mutation might accelerate seed deterioration during storage, or parental plants set seed under slightly different environmental conditions.

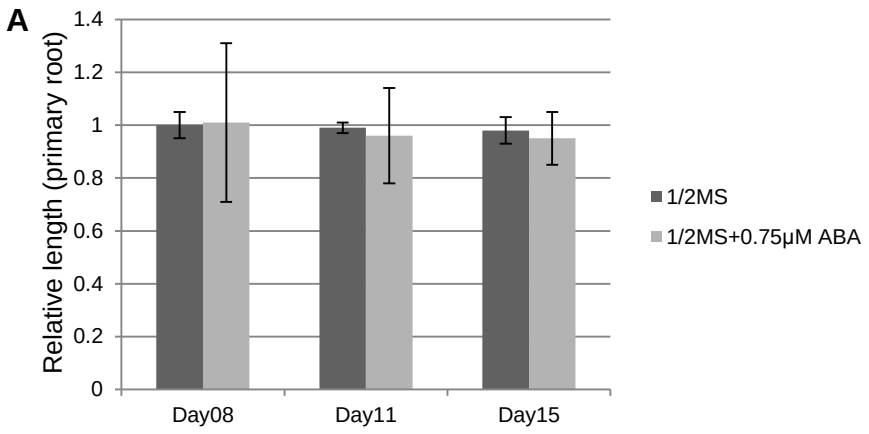
A
Relative length (primary root)
1.4
1.2
1
0.8
0.6
0.4
0.2
0
Day08
Day11
Day15
1/2MS
1/2MS+0.75μM ABA

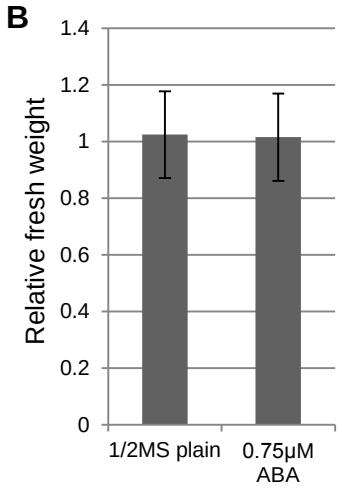
B
Relative fresh weight
1.4
1.2
1
0.8
0.6
0.4
0.2
0
1/2MS plain
0.75μM ABA

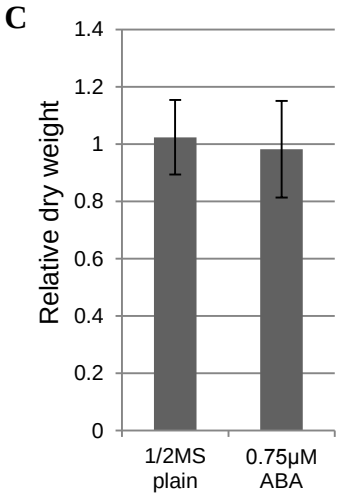
C
Relative dry weight
1.4
1.2
1
0.8
0.6
0.4
0.2
0
1/2MS plain
0.75μM ABA

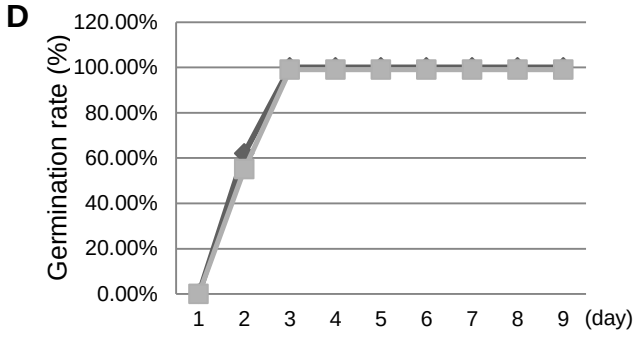
D
Germination rate (%)
120.00%
100.00%
80.00%
60.00%
40.00%
20.00%
0.00%
1 2 3 4 5 6 7 8 9 (day)

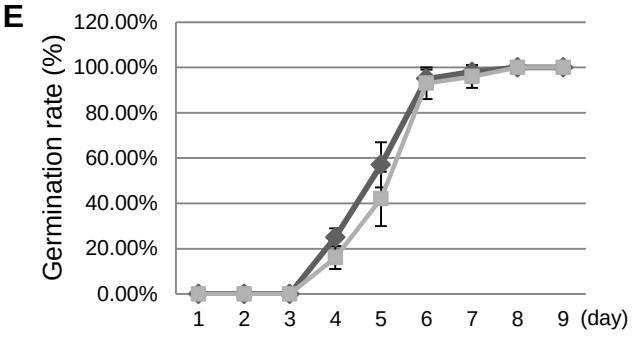
E
Germination rate (%)
120.00%
100.00%
80.00%
60.00%
40.00%
20.00%
0.00%
1 2 3 4 5 6 7 8 9 (day)

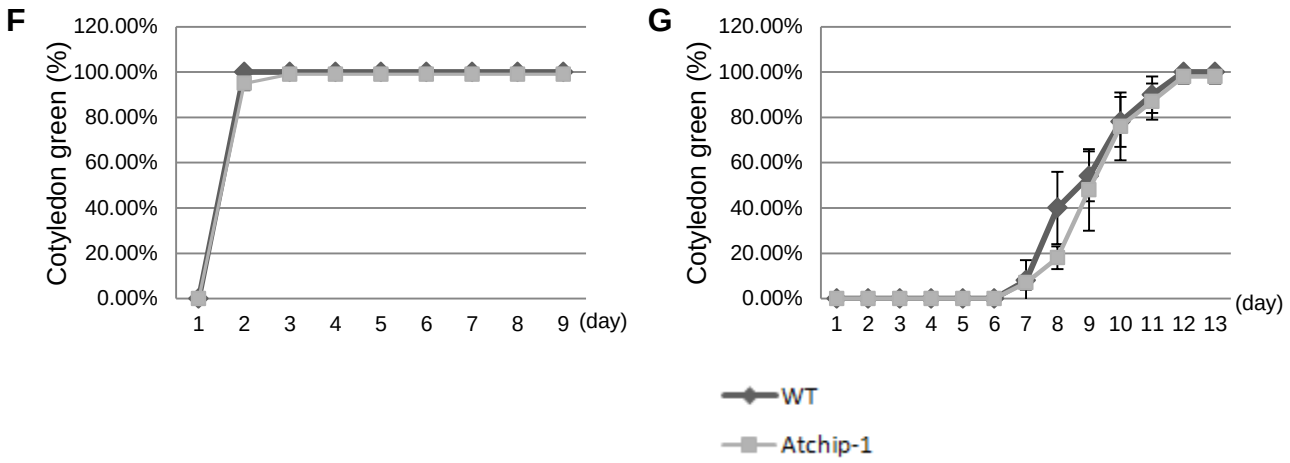


**Figure 3.6** ABA treatment analysis of *Atchip-1* and control lines grown under identical conditions. **(A)** Primary root length of *Atchip-1* mutant line (relative to wild type, 8, 11 or 15-day old plants). **(B, C)** Fresh weight **(B)** and dry weight **(C)** of *Atchip-1* mutant (relative to wild type, 15-day old plants). **(D, E)** Germination rate (%) of *Atchip-1* mutant and wild type seeds on ½ MS agar medium **(D)** and on ½ MS agar medium containing 0.75 µM ABA **(E)** between day 1 and day 9 after seed plating. **(F, G)** Cotyledon green rate (%) of *Atchip-1* mutant and wild type plants on ½ MS agar medium **(F)** and on ½ MS agar medium containing 0.75 µM ABA **(G)** between day 1 and day 11 after seed plating. Each datum represents the average of five plates, with 12 mutant and 12 control seeds or seedlings on each. Error bars represent standard deviations. For all the data points, $P > 0.01$ by *t*-test.

#### 3.1.3.2 Seed Longevity

To determine whether *Atchip-1* mutant seeds have a different rate in the loss of seed quality during seed storage, a seed longevity assay was performed. The mutant and wild type seeds harvested from plants grown under identical conditions were incubated at 37˚C under a high humidity (about 83%) for a certain period of time. After being air dried for three days, seeds were plated on ½ MS agar medium with or without 0.75 μM ABA. There was no apparent difference between the *Atchip-1* and wild type plants in terms of seed germination (Figure 3.7). Therefore, these data indicate that inactivation of *AtCHIP* does not impair seed longevity.

Interestingly, after 7 days of treatment, *Atchip-1* mutant seeds showed a slightly higher germination rate than wild type seeds in ½ MS agar medium. In order to verify the result, another round of longevity test was performed with two pairs of independent seed lots (Figure 3.8; A and B paired sets of seed lots). Each pair of seed lots were harvested under same conditions. First pair (A pair) of mutant and wild type seed lots was the same as the one used in the earlier seed longevity test, and the second pair was harvested later from plants grown under identical conditions. Comparing germination rates of two pairs of 10-day treated seed lots on ½ MS agar medium containing 0.75 μM ABA, the *Atchip-1* seeds of the initial seed lot (in B pair) seem to have a significantly higher germination rate than wild type seeds between ninth and eleventh days ($P < 0.01$ by *t*-test), while mutant and wild type seeds from the A pair of seed lots germinated very similarly (Figure 3.8). Furthermore, on ½ MS agar medium there was no observable difference in seed germination among the four seed lots (for all the data points $P > 0.01$ by *t*-test). Therefore further test is needed to draw a clear conclusion regarding whether *AtCHIP* inactivation affects the sensitivity of seed germination to ABA.

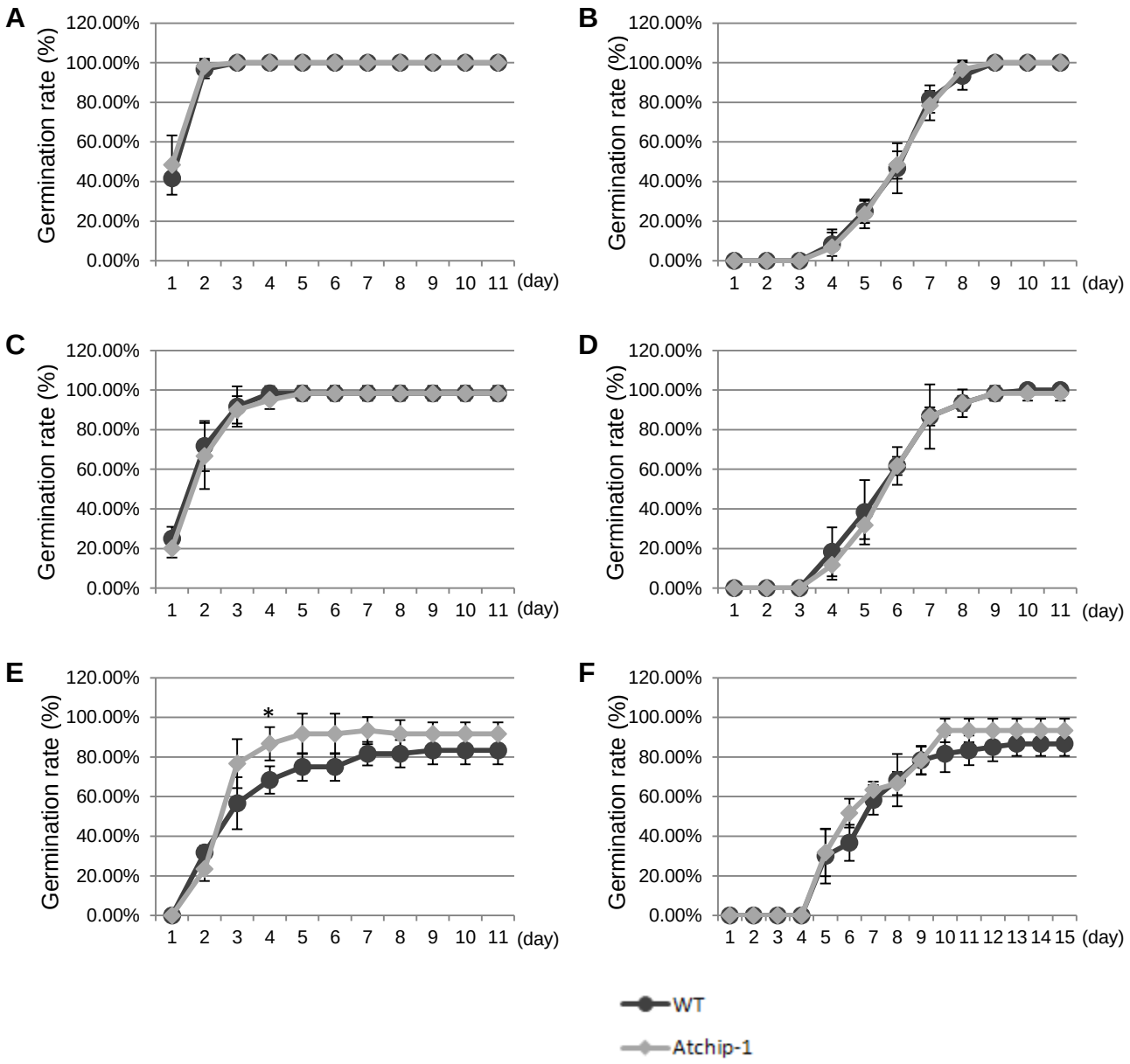


**Figure 3.7** Seed longevity analysis of *Atchip-1* mutant and wild type lines. Seeds were incubated at 37˚C under a high humidity. **(A, B)**. Germination rater (%) of: untreated *Atchip-1* mutant and wild type seeds on ½ MS agar medium **(A)** and on ½ MS agar medium containing 0.75 µM ABA **(B)**. **(C, D)** Germination rates of seeds after 3-day deterioration treatment on ½ MS agar medium **(C)** and on ½ MS agar medium containing 0.75 µM ABA **(D)**. **(E, F)** Germination rates of seeds after 7-day deterioration treatment on ½ MS agar medium **(E)** and on ½ MS agar medium containing 0.75 µM ABA **(F)**. Each datum represents the average of five plates with 16 mutant and 16 wild type plants on each. Error bars represent standard deviations. *$P$ = 0.0083 by $t$-test for the fourth-day time point in (E), while for all the other data points $P$ > 0.01.

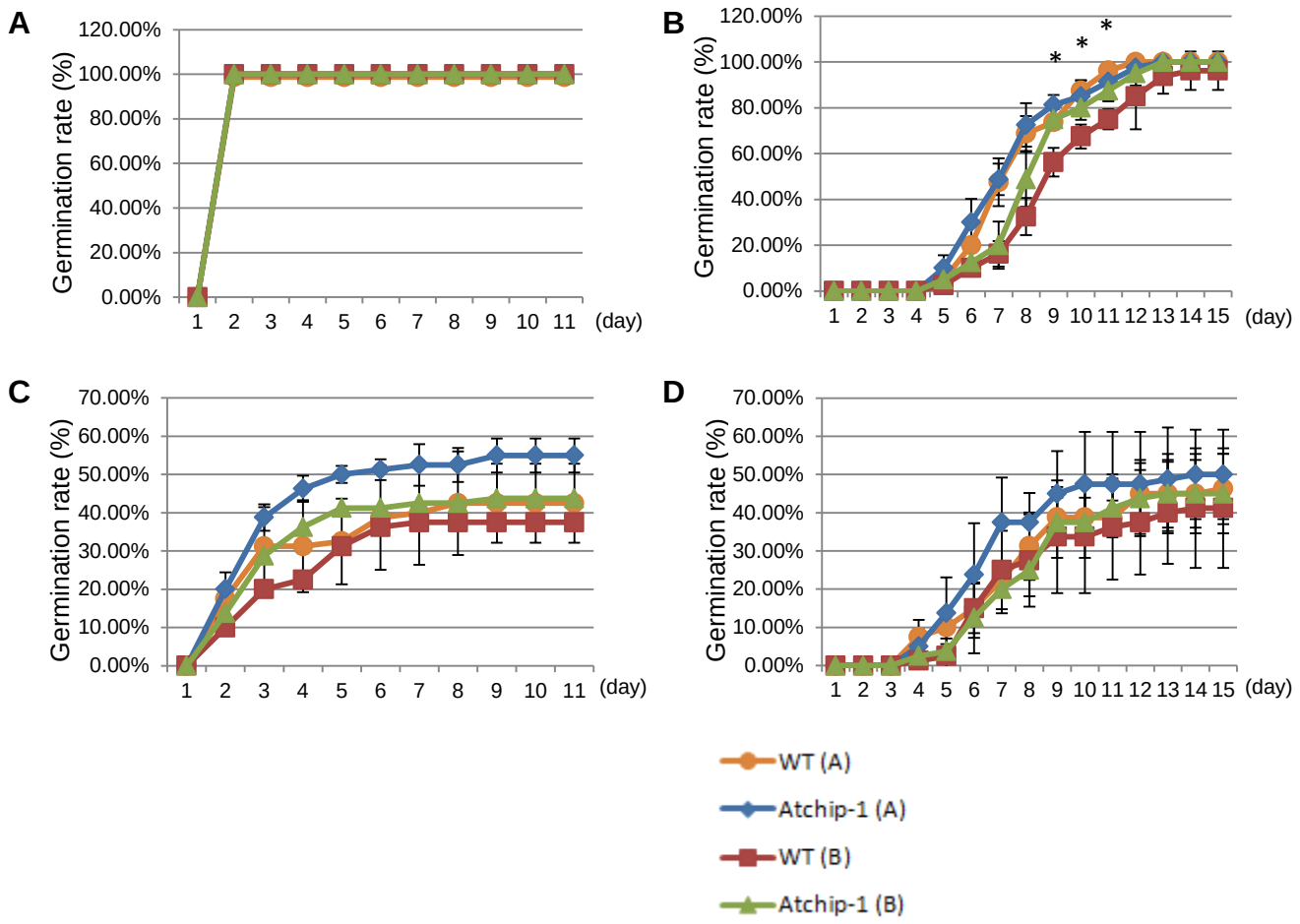


**Figure 3.8** Comparison of seed longevity of two pairs of seed lots between *Atchip-1* and the wild type. **(A, B)** Germination rate (%) of two paired seed lots of: untreated *Atchip-1* mutant and wild type seeds on ½ MS agar medium **(A)** or on ½ MS agar medium containing 0.75 µM ABA **(B)**. **(C, D)** Germination rates of seeds after 10-day deterioration treatment, Germination was on ½ MS agar medium **(C)** or on ½ MS agar medium containing 0.75 µM ABA **(D)**. Each data point represents the average of five plates and on each plate 16 mutant and 16 wild type plants were grown. Error bars represent standard deviations. *$P < 0.01$ by *t*-test comparing wild type and *Atchip-1* in pair B (matched seed lots).

In order to have a clearer conclusion on whether down-regulation of *AtCHIP* in *Atchip-1* mutant line possibly leads to altered seed germination rate, a third round of longevity test with a refined procedure was performed. In this test, a third pair of seeds (wild type and *Atchip-1* mutants) was harvested from plants grown under identical conditions to the other two pairs tested previously. Moreover, on each plate the number of treated seeds was increased for germination test to reduce the level of variation. Therefore the number of seeds tested on each plate was doubled (32 seeds) for those from 10-day treatment and tripled (48 seeds) for those from 14-day treatment. The average germination rates were calculated from three batches of wild type and *Atchip-1* seeds that had been treated for the same number of days, and the data are shown in Figure 3.9. On both 1/2 MS agar media with or without 0.75 μM ABA, *Atchip-1* mutant seeds had very similar germination rates compared to wild type seeds (for all the data points $P > 0.01$ by *t*-test), regardless of how long the seeds were incubated under high temperature and high humidity conditions. These data indicate that seeds of *Atchip-1* have a similar seed germination rate to that of wild type seeds.

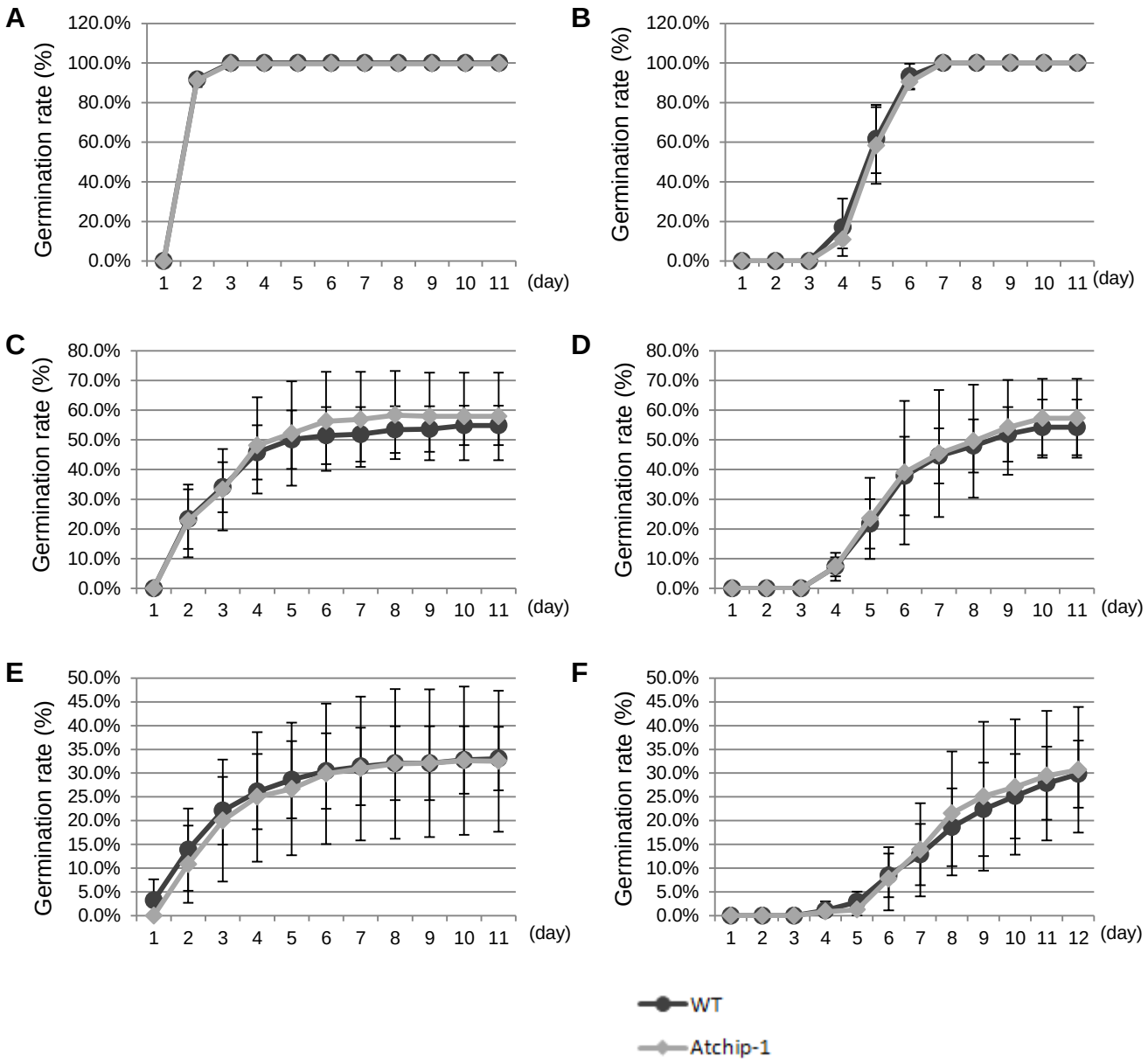


**Figure 3.9** Comparison of seed longevity of three pairs of seed lots between *Atchip-1* and the wild type. **(A, B)** Germination rate (%) of two paired seed lots of: untreated *Atchip-1* mutant and wild type seeds on ½ MS agar medium **(A)** or on ½ MS agar medium containing 0.75 µM ABA **(B)**. Each datum represents the grand average of three batches of seeds with same genotype. For each batch of seeds, five plates were used for each line, with 16 mutant and 16 wild type seedlings grown on each plate. **(C, D)** Germination rates of seeds after 10-day deterioration treatment, germination was on ½ MS agar medium **(C)** or on ½ MS agar medium containing 0.75 µM ABA **(D)**. Each datum represents the average of three batches of seeds with same genotype, and same batch of seeds were grown on five plates with 32 mutant and 32 wild

type seeds on each plate. **(E, F)** Germination rates of seeds after 14-day deterioration treatment, germination was on ½ MS agar medium **(E)** or on ½ MS agar medium containing 0.75 μM ABA **(F)**. Each datum represents the average of three batches of seeds with same genotype, and same batch of seeds were grown on five plates with 48 mutant and 48 wild type seeds on each plate. Error bars represent standard deviations. For all the data points $P > 0.01$ by *t*-test.

#### 3.1.3.3 Thermal Tolerance

It is known that the CHIP protein from animals interacts with heat shock protein Hsc70 and therefore is involved in protein-folding quality control (Hatakeyama and Nakayama, 2003). The interaction of AtCHIP with Hsc70 has been shown in *A. thaliana* (Lee *et al.*, 2009; Shen *et al.*, 2007a). Since *AtCHIP* over-expression plants have been reported to be temperature sensitive (Yan *et al.*, 2003), high temperature stress may cause an increase in protein misfolding and *Atchip-1* may show a defect in tolerating such cellular stress.

Two types of high temperature tolerance assays were used. For basal thermal tolerance, plants were incubated at 42˚C for up to 8 hours. For acquired thermal tolerance, plants were first incubated at 37 ˚C for 90 min to adapt to a high temperature environment and then placed under normal conditions for 2 hours, followed by an incubation at 45˚C for up to 8 hours. For both tests, 10-day old seedlings were treated and were then grown under normal conditions for 7 days before measurements were taken on survival rate, fresh weight and dry weight. The results shown in Figure 3.10 and Figure 3.11 did not show a clear difference in thermal tolerance between *Atchip-1* mutant and wild type plants.

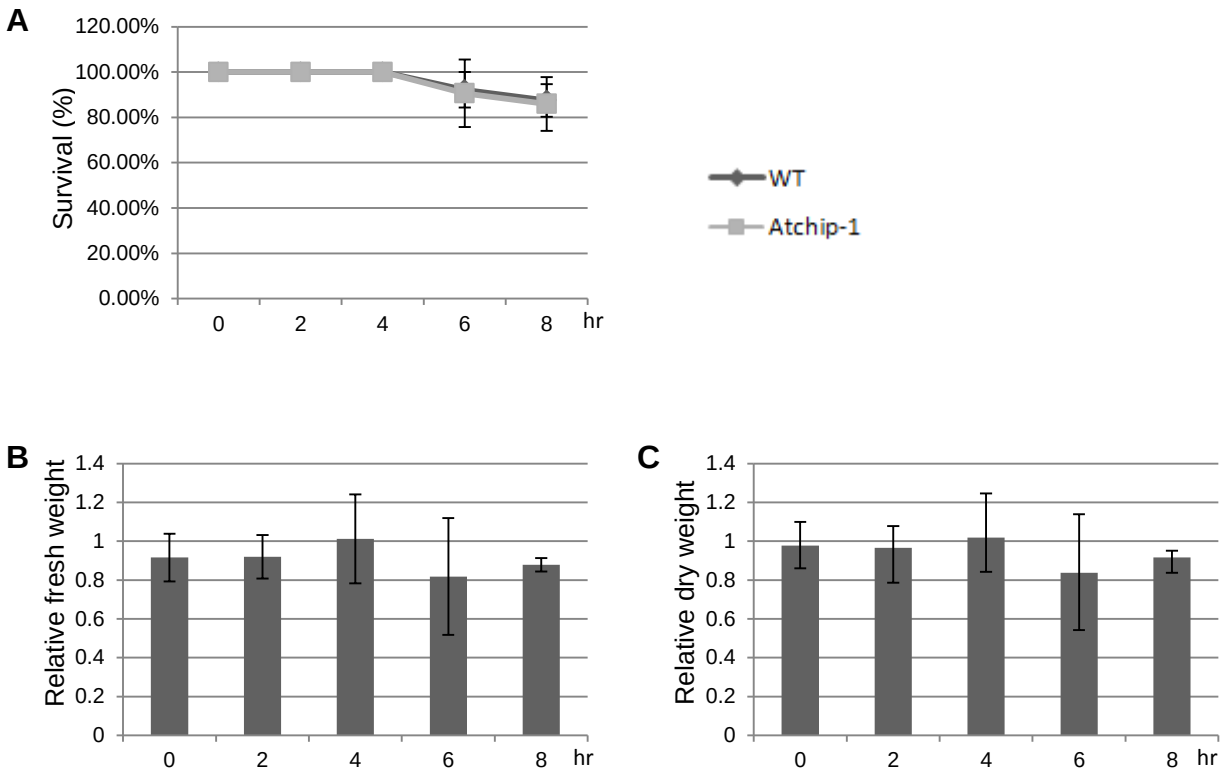


**Figure 3.10** Analysis of basal thermal tolerance. **(A)** Survival rate of *Atchip-1* mutant and wild type plants after heat stress treatment. **(B, C)** Fresh weight **(B)** and dry weight **(C)** of *Atchip-1* mutant plants (relative to the wild type plants which were set with a value of 1). All plants were analyzed on seventh day after the treatment at 42˚C. Each datum represents the average of five plates and on each plate 16 mutant and wild plants were grown. Error bars represent standard deviations. For all the data points $P > 0.01$ by *t*-test.

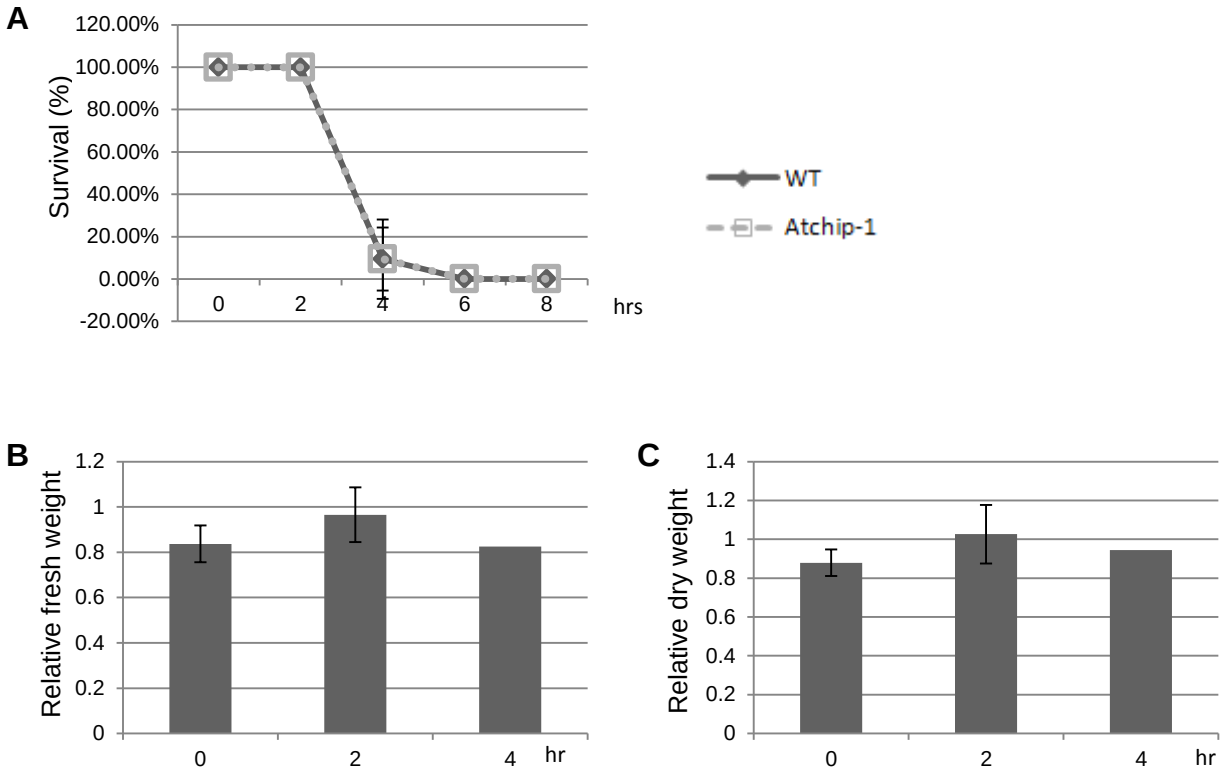


**Figure 3.11** Analysis of acquired thermal tolerance. **(A)** Survival rate of *Atchip-1* mutant and wild type plants after heat stress treatment. **(B, C)** Fresh weight **(B)** and dry weight **(C)** of survived *Atchip-1* mutant plants (relative to wild type plants which were set at 1). All the plants were analyzed on seventh day after treating plants at 45˚C. Each datum represents the average of five plates and on each plate 16 mutant and 16 wild type plants were grown. Error bars represent standard deviations.

### 3.1.3.4 Light Intensity Treatment

Since AtCHIP through its association with Hsc70 participates in controlling import of nascent proteins into the chloroplast (Lee *et al.*, 2009), one potential effect that *AtCHIP* may have is on protein turnover in the chloroplasts. On the other hand, photodamage at photosystem II can increase the level of reactive oxygen species which in turn results in protein misfolding (Shen *et*

*al.*, 2007a). Thus, high light intensity can cause damage to chloroplast proteins and hence may create stress from abnormal protein quality.

*Atchip-1* and wild type plants were grown in pots. For each tray, five pots of mutant plants and five pots of wild type plants were placed side-by-side, and five plants of the same line were grown in each pot. Beginning at two weeks of growth, one tray of plants was grown under normal light and the other under high-intensity light. After 30-day of growth, plant morphology was surveyed (Figure 3.12). Both lines grown under high-intensity light appeared to show some signs of stress - with leaf color turning purple, although they also developed faster than those under normal light. The plants under high-intensity light flowered earlier. However, there was no observable difference between the mutant plants and wild type plants.

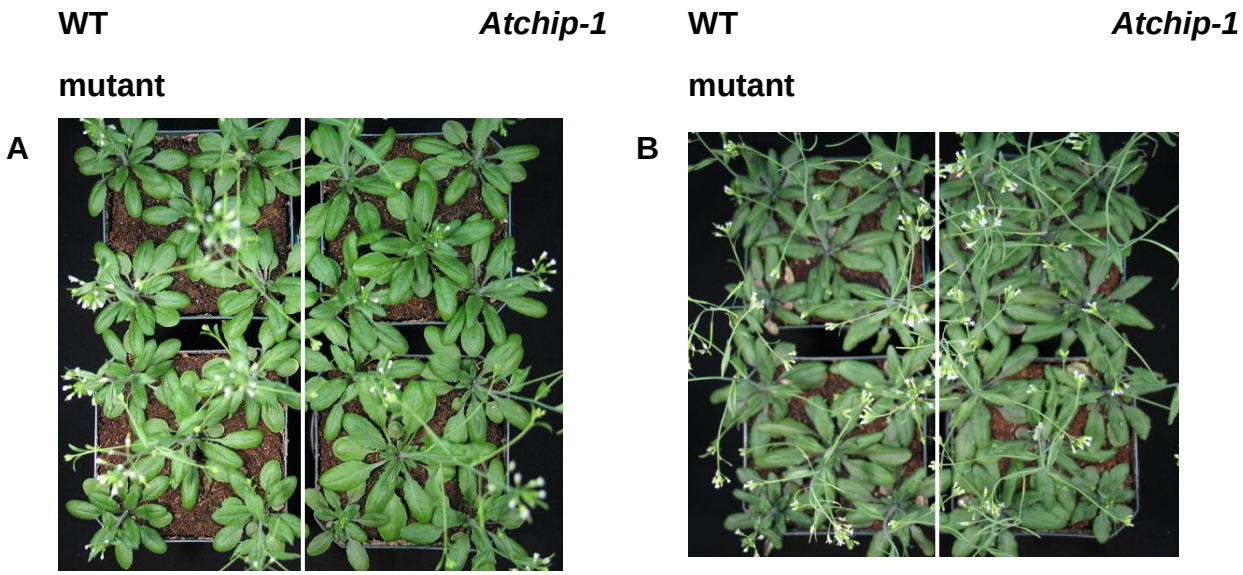


**Figure 3.12** Plant morphologies under normal and high-intensity light conditions. Plants (30-day old) were grown under **(A)** normal light and **(B)** high-intensity light conditions. On each photograph, left: wild type plants; right: *Atchip-1* mutant plants.

#### 3.1.3.5 Oxidative Stress

Oxidative stress may cause an increase in protein misfolding in the cell, and thus was used as another condition to test the phenotype of *Atchip-1*. Paraquat (also called methyl viologen) is a herbicide and widely used as a free-radical reagent. In this study paraquat dichloride was used to create oxidative stress by generating superoxide in the cells. Since this assay has not been tested previously in the laboratory, a concentration ranging from 0 to 0.2 μM in the ½ MS agar medium was tested. Seedlings did not grow on the plates with 0.2 μM paraquat dichloride. Oxidative stress can also enhance photodamage in the chloroplast (Okada *et al.*, 1996). Therefore, both wild type and mutant seeds were grown on ½ MS plates containing paraquat under either normal or intensified light condition. The primary root length was measured on the $11^{th}$ day after seeds were plated as a parameter to indicate plant development progress. However, no detectable differences were observed for the *Atchip-1* mutant in comparison with wild type seedlings (Figure 3.13).

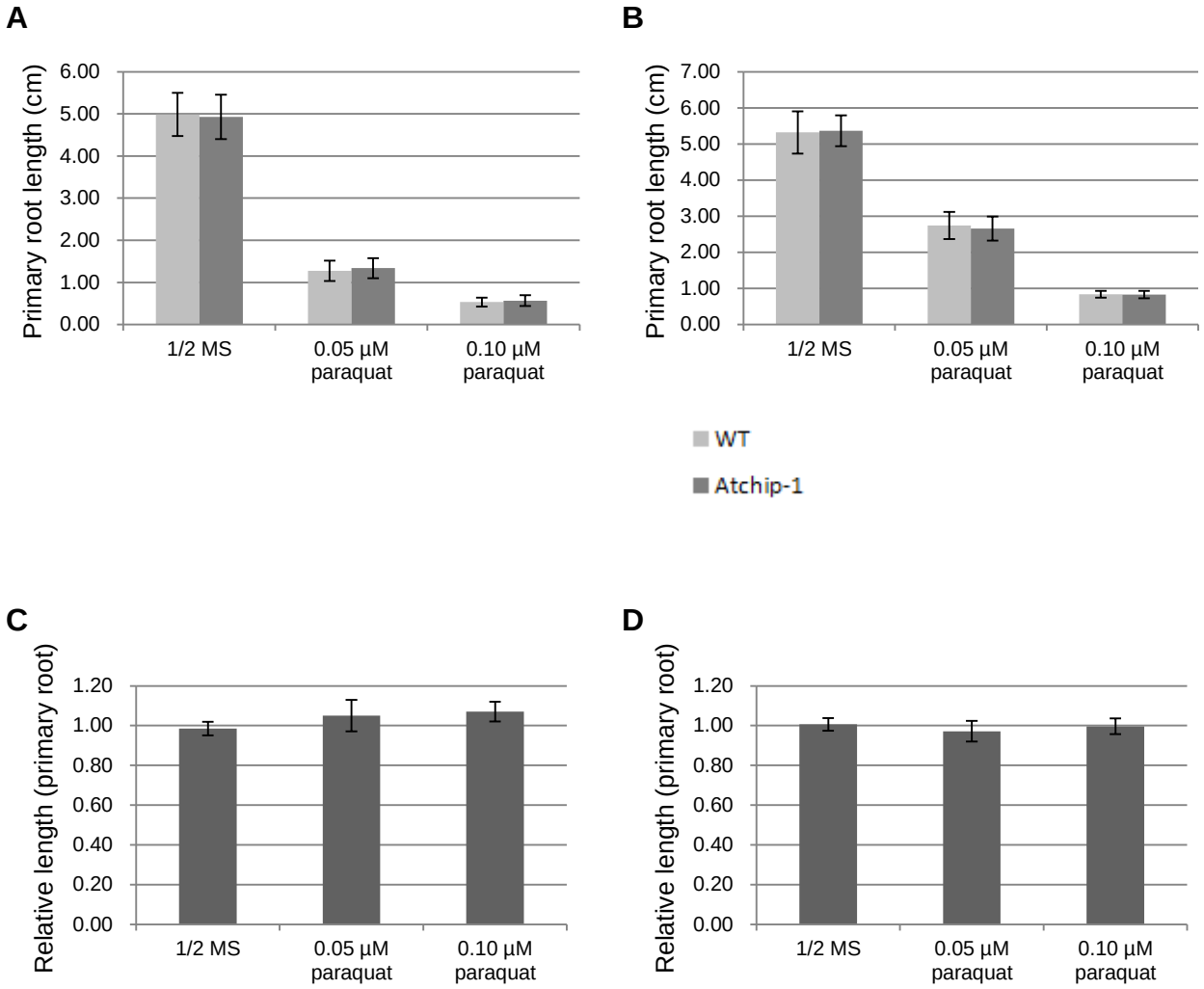


**Figure 3.13** Phenotypic survey of *Atchip-1* under oxidative stress. **(A)** Absolute primary root length (cm) of wild type and *Atchip-1* mutant line grown under normal light. **(B)** Absolute primary root length (cm) of wild type and *Atchip-1* mutant line grown under high-intensity light. **(C)** Primary root length of *Atchip-1* mutant line (relative to wild type) grown under normal light. **(D)** Primary root length of *Atchip-1* mutant line (relative to wild type) grown under high-intensity light. Primary root length was measured on 11-day old plants. For each light condition, plants were tested in ½ MS plates containing paraquat, with concentrations of 0, 0.05, 0.10 and 0.20 µM (at 0.20 µM seedlings died after germination). Each datum represents the average of five plates, and on each plate 12 mutant and 12 control seeds or seedlings were used. Error bars represent standard deviations. For all the data points $P > 0.01$ by *t*-test.

#### 3.1.3.6 DNA Damage Tolerance

Since the Arabidopsis Ubc13-Uev complex has been implicated in DNA-damage tolerance, it is interesting to examine whether AtCHIP plays a role in this function. It has been shown that the *AtUEV1D* T-DNA mutant has increased sensitivity to the DNA-damaging agent MMS (methylmethane sulfonate) (Wen *et al.* 2008). Thus, *Atchip-1* was analyzed for its sensitivity to MMS. In order to identify a proper MMS dosage for determining an effect on *Atchip-1*, a concentration ranging from 0 to 75 ppm was used in the analysis. The results showed that there was no clear difference between the wild type and *Atchip-1* plants at any of the concentrations used (Figure 3.14).

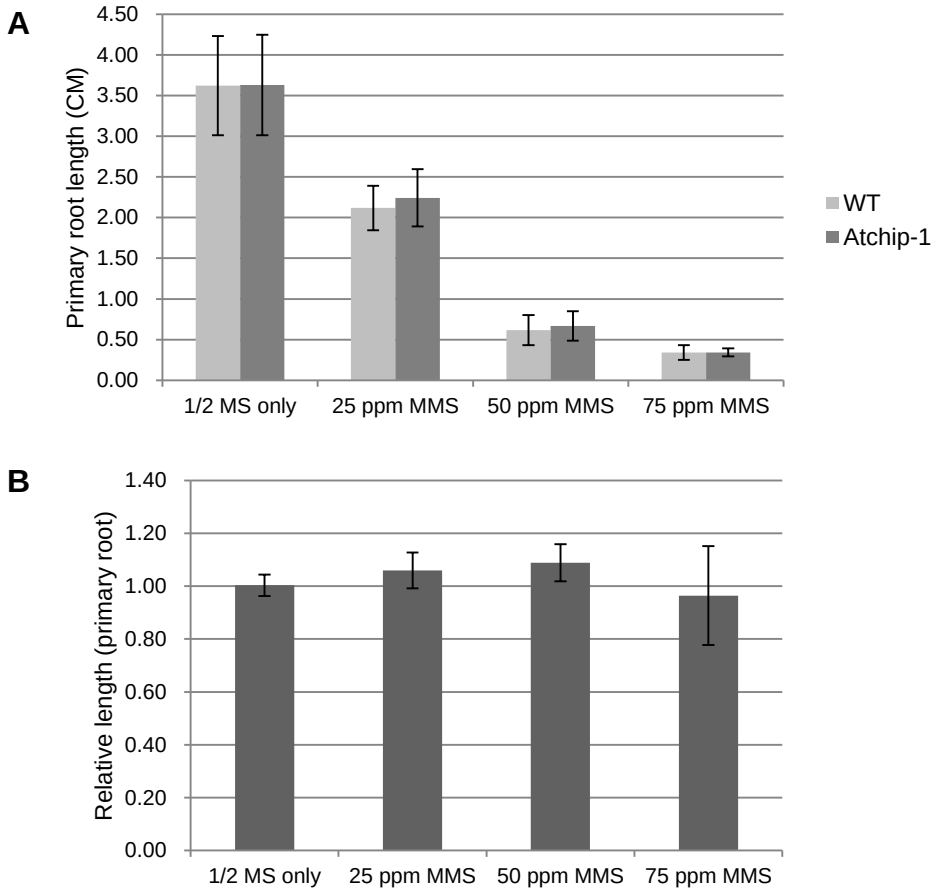


**Figure 3.14** Phenotypic survey of *Atchip-1* following DNA damaging treatments. **(A)** Absolute primary root length (cm) of wild type and *Atchip-1*. **(B)** Primary root length of *Atchip-1* (relative to wild type). Primary root length was measured on 11-day old plants. For each light condition, plants were tested in ½ MS plates containing MMS, with concentrations of 0, 25, 50 and 75 ppm. Each datum represents the average of five plates, and on each plate 12 mutant and 12 control seeds or seedlings were used. Error bars represent standard deviations. For all the data points $P > 0.01$ by *t*-test.

## 3.2 Characterization of At1g74370 (*E3-A1*) and At1g69330 (*E3-A2*) Genes

### 3.2.1 Sequence Analysis of Putative E3-A Proteins

The At1g74370 gene (tentative name *E3-A1* for this project) product was also identified in a yeast two-hybrid screen to interact with AtUBC13A (Wen, Wang, and Xiao, unpublished data). It appears that the gene belongs to a sub-family of two or three members (Figures 3.15A and 3.15B). Since the paralogous genes can be functionally redundant, the two most closely related genes (At1g69330 and At3g29270, tentatively named *E3-A2* and *E3-A3*; see Figure 3.15A) were selected for studies by down-regulation.

Based on protein information from PROSITE and SMART databases, all three E3-A proteins share very similar domain architectures (Figure 3.15C and Table 3.1). In addition to the RING finger domain, SMART program also predicted two potential transmembrane domains within the conserved region near the C-terminus of all three proteins.

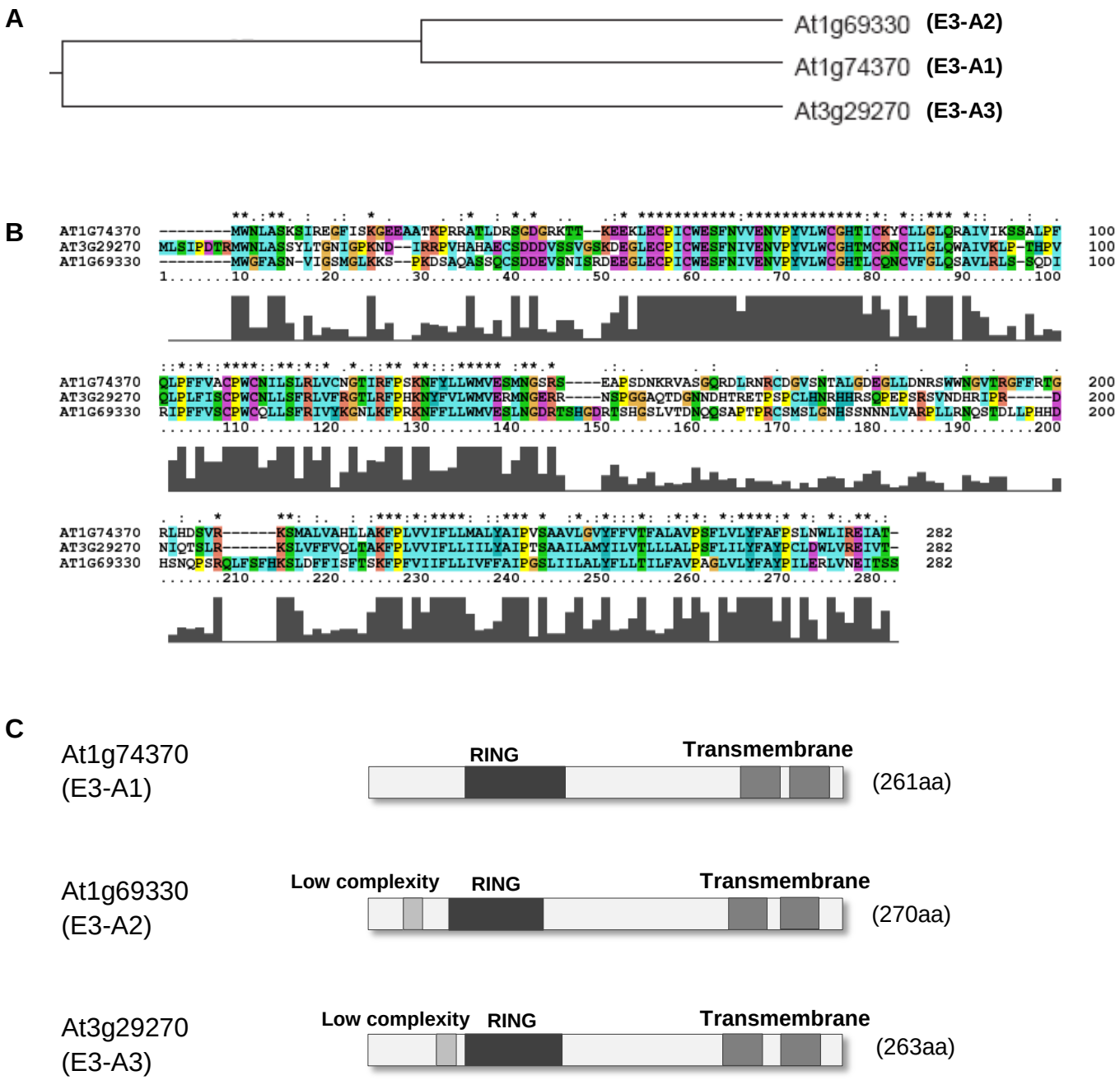


**Figure 3.15** Sequence analysis of E3s that are closely related to At1g74370 (*E3-A1*). **(A)** Phylogenetic tree by Stone *et al.* (2005) based on sequence alignment of RING domains. **(B)** Amino acid sequence alignment of closely related E3-A proteins using ClustalX with default parameters. The Consensus Line on the top indicates the degree of conservation of residues in the corresponding column: '*' indicates a column with all identical residues; ':' represents a highly conserved column; '.' represents a weakly conserved column. In the sequence alignment

the amino acid residues are colored as follows: orange for G, P, S and T; red for H, K and R; blue for F, W and Y; green for I, L, M and V. The Alignment Ruler under the sequence alignment and the numbers on the right side show the positions of the columns in the alignment. The Alignment Conservation Display Area at the bottom shows a bar chart which indicates the degree of conservation of residues in each column by the height of the corresponding bar. (**C**) Domain architecture of E3-A proteins. Full-length E3-A protein sequence was used to search PROSITE and SMART databases, and the distribution of functional domains and modification sites predicted by both databases are summarized in the diagram.

**Table 3.1** Predicted domains within sequences of E3-A proteins

| E3 protein | Low complexity | RING | Transmembrane | Transmembrane | Full length |
|---|---|---|---|---|---|
| At1g74370 (E3-A1) | | 46-101 | 198-220 | 225-247 | 1-261 |
| At1g69330 (E3-A2) | 20-31 | 45-99 | 206-228 | 235-257 | 1-270 |
| At3g29270 (E3-A3) | 38-49 | 54-108 | 197-219 | 229-251 | 1-263 |

Full-length sequences of E3-A proteins were used in the SMART program to detect potential functional domains (see http://smart.embl-heidelberg.de). The estimated locations of predicted domains in the primary protein sequences are indicated in the table.

### 3.2.2 Screen for RNAi Down-Regulation Lines of *E3-A1* and *E3-A2* Genes

*E3-A1* (At1g74370) and *E3-A2* (At1g69330) are most closely related according to a phylogenetic analysis (Stone *et al.*, 2005). However, there are no good public T-DNA insertional mutant lines (i.e. T-DNA inserted in either an exon or intron) available for either of the two *E3-A* genes. Therefore we decided to down-regulate the two genes through RNA interference (RNAi) by expressing RNAi constructs that were designed to target regions of mRNA sequences of *E3-A1* and *E3-A2*. RNAi constructs were prepared and plant transformation was performed with the help of Dr. Xianzong Shi. To ensure that the

expression pattern from the RNAi construct matches the expression of the wild type genes, each of the RNAi cassettes was placed under the control of the native promoter of the target gene. To analyze whether the expression of the target gene was down-regulated, total RNAs were extracted from the leaf or floral tissues of T1 plants (seeds produced by the infiltrated plants). According to the microarray data (Schmid *et al.*, 2005), the highest transcription level of *E3-A1* is in seeds and for *E3-A2* in floral tissues. Total RNAs were used in analysis of transcripts by RT-PCR and the gene-specific amplified PCR fragments were analyzed by 1% agarose gel electrophoresis.

To select effective down-regulation mutants, 40 T1 RNAi transformants were identified by RT-PCR for each *E3-A*. For each of the *E3-A1* and *E3-A2* RNAi constructs, 4-5 plants with effective transcript down-regulation were obtained (Figures 3.16A and 3.16B). Further functional studies on down-regulation effect require stable inheritance of effective RNAi. Therefore, seeds were harvested from the best *E3-A* down-regulating plants to select stable RNAi lines. Line 827-25 (for *E3-A1*) and line 826-51 (for *E3-A2*) were identified with stable inheritance of effective RNAi down-regulation of *E3-A1* and *E3-A2*, respectively (Figure 3.16C and 3.16D).

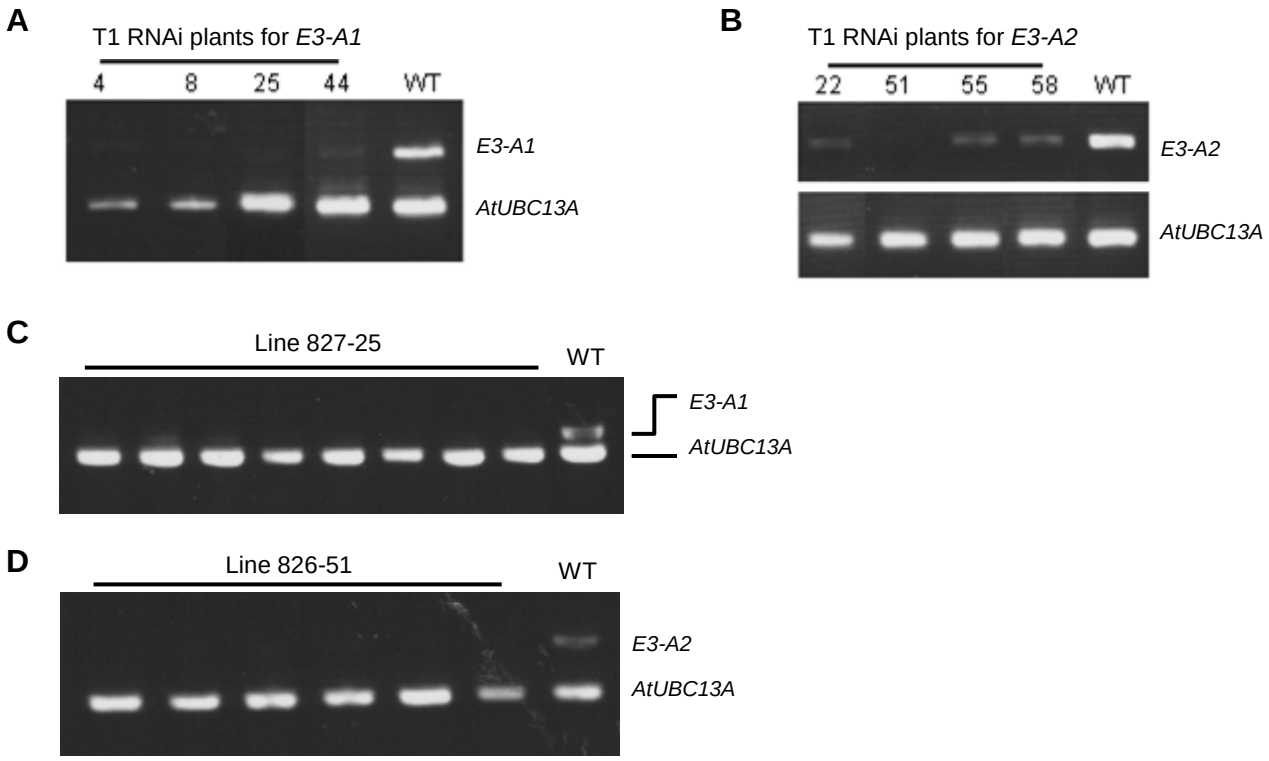


**Figure 3.16** Transcripts of *E3-A* genes in RNAi transformants analyzed by RT-PCR. **(A)** *E3-A1* transcripts were down-regulated in leaf tissue of the T1 RNAi transformants. **(B)** *E3-A2* transcripts were down-regulated in floral tissue of the T1 RNAi transformants. *AtUBC13A* is used as a reference. **(C)** Down-regulation of *E3-A1* in line 827-25. **(D)** Down-regulation of *E3-A2* in T2 plants of RNAi line 826-51. *AtUBC13A* was used as a reference gene.

### 3.2.3 Obtaining Double RNAi Lines of *E3-A1* and *E3-A2* Genes

Since down-regulation of a single gene may not produce dramatic phenotypic changes due to a functional redundancy among related genes, a double RNAi mutant line would be required to down-regulate both *E3-A1* and *E3-A2* simultaneously. To obtain such a double RNAi line, two parents with stable down-regulation of the target gene are required. Thus, the two best T2 RNAi lines (line 827-25-12 for *E3-A1* and line 826-51-28 for *E3-A2*) were crossed. The F1 plants (the first generation from the cross) were screened by RT-PCR, and several plants with both genes down-regulated were obtained (Figure 3.17). Among them, the line Cr7-33 was subject to further phenotypic characterization.

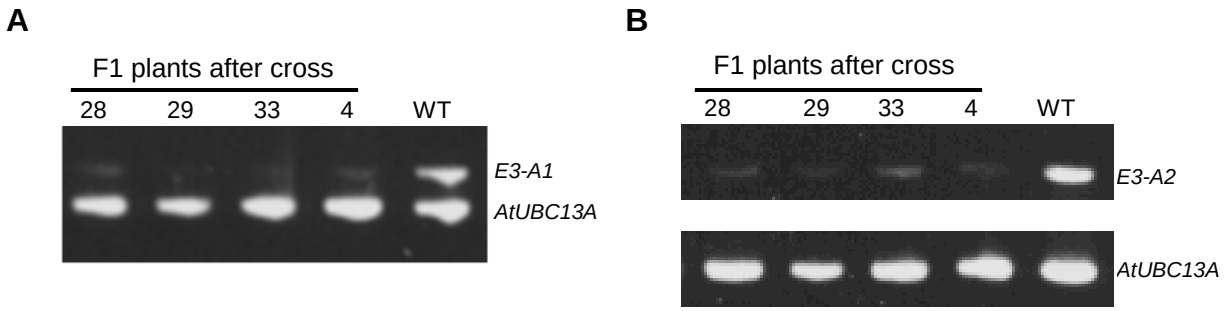


Figure 3.17 Down-regulation of *E3-A1* and *E3-A2* in hybrid RNAi plants (F1 generation). **(A)** F1 RNAi plants with down-regulated *E3-A1* transcripts were identified by RT-PCR. **(B)** F1 RNAi plants with down-regulated *E3-A2* transcripts were identified by RT-PCR.

### 3.2.4 Phenotypic Characterization of *E3-A1 and E3-A2* RNAi lines

In order to search for possible phenotypes induced by down-regulation of *E3* genes, an *E3-A1* RNAi line (827-25-12) and an *E3-A1/A2* double RNAi line (Cr7-33-7; F2 generation line) were subject to a series of hormonal and osmotic treatments. Seeds were plated on ½ MS agar medium containing one of the following ingredients: 5% sucrose, 150 mM NaCl, 50 µM SA or 0.75 µM ABA. Root length, fresh weight and dry weight were measured as in the phenotyping of *Atchip-1*, and control plants were from the same wild type segregant line (from SALK_112098). Root length differences were observed in the mutant plants on ABA containing plates (Figure 3.18). Mutant seeds started germination and cotyledon emergence later than wild type seeds on 1/2 MS agar medium containing 0.75 µM ABA. Also the overall developmental progress of mutant seedlings was behind that of wild type seedlings, as indicated by primary root length, fresh weight and dry weight of seedlings.

However, since the seeds of different lines used in this experiment were not harvested from plants grown under strictly controlled identical conditions, minor difference in seed quality might be a contributing factor again. Therefore, seed germination and cotyledon greening assays were done on 1/2 MS agar medium containing 0.75 µM ABA to compare the viability and seedling initiation of RNAi seeds with seeds of wild type and a T-DNA line SK353 (SALK_058353c, used as another control, harvested at the same time with RNAi seeds).

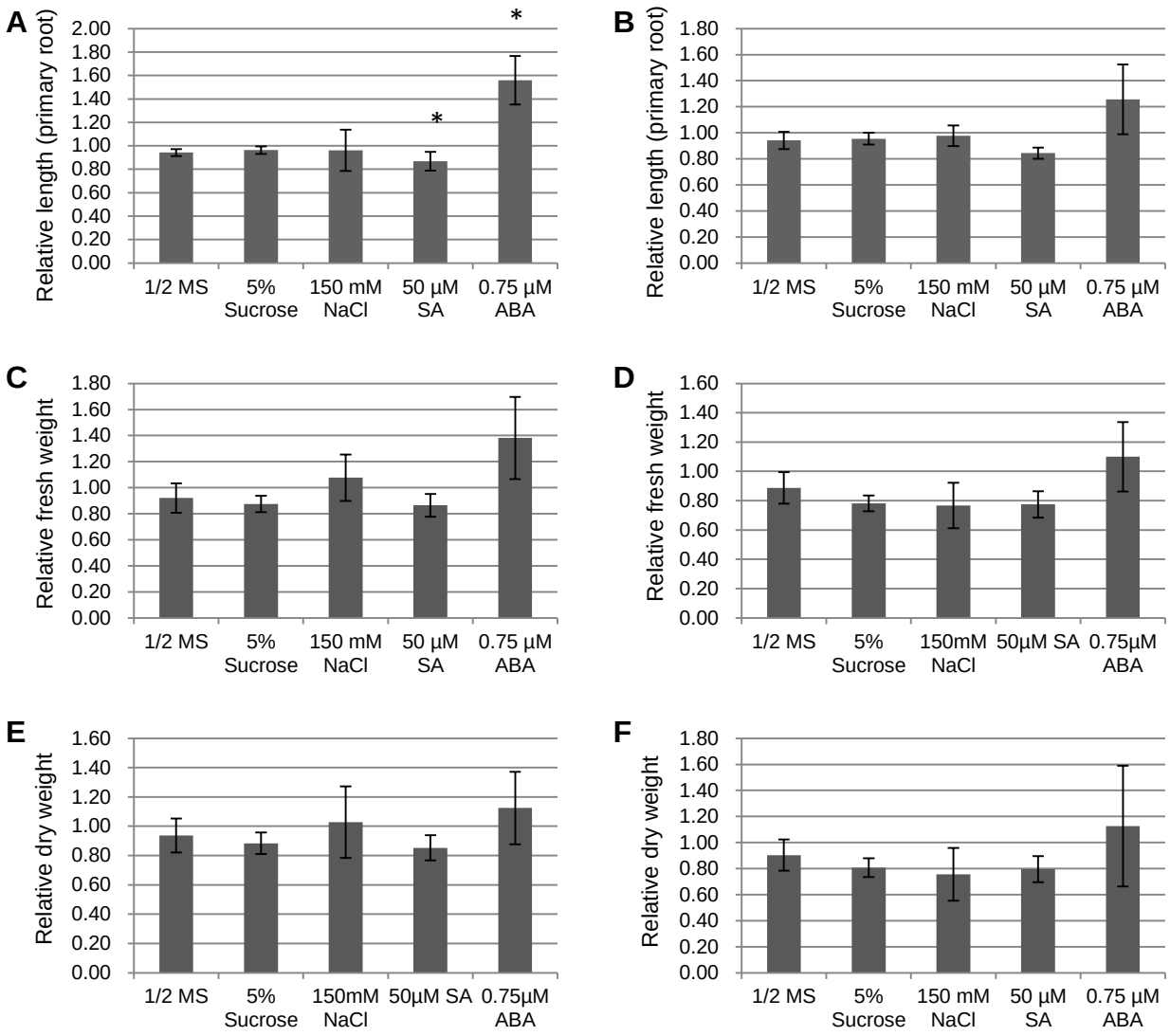


**Figure 3.18** Phenotypic survey of E3-A1 and E3-A2 RNAi lines in response to hormonal treatments and osmotic stress. **(A, B)** Relative root length of **(A)** *E3-A1* RNAi line (827-25-12) and of **(B)** *E3-A1/A2* double RNAi line (Cr7-33) (to wild type, 11-day old plants). **(C, D)** Relative fresh weight of **(C)** line 827-25-12 and of **(D)** Cr7-33 (to wild type, 11-day old plants). **(E, F)** Relative dry weight of **(E)** line 827-25-12 and of **(F)** Cr7-33 (to wild type, 11-day old plants). The data for each treatment represents the average of five plates and on each plate 12 RNAi and 12 control plants were measured. Error bars represent standard deviations. * indicates $P < 0.01$ by *t*-test.

According to the data from this experiment (Figure 3.19A), no clear difference was observed in seed germination and cotyledon greening of the RNAi line compared to the wild type in the absence of ABA. However, on the seventh day after seed plating on 1/2 MS agar medium containing 0.75 μM ABA (Figure 3.19B), the wild type seeds showed a lower germination rate in comparison to all the other lines tested, including the control line SK353. Yet on normal 1/2 MS medium the wild type seeds had a similar germination rate with all the other seed lots tested. The germination rates of three RNAi lines and the SK353 line were similar to each other even in the presence of 0.75 μM ABA, which suggests that seeds from the RNAi lines did not respond to ABA differently. In the case of previous ABA treatment (Figure 3.18), since the seeds were harvested at different times, the difference in seed germination rate might be due to minor difference in seed quality. Therefore, the phenotype of the RNAi lines with ABA treatment does not seem to be a result of down-regulation of *E3-A* genes.

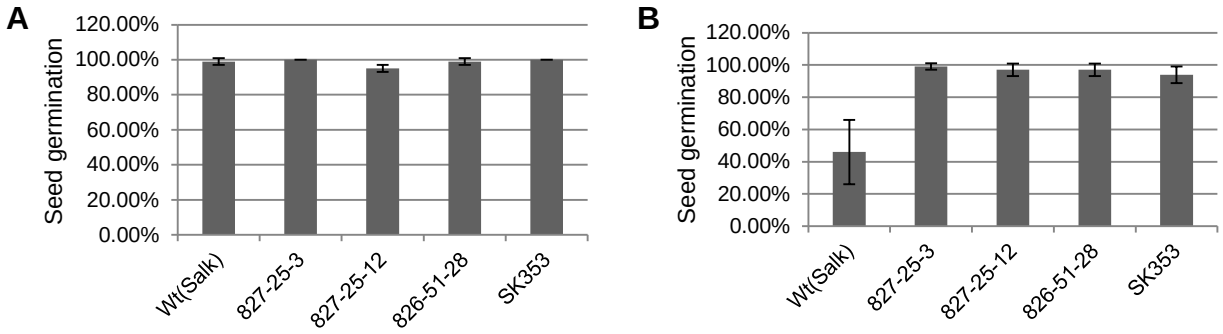


**Figure 3.19** Analysis of seed germination of RNAi lines, wild type line and unrelated T-DNA mutant line as control. Seeds were plated on ½ MS agar medium, seed germination rate (%) of wild type plants, *E3-A1* RNAi lines (827-25-3 and 827-25-12), *E3-A2* RNAi line (826-51-28) and unrelated T-DNA mutant line SK353 (no phenotype on ABA plate) were recorded after seven days after. **(A)** Seed germination on plates without ABA. **(B)** Seed germination on plates containing 0.75 μM ABA. The datum for each treatment represents the average of five plates, with each plate containing 25 seeds. Error bars represent standard deviations.

### 3.2.5 Identification of "Stem-Fusion" Phenotype on *E3-A2* RNAi Transformants

When grown in soil under normal conditions, some plants from the *E3-A2* RNAi line (826-51) were found to have widened stems which appeared like two normal stems fused together. The same "stem fusion" phenotype was observed in T1 transformed plants (the first generation after plant transformation) of an independent RNAi line (828) grown in soil (Figure 3.20). Among 150 screened T1 plants from the 828 line, six of them had the "stem-fusion" phenotype. According to the microarray data (Schmid *et al.*, 2005), the highest transcription level of *E3-A2* is in floral tissue, therefore this phenotype might be a result of abnormal emergence of the shoot apical meristem before flowering. However, this "stem-fusion" phenotype did not occur on the other RNAi plants even with effective down-regulation of the *E3-A2* gene.

It is possible that this "stem fusion" phenotype was a result of interaction between the down-regulation of *E3-A2* and some environmental factors. To determine this possibility, several treatments were applied to the progeny of the *E3-A2* RNAi line (826-51-28) which had displayed the "stem-fusion" phenotype. The RNAi and wild type plants (five pots for each type, thus 25 RNAi plants and 25 wild type plants) were grown side-by-side in each tray and one of the following treatments was applied: control (no additional treatment), repeatedly trimming of floral stalks to encourage the generation of new stalks, fertilizer applied (watering plants with half-strength garden fertilizer), high moisture (spraying plants with water twice a day), drought and spraying auxin (2 μM NAA solution). However, none of the treatments was able to induce "stem-fusion" phenotype. Thus, no conditions can be found so far to specifically induce "stem-fusion" when *E3-A2* is down-regulated.

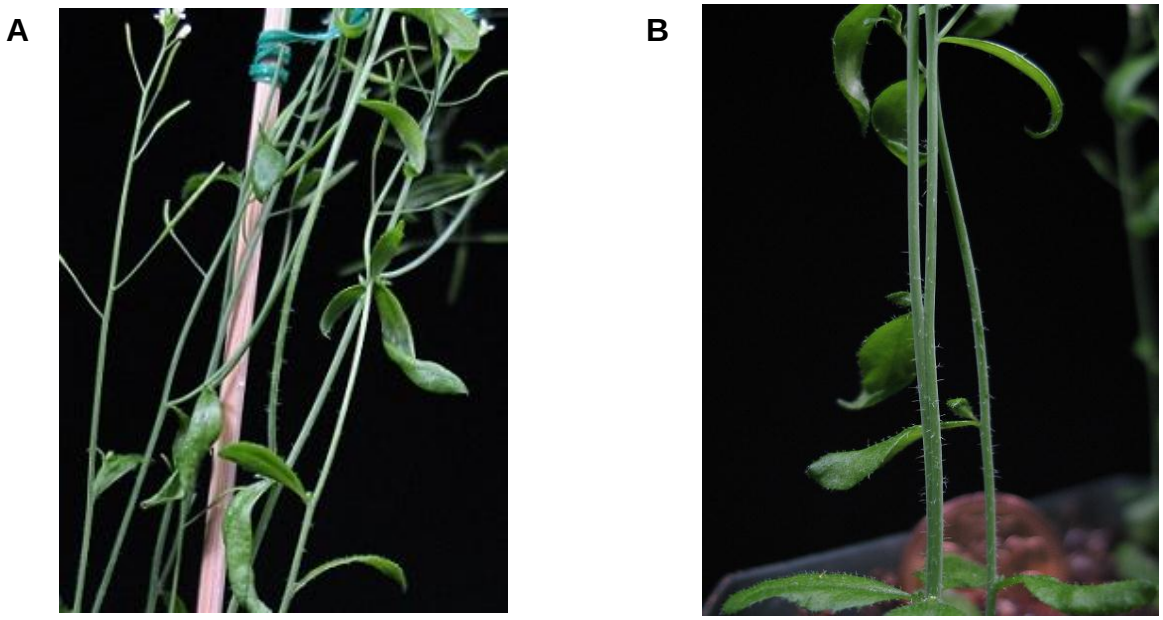


**Figure 3.20** Plant morphology of **(A)** normal stems of a wild type plant and **(B)** a "fused stem" of an *E3-A2* RNAi transformant (828-9). Plants in the photographs were 30-day old.

## 3.3 Summary of Phenotypic Surveys

The phenotypic surveys that have been done are summarized in Tables 3.2 and 3.3.

**Table 3.2** Phenotypic surveys for *Atchip-1* mutant line

| Treatments | Conditions | Parameters analyzed | Results |
|---|---|---|---|
| **Hormones and osmotic stress** | ½ MS medium (0.7% agar, 1% Sucrose)<br>½ MS medium (0.7% agar, 5% Sucrose)<br>½ MS + 0.1 µM NAA<br>½ MS + 50 µM SA<br>½ MS + 0.75 µM ABA[1]<br>½ MS + 25 µM MeJA<br>½ MS + 2.5 µM KN | Root length<br>Fresh weight<br>Dry weight<br>Seed germination rate<br>Cotyledon green rate | *Atchip-1* mutant showed more sensitivity to ABA than wild type plants. However, this phenotype was not observed with other seed lots |
| **ABA treatment[2]** | ½ MS + 0.75 µM ABA | Root length<br>Fresh weight<br>Dry weight<br>Seed germination rate<br>Cotyledon green rate | No difference was observed between *Atchip-1* mutant and wild type plants |
| **Seed longevity** | Deterioration of seeds: incubate seeds at 37 ˚C in high humidity<br>Plating: ½ MS medium (0.7% agar, 1% Sucrose) and ½ MS + 0.75 µM ABA | Seed germination rate<br>Cotyledon green rate<br>Fresh weight<br>Dry weight | *Atchip-1* plants showed slightly better viability in one pair of seed lot, but no in another |
| **Thermal tolerance** | Basal thermal tolerance: incubate seedlings at 42˚C<br>Acquired thermal tolerance: preincubate seedlings at 37˚C before incubation at 45˚C | Survival rate<br>Fresh weight<br>Dry weight | No distinct phenotype detected |
| **Light** | Normal light<br>High-intensity light | Morphology observation on soil | No distinct phenotype detected |

| | | | |
|---|---|---|---|
| **Oxidative stress** | ½ MS medium<br>½ MS + 0.05, 0.1 and 0.2 µM paraquat dichloride<br>Normal light<br>High-intensity light | Root length<br>Fresh weight<br>Dry weight<br>Seed germination rate<br>Cotyledon green rate | No difference was observed between wild type and *Atchip-1* plants |
| **DNA damage tolerance** | ½ MS medium<br>½ MS + 25, 50 and 75 ppm MMS | Root length<br>Fresh weight<br>Dry weight | No difference was observed between wild type and *Atchip-1* plants |

1. In first round of hormonal phenotypic survey, *Atchip-1* mutant seeds and wild type seeds were harvested at different times. Therefore there might be a difference in seed quality.
2. *Atchip-1* mutant and wild type plants were grown side-by-side under the same conditions. Seeds were harvested at the same time and in the same way to ensure that seed quality of both lines was as similar as possible. These seeds were used for phenotypic survey on ABA containing plates.

**Table 3.3** Phenotypic analysis of *E3-A1* and *E3-A2* RNAi transformants

| Treatments | Conditions | Parameters analyzed | Results |
|---|---|---|---|
| **Hormones and osmotic stress** | ½ MS medium (0.7% agar, 1% Sucrose)<br>½ MS medium (0.7% agar, 5% Sucrose)<br>½ MS + 150 mM NaCl<br>½ MS + 50 µM SA<br>½ MS + 0.75 µM ABA | Root length<br>Fresh weight<br>Dry weight<br>Seed germination rate<br>Cotyledon green rate | No clear phenotype detected |
| **Growth condition test** | Repeatedly trimming<br>Fertilizer<br>High moisture<br>Drought<br>Spray auxin | Morphology on soil | No clear phenotype detected |

# 4 DISCUSSION

## 4.1 AtCHIP and Protein Quality Control

Molecular chaperones such as the Hsp70 and Hsp90 families of proteins participate in protein quality control. These chaperones either catalyze refolding of misfolded polypeptides or cause them to be degraded in UPS. This well-tuned two-way system is known as the "molecular triage". The CHIP protein in mouse has been shown to inhibit ATPase activity and substrate binding affinity of Hsp70, and its E3 ligase activity polyubiquitinates substrates of Hsp70 and Hsp90 for degradation (McDonough and Patterson, 2003). This role of the CHIP protein appears to be vital for animals, as CHIP knockout in mice and CHIP knockdown in *C. elegans* both resulted in severe phenotypes. The down-regulation by RNAi and knockout of CHIP in *C. elegans* caused arrests of larval development (Khan and Nukina, 2004). CHIP knockout mice had significantly shortened life span and accelerated aging (Min *et al.*, 2008).

The AtCHIP protein shares a high degree of sequence similarity with animal CHIPs, and like animal CHIPs it also interacts with the Hsp70 chaperone proteins which are located in the cytoplasm (Lee *et al.*, 2009; Shen *et al.*, 2007a). Therefore it is reasonable that AtCHIP plays similar roles in plants as its orthologs in animals. In the plant Arabidopsis, a protein quality control machinery similar to that in animals has not yet been shown. However, the transcriptional level from the *AtCHIP* gene was upregulated by stress conditions, and overexpression of the *AtCHIP* gene resulted in hyper-sensitivity to temperature stress (Yan *et al.*, 2003). Since environmental stress conditions will likely result in an increase in the amount of misfolded proteins, AtCHIP may function to degrade Hsp70-associated non-native proteins. Based on this assumption, *Atchip-1* mutants may display certain defects under stress conditions due to the loss of the protein degradation function in the proposed "molecular triage". The rationale for using different stress conditions in this study was that damaged and misfolded proteins would increase under certain conditions, resulting in an imbalance of protein turnover

in *Atchip-1* mutant plants. However, present results showed that *Atchip-1* mutants did not have any apparent phenotypic defects under various stress conditions tested in this study.

High temperature stress creates pressure on intracellular protein folding, by affecting structural stability of functional proteins and the folding process of newly synthesized proteins. Therefore, plants with defects in protein misfolding response may show decreased heat tolerance. In this study, two types of thermotolerance test were used: to test basal thermotolerance seedlings were treated with a high temperature directly, and to test acquired thermotolerance seedlings were exposed to a moderately high temperature for a short period before being exposed to a higher temperature. As shown in Figures 3.10 and 3.11, *Atchip-1* seedlings had a similar survival rate compared to wild type seedlings in both thermotolerance tests. Two weeks after the treatments, *Atchip-1* seedlings and wild type seedlings had comparable average fresh and dry weights. Therefore, both genotypes of plants had similar recovery progress.

Since photodamage in the chloroplast can increase the level of reactive oxygen species which in turn causes protein misfolding, *Atchip-1* plants growing in pots were exposed to high-intensity light to test in tolerance to strong light. However, the morphologies of *Atchip-1* mutant and wild type plants were similar to each other as shown in Figure 3.12. It seems that the *AtCHIP* knock-out did not cause a defect in response to high-intensity light.

Oxidative stress is another factor that can induce unfolded protein stress in cells. It can affect the formation of disulfide bond and cause protein misfolding. Therefore, paraquat, a herbicide and free-radical reagent, was added into 1/2 MS medium. The oxidative stress test was done in both normal and high-intensity light conditions, as oxidative stress can enhance photodamage in the chloroplast. Under both normal and high-intensity light conditions, the average primary root length of *Atchip-1* was indistinguishable from that of wild type seedlings (Figure 3.13). *Atchip-1* did not show any observable defect under oxidative stress.

In addition, results from seed longevity tests (Figures 3.7 - 3.9) showed that after enduring a period of high temperature and high humidity storage conditions, the *Atchip-1* and wild type

seeds germinated similarly. Therefore, the *AtCHIP* knock-out does not alter the seed viability during storage and does not lead to a defective response to protein misfolding induced by environmental stress during seed development.

The lack of a clear phenotype in the *Atchip-1* mutant might be due to a narrow range of substrates or functional redundancy with other E3 ligases. In this regard, several AtCHIP substrates reported to be ubiquitinated by AtCHIP for degradation are so far all chloroplast proteins (Lee *et al.*, 2009; Shen *et al.*, 2007a; Shen *et al.*, 2007b). Moreover, it is possible that E3s other than AtCHIP may interact with Hsp70 proteins. For example, Arabidopsis SGT1 interacts with Hsc70 chaperones (Noel *et al.*, 2007), and SGT1 is known to be associated with some subunits of SCF-type E3 (Azevedo *et al.*, 2002; Liu *et al.*, 2002). Therefore, mediated by SGT1, SCF-type E3s may be recruited to Hsc70 for the degradation of unfolded substrates. In animals, one E3 ligase that may be functionally redundant is Parkin which is an E3 ligase capable of interacting with Hsp70 in mammalian cells (Tsai *et al.*, 2003; Zhang *et al.*, 2000). The loss-of-function mutation of Parkin is related to Parkinson disease (Kitada *et al.*, 1998). Interestingly, in mouse cells Parkin was found to be able to interact with two substrates of CHIP, neuronal nitric-oxide synthase (nNOS) and a polyglutamine-expanded protein (Q78 ataxin-3), and to induce degradation of both CHIP substrate proteins (Morishima *et al.*, 2008). Although evidence is yet to be obtained, it is tempting to speculate that there may be one or more E3s that function redundantly with AtCHIP in Arabidopsis. However, based on sequence analysis alone no Parkin orthologs have been identified in Arabidopsis. Parkin is a RING-IBR-RING (RBR)-type protein which possesses two RING finger domains and an in-between ring-finger (IBR). A phylogenetic analysis indicates that subfamilies of RBR proteins in Arabidopsis are quite distinct from Parkin (Marin and Ferrus, 2002). Moreover, there are at least 42 RBR proteins in Arabidopsis (Marin, 2010), and further experimental work will be needed to determine whether one or more of the RBR proteins share any functional redundancy with AtCHIP.

## 4.2 AtCHIP and Homeostasis of Chloroplast Protein Turnover

In plants, Hsp70 molecular chaperones are involved in the import of chloroplast proteins (Wang *et al.*, 2004). Cytosolic Hsp70 proteins may assist the import process through association with chloroplast-destined precursor proteins and maintain these proteins in the unfolded state until being recognized by the translocation machinery on the surface of the chloroplast. AtCHIP may regulate the degradation of chloroplast proteins through its interaction with Hsp70 proteins. AtCHIP has been found to induce degradation of FtsH1 and ClpP4 which are subunits of the protease complexes FtsH and Clp, respectively (Shen *et al.*, 2007a; Shen *et al.*, 2007b). AtCHIP was also shown to reduce the level of a reporter polypeptide, which accumulated in the cytosol due to delayed import into the chloroplast (Lee *et al.*, 2009).

High-intensity light can induce photodamage of chloroplast proteins, which in turn will affect the homeostasis of protein turnover in the chloroplast. It remains a question whether the loss of AtCHIP function in degrading chloroplast precursor proteins in the cytosol would have any impact on chloroplast homeostasis. *Atchip-1* plants did not show any difference from wild type plants under high-intensity light (Figure 3.12B), although both wild type and mutant plants flowered earlier compared to corresponding plants under normal light conditions. Since the light intensity was not very high in the growth facilities we had, we reasoned that strong light and oxidative stress (by including Paraquat in the growth medium) simultaneously could increase photodamage in the chloroplast. However, the mutant plants did not show any difference from wild type plants either (see Figures 3.13B and D). Interestingly, overexpression of *AtCHIP* resulted in a necrosis phenotype on the leaves of Arabidopsis plants (Shen *et al.*, 2007a). It was hypothesized that, because a high level of AtCHIP led to excess degradation of precursors of some FtsH protease subunits, certain damaged proteins inside the chloroplast could not be metabolized (Shen *et al.*, 2007a). If this is true, the present results suggest that either the removal of chloroplast-destined precursor proteins in the cytosol by AtCHIP does not have a vital role in response to photodamage in the chloroplast, or another E3

can carry out this function.

### 4.3 Other Potential Functions of AtCHIP

In animal cells the CHIP protein also has non-degradative roles by modifying substrates. Animal CHIP autoubiquitinates itself *in vitro* and is also found to modify Hsc70 (a member of Hsp70 family) with an atypical polyUb chain (Lys63- or Lys29- linkage) that does not induce protein degradation by UPS (Jiang *et al.*, 2001). This is supported by the evidence that CHIP interacts with the Ubc13-Uev1a complex which is an E2 specifically catalyzing Lys63-linked polyubiquitination (Zhang *et al.*, 2005). Such a UPS independent function was also discovered in the case of AtCHIP in *A. thaliana*. AtCHIP was found to monoubiquitinate PP2A, and overexpressing AtCHIP resulted in increased enzymatic activity of PP2A (Luo *et al.*, 2006). In addition, AtCHIP can possibly catalyze Lys63-linked polyubiquitination, as it interacts with the Arabidopsis Ubc13-Uev E2 complex (Supplement Figure S1).

We reasoned that AtCHIP might participate in functions regulated by plant hormones. For instance monoubiquitination of PP2A by AtCHIP might affect the ABA response of Arabidopsis plants (Luo *et al.*, 2006). In this research, six major plant hormones plus high sucrose concentration were used to test *Atchip-1*. The results (Figure 3.1) indicate that *Atchip-1* did not appear to respond differently from wild type plants to the test conditions.

A T-DNA null mutation in *AtUEV1D* that encodes a component of an E2 catalyzing Lys63-linked polyubiquitination has led to increased sensitivity of Arabidopsis plants to the DNA damaging reagent MMS (Wen *et al.*, 2008). MMS was also used to test *Atchip-1* in this study. Based on primary root length data, in the presence of MMS *Atchip-1* seedlings grew similarly to wild type seedlings. Thus, it seems that the DNA-damage response is not affected by the disruption of *AtCHIP*.

The objective of the hormonal and MMS tests was to see if *Atchip-1* mutants display any observable phenotypes and if so to investigate the biochemical and cellular basis underlying

such a phenotype. Unfortunately, no clear phenotype was observed under the hormonal and DNA-damage treatment conditions used.

### 4.4 E3-A Family

An *in vitro* ubiquitination assay by Stone *et al.* (2005) showed that the product of At1g74370 (tentatively named E3-A1) was able to assemble polyUb chain with AtUBC13A and AtUBC13B as E2s. Further functional characterization of E3-A1 can lead to a better understanding of Lys63-linked polyubiquitination in plants. Thus, we were interested in determining the function of this gene family in plants. Sequence analysis showed that there are at least three related proteins in the E3-A family (At1g74370, At1g69330 and At3g29270), with two of the three more closely related to each other (Figure 3.15A). E3-A1, A2 and A3 share a high degree of sequence identity in regions of the N-terminal RING domain and two possible C-terminal transmembrane domains (according to domain prediction by the SMART program, see Figure 3.15B, C and Table 3.1).

In order to identify possible effects from the down-regulation of *E3-A* genes, transgenic lines expressing micro RNA constructs which specifically silence *E3-A1* and *E3-A2* gene transcripts were generated in our lab (Figures 3.16 and 3.17). Several hormonal and salt stress treatments were applied to the RNAi plants. However, neither single RNAi transformants nor double RNAi transformants showed any observable difference from wild type plants under the test conditions (Figure 3.18). It is likely that E3-A3, the third member of E3-A family, is functionally redundant with the other two E3-As. Based on the E3-A3 protein sequence, it also possesses a RING finger at the N-terminus and two putative transmembrane domains at the C-terminus similar to E3-A1 and E3-A2 proteins. This similarity indicates that the E3-A3 protein may have same subcellular localization (cytoplasmic surface of plasma membrane or intracellular organelles) and overlapping E3 ligase specificity. On the other hand, results of *in vitro* ubiquitination assays using different pairs of E2s and RING-type E3s (supplement data of

Stone *et al.*, 2005) showed that E3-A1 catalyzed polyUb chain formation with AtUBC13A and AtUBC13B whereas E3-A3 did not. Thus, although these two E3s share a certain degree of sequence similarity, E3-A3 may not catalyze Lys63-linked polyubiquitination. However, possibilities still remain that atypical polyUb chain linkages other than a Lys63-linkage are assembled by E3-As with different E2s, and these different types of polyUb signal may contribute to the overlapping activities among E3-A family members. Therefore, down-regulation of all three *E3-A* genes by crossing the double RNAi line with T-DNA null mutant of *E3-A3* gene will be required to address this issue and increase the possibility of observing a phenotype.

Although the RNAi mutants used in this study showed significant down-regulation of both *E3-A1* and *E3-A2* transcripts with mRNA levels decreased by over 90 percent compared to wild type plants based on RT-PCR results, it is difficult to completely eliminate gene expression by the RNAi approach. The remaining level of E3-A1 and E3-A2 expression may be able to provide a low level of activity for each protein, alleviating the severity of a possible phenotype from down-regulation. On the other hand, if a gene is essential for plant development or a biological process, a complete knock-out of such a gene often leads to severe developmental defects or infertility.

### 4.5 Phenotypic Analyses of *A. thaliana*

Considering the wide range of functions ubiquitination (E3 ligases) may be involved in, the number of conditions included for testing in the present research is still limited (Smalle and Vierstra, 2004). In addition, in many cases a phenotype in a loss-of-function mutant can only be identified by treating plants with a combination of conditions, and sometimes effects of down-regulation may not be observed until plants are grown for several generations (Bouche and Bouchez, 2001). Thus, it is difficult to conduct all possible assays for identifying a phenotype. In this study, we selected conditions which we reasoned could provide a good

chance for identifying a phenotype in hormonal regulation and response to environmental conditions. These assays were also chosen since we could establish the experimental conditions with the facilities available.

It was observed initially that *Atchip-1* plants showed an increased sensitivity to ABA in terms of germination and cotyledon greening while they showed no difference in the absence of ABA (Figures 3.4 and 3.5). Subsequently, the same experiment was repeated using mutant and wild type seeds harvested at the exact same time from plants grown side-by-side. In this new round of ABA experiment (Figure 3.6), however, seed germination and greening rates were similar between mutant and wild type plants. In addition, the primary root length, fresh weight and dry weight of seedlings were also comparable. Thus, it appears that a minor difference in seed quality was the underlying reason for the increased inhibition of *Atchip-1* seed germination and development by ABA. Furthermore, in seed longevity tests *Atchip-1* seeds did not show accelerated deterioration compared to wild type seeds (Figures 3.7-3.9). Although eventually an effect on ABA response or seed longevity could not be found due to *AtCHIP* inactivation, it seems that minor seed quality differences not observable when seedlings are grown under normal conditions can cause differences in seed germination and seedling growth in the presence of ABA. This observation will be helpful for future phenotypic studies. In fact, a similar phenomenon was also observed when RNAi transformants for the *E3-A* genes were analyzed with ABA (comparing Figure 3.18 and Figure 3.19). The RNAi transformants and wild type seeds grew differently in ABA plates, which was however probably due to different seed quality.

ABA inhibits seed germination, and it has been reported that a decrease of ABA content in the seeds can trigger the release of seed dormancy (Sondheim *et al.*, 1968). It is also known that seed metabolites during seed dormancy release and germination can serve as regulatory signals (Wobus and Weber, 1999). For example, metabolism of certain types of sugar could affect the ABA content in seeds (Gubler *et al.*, 2005). After seed maturation, seeds turn into dormant state during seed storage until this state is released when growth conditions are suitable

for germination. It is possible that during seed maturation and storage, environmental conditions may affect seed metabolism, resulting in slight variations in ABA levels during seed germination. Regardless of the mechanism underlying this variation in response to ABA treatment, the present results highlight the importance of uniformity in seed quality when comparing different Arabidopsis lines (control vs. test lines) particularly for ABA sensitivity. Extra care needs to be taken in evaluating the phenotype of mutants under stress conditions compared to wild type plants.

### 4.6 General Discussion and Future Work

While the Ub system in plants has its general biochemical significance like that of yeast and animals, it also has characteristics unique to plants such as involvement in hormonal regulation and in complex environmental response mechanisms (Smalle and Vierstra, 2004). Studies on E3 ligases can provide valuable perspective on detailed roles of protein ubiquitination in specific cellular activities. For a well-studied model organism like *A. thaliana*, the entire genome of which has been sequenced, one of the most popular ways to characterize a given gene and its product is to down-regulate gene expression in order to gain an understanding of the role in the plant. For E3 ligases which catalyze noncanonical ubiquitination, as their activities are believed to activate some components of intracellular signaling pathways instead of eliminating substrates through the UPS, it is hoped that the gene knockout approach can generate much needed information regarding their roles in specific cellular processes.

There are at least two major challenges in searching for possible phenotypes. The first challenge is the redundancy of gene functions (Cutler and McCourt, 2005). Second, in many cases phenotypic changes will not be seen in an ideal growth environment in laboratories unless mutant plants are exposed to abnormal conditions (Bouche and Bouchez, 2001). One way to address functional redundancy in the genome is to abolish the expression of closely related genes simultaneously, and thus eliminate related gene products that have overlapping roles. In

this study, a loss-of-function T-DNA insertion mutant of the *AtCHIP* gene was identified, and effective RNAi transformant lines for *E3-A1* and *E3-A2* genes were generated in our laboratory. An advantage with the *AtCHIP* gene is its apparently unique sequence, for no closely related sequence is found in the Arabidopsis genome. For *E3-A* gene family, however, *E3-A1* and *E3-A2* genes were down-regulated simultaneously by expressing RNAi constructs targeting both genes in the plants. In order to identify potential phenotypes not observed in normal condition, typical hormones and stress conditions were based on to test mutant plants. However, in spite of considerable efforts made to obtain distinct phenotypes of mutants, so far no clear phenotypes have been observed.

Although the phenotypic analyses in this study did not uncover roles for AtCHIP and E3-A ligases in specific cellular and biological processes, the analytical system which has been established in this research can be helpful in the characterization of other genes in Arabidopsis. Based on similar sets of parameters to be measured, a broader range of hormones, other chemicals and abiotic conditions can be used to test mutant plants. By trying more treatments in future, it may still be possible to identify a mutant phenotype. Bioinformatics and biochemical analyses may help to focus on aspects of plant growth and stress response that should be examined.

To further understanding AtCHIP functions, its activity in catalyzing noncanonical ubiquitination will continue to be an interesting subject. The significance of such a biochemical function will be enhanced when a role in a cellular or biological process is identified. Since the Lys63-linked polyubiquitination is widely involved in endocytosis of membrane proteins, some work may be done in this area in future. It is still unclear whether the same protein quality control system exists in plants as in animal models. The knockout of *AtCHIP* did not cause severe phenotype in morphology in normal growth environment as *CHIP* gene knockout did in animal models, which may be a reflection of differences between plants and animals. This difference suggests that plants have more diverse stress-tolerance mechanisms. Perhaps due to the lack of a nervous system and mobility, plants have to adapt

their metabolism to harsh environments more readily than animals. Therefore, future studies on the regulation of related molecular pathways in plant cells may help understand the special roles of AtCHIP in plant cytosolic protein quality control or in other functions unique to plants. For members of the E3-A family, though, the *E3-A3* gene may have to be interrupted at the same time as the other two *E3-A* genes are silenced by an RNAi approach, in order to eliminate the possible overlapping function of these E3-A proteins. Furthermore, the predicted transmembrane domains imply a possible phenotype as a result of blocking E3-A functions in triggering endocytosis of cytoplasmic membrane proteins or cellular signal transduction involving the membrane structures.

## APPENDICES

The interaction between AtCHIP and AtUBC13A was confirmed in the yeast two-hybrid system and also by a glutathione S-transferase (GST)-affinity pull-down assay. Yeast two-hybrid assay was done by Rui Wen as described in Rui *et al.* (2008). The U-box domain (RF) or full length (FL) AtCHIP was fused with a Gal4 activation domain and AtUBC13A with a Gal4 DNA binding domain. The yeast two-hybrid strain was co-transformed with $Gal4_{BD}$ and $Gal4_{AD}$ constructs and co-transformed colonies were first selected on SD-Leu-Trp plates. As shown in Figure S1, both the U-box domain and full-length AtCHIP interact with AtUBC13A.

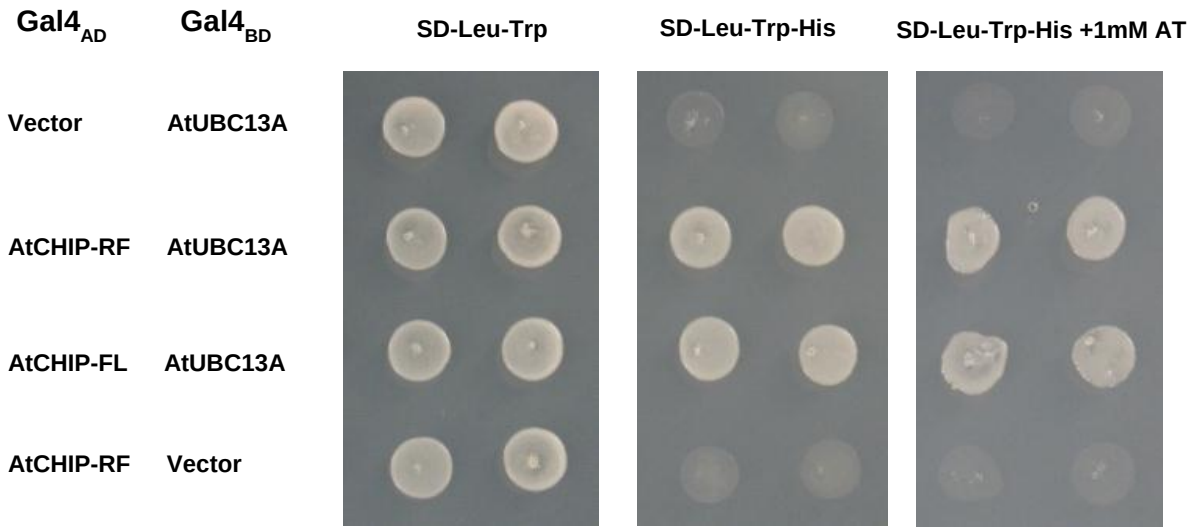


**Figure S1** Interactions between full-length (FL) or U-box (RF) domain of AtCHIP and AtUbc13A in a yeast two-hybrid assay. $Gal4_{AD}$: constructs in the Gal4 activation domain (AD) vector. $Gal4_{BD}$: constructs in the Gal4 DNA-binding domain (BD) vector. The transformants carrying one $Gal4_{AD}$ construct and one $Gal4_{BD}$ construct were plated on: SD-Leu-Trp plates (left panel), or SD-Leu-Trp-His (middle panel), or SD-His-Leu-Trp + 1 mM 3-AT plates (right panel), and incubated for three days. Empty pGAD424 and pGBT9 vectors were used as negative controls for $Gal4_{AD}$ and $Gal4_{BD}$, respectively. In the same panel each row is a duplication of the same combination of $Gal4_{AD}$ and $Gal4_{BD}$ constructs.

The interaction between AtCHIP and AtUBC13A was also shown in a GST pull-down assay. As described by Rui *et al.* (2008), AtCHIP with a GST tag was expressed in bacterial cells and purified. After the GST tag was cleaved off, purified AtCHIP was added to a microspin column bound with GST and to one with GST-AtUBC13A. After incubation and washing, AtCHIP was eluted together with GST-AtUBC13A, yet not with GST (Figure S2), which indicates the interaction between AtCHIP and AtUBC13A.

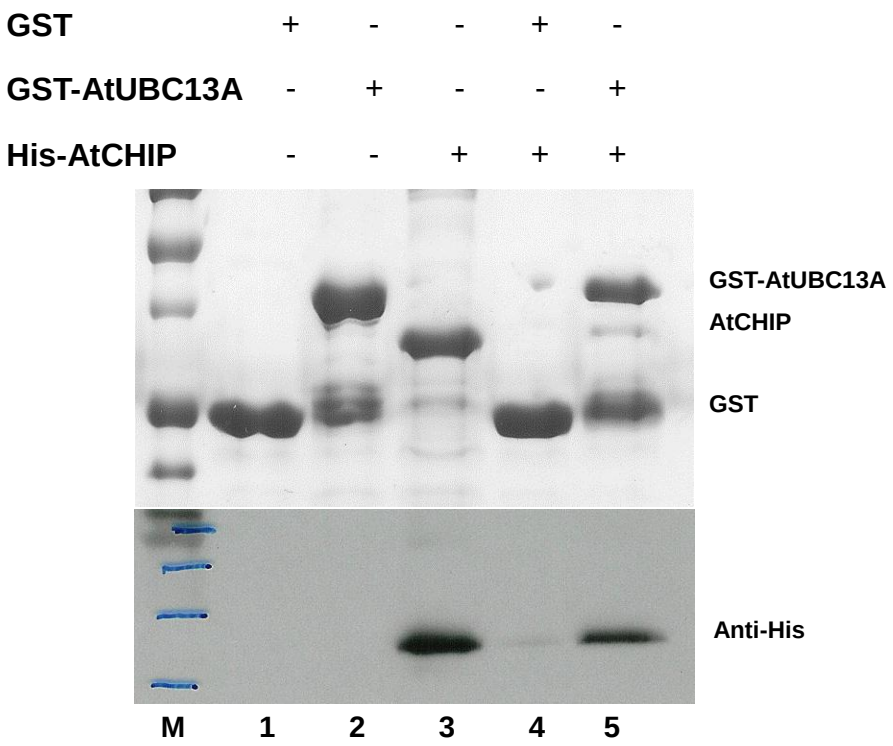


**Figure S2** Protein interaction between AtCHIP and AtUBC13A is shown by a GST pull-down assay. Purified GST or GST-AtUBC13A was added to a microspin column. After incubation, columns were spun and washed. Following that, purified AtCHIP was added, and columns were again incubated, spun and washed. In the end, columns were eluted with reduced glutathione, and the eluent separated by SDS-PAGE gel electrophoresis. Purified GST, GST-AtUBC13A and His-AtCHIP as input in pull-down assay are shown in lanes 1 to 3, respectively; lane 4 shows the eluent from the column bound with GST (lane 1); lane 5 shows the eluent from the columns bound with GST-AtUBC13 (lane 2).

Reference List

Agne, B., and Kessler, F. (2009). Protein transport in organelles: the Toc complex way of preprotein import. FEBS J. *276,* 1156-1165.

Alonso, J.M., Stepanova, A., Leisse, T., Kim, C., Chen, H., Shinn, P., Stevenson, D., Zimmerman, J., Barajas, P., Cheuk, R., *et al.* (2003). Genome-wide insertional mutagenesis of *Arabidopsis thaliana* . Science *301,* 653-657.

Andersen, P.L., Zhou, H.L., Pastushok, L., Moraes, T., McKenna, S., Ziola, B., Ellison, M.J., Dixit, V.M., and Xiao, W. (2005). Distinct regulation of Ubc13 functions by the two ubiquitin-conjugating enzyme variants Mms2 and Uev1A. J. Cell Biol. *170,* 745-755.

Aravind, L., and Koonin, E.V. (2000). The U box is a modified RING finger - a common domain in ubiquitination. Curr. Biol. *10,* R132-R134.

Azevedo, C., Sadanandom, A., Kitagawa, K., Freialdenhoven, A., Shirasu, K., and Schulze-Lefert, P. (2002). The RAR1 interactor SGT1, an essential component of *R* gene-triggered disease resistance. Science *295,* 2073-2076.

Bache, K.G., Slagsvold, T., and Stenmark, H. (2004). Defective downregulation of receptor tyrosine kinases in cancer. EMBO J. *23,* 2707-2712.

Bachmair, A., Novatchkova, M., Potuschak, T., and Eisenhaber, F. (2001). Ubiquitylation in plants: a post-genomic look at a post-translational modification. Trends Plant Sci. *6,* 463-470.

Ballinger, C.A., Connell, P., Wu, Y.X., Hu, Z.Y., Thompson, L.J., Yin, L.Y., and Patterson, C. (1999). Identification of CHIP, a novel tetratricopeptide repeat-containing protein that interacts with heat shock proteins and negatively regulates chaperone functions. Mol. Cell. Biol. *19,* 4535-4545.

Barriere, H., Nemes, C., Du, K., and Lukacs, G.L. (2007). Plasticity of polyubiquitin recognition as lysosomal targeting signals by the endosomal sorting machinery. Mol. Biol. Cell *18,* 3952-3965.

Behrends, C., and Harper, J.W. (2011). Constructing and decoding unconventional ubiquitin chains. Nat. Struct. Mol. Biol. *18,* 520-528.

Bennett, E.J., and Harper, J.W. (2008). DNA damage: ubiquitin marks the spot. Nat. Struct. Mol. Biol. *15,* 20-22.

Bennetzen, J.L. (2001). Arabidopsis arrives. Nat. Genet. *27,* 3-5.

Bernassola, F., Karin, M., Ciechanover, A., and Melino, G. (2008). The HECT family of E3 ubiquitin ligases: Multiple players in cancer development. Cancer Cell *14,* 10-21.

Bouche, N., and Bouchez, D. (2001). Arabidopsis gene knockout: phenotypes wanted. Curr. Opin. Plant Biol. *4,* 111-117.

Broomfield, S., Chow, B.L., and Xiao, W. (1998). MMS2, encoding a ubiquitin-conjugating-enzyme-like protein, is a member of the yeast error-free postreplication repair pathway. Proc. Natl. Acad. Sci. USA *95,* 5678-5683.

Brummelkamp, T.R., Nijman, S.M.B., Dirac, A.M.G., and Bernards, R. (2003). Loss of the cylindromatosis tumour suppressor inhibits apoptosis by activating NF-kappa B. Nature *424,* 797-801.

Callis, J., Carpenter, T., Sun, C.W., and Vierstra, R.D. (1995). Structure and evolution of genes encoding polyubiquitin and ubiquitin-like proteins in *Arabidopsis thaliana* ecotype Columbia. Genetics *139,* 921-939.

Callis, J., Raasch, J.A., and Vierstra, R.D. (1990). Ubiquitin extension proteins of *Arabidopsis thaliana*: structure, localization, and expression of their promoters in transgenic tobacco. J. Biol. Chem. *265,* 12486-12493.

Cao, Y., Dai, Y., Cui, S., and Ma, L. (2008). Histone H2B monoubiquitination in the chromatin of *FLOWERING LOCUS C* regulates flowering time in Arabidopsis. Plant Cell *20,* 2586-2602.

Cardozo, T., and Pagano, M. (2004). The SCF ubiquitin ligase: insights into a molecular machine. Nat. Rev. Mol. Cell Biol. *5,* 739-751.

Chen, Z.J., and Sun, L.J. (2009). Nonproteolytic Functions of Ubiquitin in Cell Signaling. Mol. Cell *33,* 275-286.

Christensen, D.E., Brzovic, P.S., and Klevit, R.E. (2007). E2-BRCA1 RING interactions dictate synthesis of mono- or specific polyubiquitin chain linkages. Nat. Struct. Mol. Biol. *14,* 941-948.

Ciechanover, A., Elias, S., Heller, H., and Hershko, A. (1982). "Covalent affinity" purification of ubiquitin-activating enzyme. J. Biol. Chem. *257,* 2537-2542.

Ciechanover, A., Heller, H., Katzetzion, R., and Hershko, A. (1981). Activation of the heat-stable polypeptide of the ATP-dependent proteolytic system. Proc. Natl. Acad. Sci. USA *78,* 761-765.

Clough, S.J., and Bent, A.F. (1998). Floral dip: a simplified method for *Agrobacterium*-mediated transformation of *Arabidopsis thaliana* . Plant J. *16,* 735-743.

Connell, P., Ballinger, C.A., Jiang, J.H., Wu, Y.X., Thompson, L.J., Hohfeld, J., and Patterson, C. (2001). The co-chaperone CHIP regulates protein triage decisions mediated by heat-shock proteins. Nat. Cell Biol. *3,* 93-96.

Cutler, S., and McCourt, P. (2005). Dude, where's my phenotype? Dealing with redundancy in signaling networks. Plant Physiol. *138,* 558-559.

Deng, L., Wang, C., Spencer, E., Yang, L.Y., Braun, A., You, J.X., Slaughter, C., Pickart, C., and Chen, Z.J. (2000). Activation of the I kappa B kinase complex by TRAF6 requires a dimeric ubiquitin-conjugating enzyme complex and a unique polyubiquitin chain. Cell *103,* 351-361.

Deshaies, R.J., and Joazeiro, C.A.P. (2009). RING domain E3 ubiquitin ligases. Annu. Rev. Biochem. *78,* 399-434.

Dharmasiri, N., Dharmasiri, S., Weijers, D., Lechner, E., Yamada, M., Hobbie, L., Ehrismann, J.S., Jurgens, G., and Estelle, M. (2005). Plant development is regulated by a family of auxin receptor F box proteins. Dev. Cell *9,* 109-119.

Disteche, C.M., Zacksenhaus, E., Adler, D.A., Bressler, S.L., Keitz, B.T., and Chapman, V.M. (1992). Mapping and expression of the ubiquitin-activating enzyme E1 (*Ube1*) gene in the mouse. Mamm. Genome *3,* 156-161.

Doil, C., Mailand, N., Bekker-Jensen, S., Menard, P., Larsen, D.H., Pepperkok, R., Ellenberg, J., Panier, S., Durocher, D., Bartek, J., Lukas, J., and Lukas, C. (2009). RNF168 binds and amplifies ubiquitin conjugates on damaged chromosomes to allow accumulation of repair proteins. Cell *136,* 435-446.

Downes, B., and Vierstra, R. (2005). Post-translational regulation in plants employing a diverse set of polypeptide tags. Biochem. Soc. Trans. *33,* 393-399.

Downes, B.P., Stupar, R.M., Gingerich, D.J., and Vierstra, R.D. (2003). The HECT ubiquitin-protein ligase (UPL) family in Arabidopsis: UPL3 has a specific role in trichome development. Plant J. *35,* 729-742.

Dunn, R., Klos, D., Adler, A., and Hicke, L. (2004). The C2 domain of the Rsp5 ubiquitin ligase binds membrane phosphoinositides and directs ubiquitination of endosomal cargo. J. Cell Biol. *165,* 135-144.

Ea, C.K., Deng, L., Xia, Z.P., Pineda, G., and Chen, Z.J.J. (2006). Activation of IKK by TNF alpha requires site-specific ubiquitination of RIP1 and polyubiquitin binding by NEMO. Mol. Cell *22,* 245-257.

Eddins, M.J., Carlile, C.M., Gomez, K.M., Pickart, C.M., and Wolberger, C. (2006). Mms2-Ubc13 covalently bound to ubiquitin reveals the structural basis of linkage-specific polyubiquitin chain formation. Nat. Struct. Mol. Biol. *13,* 915-920.

Edwards, K., Johnstone, C., and Thompson, C. (1991). A simple and rapid method for the preparation of plant genomic DNA for PCR analysis. Nucleic Acids Res. *19,* 1349-1349.

Finley, D., Sadis, S., Monia, B.P., Boucher, P., Ecker, D.J., Crooke, S.T., and Chau, V. (1994). Inhibition of proteolysis and cell cycle progression in a multiubiquitination-deficient yeast mutant. Mol. Cell. Biol. *14,* 5501-5509.

Finley, D. (2009). Recognition and processing of ubiquitin-protein conjugates by the proteasome. Annu. Rev. Biochem. *78,* 477-513.

Freemont, P.S. (1993). The RING finger - a novel protein-sequence motif related to the zinc-finger. Ann. NY Acad. Sci. *684,* 174-192.

Galan, J.M., and HaguenauerTsapis, R. (1997). Ubiquitin Lys63 is involved in ubiquitination of a yeast plasma membrane protein. EMBO J. *16,* 5847-5854.

Garoff, H., Hewson, R., and Opstelten, D.J.E. (1998). Virus maturation by budding. Microbiol. Mol. Biol. Rev. *62,* 1171-1190.

Geetha, T., Jiang, J.X., and Wooten, M.W. (2005). Lysine 63 polyubiquitination of the nerve growth factor receptor TrkA directs internalization and signaling. Mol. Cell *20,* 301-312.

Glickman, M.H., and Ciechanover, A. (2002). The ubiquitin-proteasome proteolytic pathway: destruction for the sake of construction. Physiol. Rev. *82,* 373-428.

Glickman, M.H., Rubin, D.M., Coux, O., Wefes, I., Pfeifer, G., Cjeka, Z., Baumeister, W., Fried, V.A., and Finley, D. (1998). A subcomplex of the proteasome regulatory particle required for ubiquitin-conjugate degradation and related to the COP9-signalosome and eIF3. Cell *94,* 615-623.

Goettsch, S., and Bayer, P. (2002). Structural attributes in the conjugation of ubiquitin, SUMO and RUB to protein substrates. Front. Biosci. *7,* A148-A162.

Groettrup, M., Pelzer, C., Schmidtke, G., and Hofmann, K. (2008). Activating the ubiquitin family: UBA6 challenges the field. Trends Biochem. Sci. *33,* 230-237.

Gubler, F., Millar, A.A., and Jacobsen, J.V. (2005). Dormancy release, ABA and pre-harvest sprouting. Curr. Opin. Plant Biol. *8,* 183-187.

Haas, A.L., Warms, J.V.B., Hershko, A., and Rose, I.A. (1982). Ubiquitin-activating enzyme: mechanism and role in protein-ubiquitin conjugation. J. Biol. Chem. *257,* 2543-2548.

Haglund, K., Di Fiore, P.P., and Dikic, I. (2003). Distinct monoubiquitin signals in receptor endocytosis. Trends Biochem. Sci. *28,* 598-603.

Haglund, K., and Dikic, I. (2005). Ubiquitylation and cell signaling. EMBO J. *24,* 3353-3359.

Hanna, J., Hathaway, N.A., Tone, Y., Crosas, B., Elsasser, S., Kirkpatrick, D.S., Leggett, D.S., Gygi, S.P., King, R.W., and Finley, D. (2006). Deubiquitinating enzyme Ubp6 functions noncatalytically to delay proteasomal degradation. Cell *127,* 99-111.

Hatakeyama, S., and Nakayama, K. (2003). U-box proteins as a new family of ubiquitin ligases. Biochem. Biophys. Res. Commun. *302,* 635-645.

Hatakeyama, S., Yada, M., Matsumoto, M., Ishida, N., and Nakayama, K.I. (2001). U box proteins as a new family of ubiquitin-protein ligases. J. Biol. Chem. *276,* 33111-33120.

Hatfield, P.M., Callis, J., and Vierstra, R.D. (1990). Cloning of ubiquitin activating enzyme from wheat and expression of a functional protein in *Escherichia coli*.. J. Biol. Chem. *265,* 15813-15817.

Hatfield, P.M., Gosink, M.M., Carpenter, T.B., and Vierstra, R.D. (1997). The ubiquitin-activating enzyme (E1) gene family in *Arabidopsis thaliana*. Plant J. *11,* 213-226.

Hershko, A., and Ciechanover, A. (1998). The ubiquitin system. Annu. Rev. Biochem. *67,* 425-479.

Hicke, L. (2001). Protein regulation by monoubiquitin. Nat. Rev. Mol. Cell Biol. *2,* 195-201.

Hicke, L. (1999). Gettin' down with ubiquitin: turning off cell-surface receptors, transporters and channels. Trends Cell Biol. *9,* 107-112.

Hicke, L., and Riezman, H. (1996). Ubiquitination of a yeast plasma membrane receptor signals its ligand-stimulated endocytosis. Cell *84*, 277-287.

Hochstrasser, M. (1996). Ubiquitin-dependent protein degradation. Annu. Rev. Genet. *30*, 405-439.

Hofmann, R.M., and Pickart, C.M. (1999). Noncanonical MMS2-encoded ubiquitin-conjugating enzyme functions in assembly of novel polyubiquitin chains for DNA repair. Cell *96*, 645-653.

Huang, F., Kirkpatrick, D., Jiang, X., Gygi, S., and Sorkin, A. (2006). Differential regulation of EGF receptor internalization and degradation by multiubiquitination within the kinase domain. Mol. Cell *21*, 737-748.

Huen, M.S.Y., Sy, S.M.H., and Chen, J. (2010). BRCA1 and its toolbox for the maintenance of genome integrity. Nat. Rev. Mol. Cell Biol. *11*, 138-148.

Huibregtse, J.M., Scheffner, M., Beaudenon, S., and Howley, P.M. (1995). A family of proteins structurally and functionally related to the E6-AP ubiquitin-protein ligase. Proc. Natl. Acad. Sci. USA *92*, 2563-2567.

Hurley, J.H., and Emr, S.D. (2006). The ESCRT complexes: Structure and mechanism of a membrane-trafficking network. Annu. Rev. Biophys. Biomol. Struct. *35*, 277-298.

Ikeda, F., and Dikic, I. (2008). Atypical ubiquitin chains: new molecular signals - 'protein modifications: beyond the usual suspects' review series. EMBO Rep. *9*, 536-542.

Jackson, S.E. (2006). Ubiquitin: a small protein folding paradigm. Org.Biomol.Chem. *4*, 1845-1853.

Jentsch, S. (1992). The ubiquitin-conjugation system. Annu. Rev. Genet. *26*, 179-207.

Jiang, J.H., Ballinger, C.A., Wu, Y.X., Dai, Q., Cyr, D.M., Hohfeld, J., and Patterson, C. (2001). CHIP is a U-box-dependent E3 ubiquitin ligase: identification of Hsc70 as a target for ubiquitylation. J. Biol. Chem. *276*, 42938-42944.

Jones, A.M., Chory, J., Dangl, J.L., Estelle, M., Jacobsen, S.E., Meyerowitz, E.M., Nordborg, M., and Weigel, D. (2008). The impact of Arabidopsis on human health: diversifying our portfolio. Cell *133*, 939-943.

Kanayama, A., Seth, R.B., Sun, L.J., Ea, C.K., Hong, M., Shaito, A., Chiu, Y.H., Deng, L., and Chen, Z.J. (2004). TAB2 and TAB3 activate the NF-kappa B pathway through binding to polyubiquitin chains. Mol. Cell *15,* 535-548.

Kay, G.F., Ashworth, A., Penny, G.D., Dunlop, M., Swift, S., Brockdorff, N., and Rastan, S. (1991). A candidate spermatogenesis gene on the mouse Y chromosome is homologous to ubiquitin-activating enzyme E1. Nature *354,* 486-489.

Kee, Y., and Huibregtse, J.M. (2007). Regulation of catalytic activities of HECT ubiquitin ligases. Biochem. Biophys. Res. Commun. *354,* 329-333.

Kee, Y., Munoz, W., Lyon, N., and Huibregtse, J.M. (2006). The deubiquitinating enzyme Ubp2 modulates Rsp5-dependent Lys(63)-linked polyubiquitin conjugates in *Saccharomyces cerevisiae* . J. Biol. Chem. *281,* 36724-36731.

Kepinski, S., and Leyser, O. (2005). The Arabidopsis F-box protein TIR1 is an auxin receptor. Nature *435,* 446-451.

Khan, L.A., and Nukina, N. (2004). Molecular and functional analysis of *Caenorhabditis elegans* CHIP, a homologue of Mammalian CHIP. FEBS Lett. *565,* 11-18.

Kim, H.T., Kim, K.P., Lledias, F., Kisselev, A.F., Scaglione, K.M., Skowyra, D., Gygi, S.P., and Goldberg, A.L. (2007). Certain pairs of ubiquitin-conjugating enzymes (E2s) and ubiquitin-protein ligases (E3s) synthesize nondegradable forked ubiquitin chains containing all possible isopeptide linkages. J. Biol. Chem. *282,* 17375-17386.

Kitada, T., Asakawa, S., Hattori, N., Matsumine, H., Yamamura, Y., Minoshima, S., Yokochi, M., Mizuno, Y., and Shimizu, N. (1998). Mutations in the parkin gene cause autosomal recessive juvenile parkinsonism. Nature *392,* 605-608.

Komada, M., and Kitamura, N. (2005). The Hrs/STAM complex in the downregulation of receptor tyrosine kinases. J. Biochem. *137,* 1-8.

Komander, D. (2009). The emerging complexity of protein ubiquitination. Biochem. Soc. Trans. *37,* 937-953.

Komander, D., Reyes-Turcu, F., Licchesi, J.D.F., Odenwaelder, P., Wilkinson, K.D., and Barford, D. (2009). Molecular discrimination of structurally equivalent Lys 63-linked and linear polyubiquitin chains. EMBO Rep. *10,* 466-473.

Kraft, E., Stone, S.L., Ma, L.G., Su, N., Gao, Y., Lau, O.S., Deng, X.W., and Callis, J. (2005). Genome analysis and functional characterization of the E2 and RING-type E3 ligase ubiquitination enzymes of Arabidopsis. Plant Physiol. *139,* 1597-1611.

Krappmann, D., and Scheidereit, C. (2005). A pervasive role of ubiquitin conjugation in activation and termination of I kappa B kinase pathways. EMBO Rep. *6,* 321-326.

Lauwers, E., Jacob, C., and Andre, B. (2009). K63-linked ubiquitin chains as a specific signal for protein sorting into the multivesicular body pathway. J. Cell Biol. *185,* 493-502.

Lecker, S.H., Goldberg, A.L., and Mitch, W.E. (2006). Protein degradation by the ubiquitin-proteasome pathway in normal and disease states. J. Am. Soc. Nephrol. *17,* 1807-1819.

Lee, S., Lee, D.W., Lee, Y., Mayer, U., Stierhof, Y., Lee, S., Juergens, G., and Hwang, I. (2009). Heat shock protein cognate 70-4 and an E3 ubiquitin ligase, CHIP, mediate plastid-destined precursor degradation through the ubiquitin-26S proteasome system in Arabidopsis. Plant Cell *21,* 3984-4001.

Li, W., Bengtson, M.H., Ulbrich, A., Matsuda, A., Reddy, V.A., Orth, A., Chanda, S.K., Batalov, S., and Joazeiro, C.A.P. (2008). Genome-wide and functional annotation of human E3 ubiquitin ligases identifies MULAN, a mitochondrial E3 that regulates the organelle's dynamics and signaling. PloS ONE *3,* e1487.

Liu, Y., Schiff, M., Serino, G., Deng, X.W., and Dinesh-Kumar, S.P. (2002). Role of SCF ubiquitin-ligase and the COP9 signalosome in the *N* gene-mediated resistance response to *Tobacco mosaic virus*. Plant Cell *14,* 1483-1496.

Liu, Y., Koornneef, M., and Soppe, W.J.J. (2007).
The absence of histone H2B monoubiquitination in the Arabidopsis *hub1 (rdo4)* mutant reveals a role for chromatin remodeling in seed dormancy. Plant Cell *19,* 433-444.

Lovering, R., Hanson, I.M., Borden, K.L.B., Martin, S., Oreilly, N.J., Evan, G.I., Rahman, D., Pappin, D.J.C., Trowsdale, J., and Freemont, P.S. (1993). Identification and preliminary characterization of a protein motif related to the zinc finger. Proc. Natl. Acad. Sci. USA *90,* 2112-2116.

Luo, J., Shen, G., Yan, J., He, C., and Zhang, H. (2006). AtCHIP functions as an E3 ubiquitin ligase of protein phosphatase 2A subunits and alters plant response to abscisic acid treatment. Plant J. *46,* 649-657.

Marin, I., and Ferrus, A. (2002). Comparative genomics of the RBR family, including the Parkinson's disease-related gene Parkin and the genes of the Ariadne subfamily. Mol. Biol. Evol. *19,* 2039-2050.

Marin, I. (2010). Diversification and specialization of plant RBR ubiquitin ligases. PloS ONE *5,* e11579.

Markson, G., Kiel, C., Hyde, R., Brown, S., Charalabous, P., Bremm, A., Semple, J., Woodsmith, J., Duley, S., Salehi-Ashtiani, K., *et al.* (2009). Analysis of the human E2 ubiquitin conjugating enzyme protein interaction network. Genome Res. *19,* 1905-1911.

McDonough, H., and Patterson, C. (2003). CHIP: a link between the chaperone and proteasome systems. Cell Stress Chaperone *8,* 303-308.

Mcgrath, J.P., Jentsch, S., and Varshavsky, A. (1991). UBA 1: an essential yeast gene encoding ubiquitin-activating enzyme. EMBO J. *10,* 227-236.

McKenna, S., Moraes, T., Pastushok, L., Ptak, C., Xiao, W., Spyracopoulos, L., and Ellison, M.J. (2003). An NMR-based model of the ubiquitin-bound human ubiquitin conjugation complex Mms2 center dot Ubc13: the structural basis for lysine 63 chain catalysis. J. Biol. Chem. *278,* 13151-13158.

Meinke, D.W., Cherry, J.M., Dean, C., Rounsley, S.D., and Koornneef, M. (1998). Arabidopsis thaliana: a model plant for genome analysis. Science *282,* 662-682.

Miao, Y., and Zentgraf, U. (2010). A HECT E3 ubiquitin ligase negatively regulates Arabidopsis leaf senescence through degradation of the transcription factor WRKY53. Plant J. *63,* 179-188.

Min, J., Whaley, R.A., Sharpless, N.E., Lockyer, P., Portbury, A.L., and Patterson, C. (2008). CHIP deficiency decreases longevity, with accelerated aging phenotypes accompanied by altered protein quality control. Mol. Cell. Biol. *28,* 4018-4025.

Mitchell, M.J., Woods, D.R., Wilcox, S.A., Graves, J.A.M., and Bishop, C.E. (1992). Marsupial Y chromosome encodes a homologue of the mouse Y-linked candidate spermatogenesis gene *Ube1y*. Nature *359,* 528-531.

Mockaitis, K., and Estelle, M. (2008). Auxin receptors and plant development: a new signaling paradigm. Annu. Rev. Cell Dev. Biol. *24,* 55-80.

Morishima, Y., Wang, A.M., Yu, Z., Pratt, W.B., Osawa, Y., and Lieberman, A.P. (2008). CHIP deletion reveals functional redundancy of E3 ligases in promoting degradation of both signaling proteins and expanded glutamine proteins. Hum. Mol. Genet. *17,* 3942-3952.

Mukhopadhyay, D., and Riezman, H. (2007). Proteasome-independent functions of ubiquitin in endocytosis and signaling. Science *315,* 201-205.

Noel, L.D., Cagna, G., Stuttmann, J., Wirthmueller, L., Betsuyaku, S., Witte, C., Bhat, R., Pochon, N., Colby, T., and Parker, J.E. (2007). Interaction between SGT1 and cytosolic/nuclear HSC70 chaperones regulates Arabidopsis immune responses. Plant Cell *19,* 4061-4076.

Ohi, M.D., Vander Kooi, C.W., Rosenberg, J.A., Chazin, W.J., and Gould, K.L. (2003). Structural insights into the U-box, a domain associated with multi-ubiquitination. Nat. Struct. Biol. *10,* 250-255.

Okada, K., Ikeuchi, M., Yamamoto, N., Ono, T.A., and Miyao, M. (1996). Selective and specific cleavage of the D1 and D2 proteins of Photosystem II by exposure to singlet oxygen: factors responsible for the susceptibility to cleavage of the proteins. BBA-Bioenergetics *1274,* 73-79.

Ordureau, A., Smith, H., Windheim, M., Peggie, M., Carrick, E., Morrice, N., and Cohen, P. (2008). The IRAK-catalysed activation of the E3 ligase function of Pellino isoforms induces the Lys(63)-linked polyubiquitination of IRAK1. Biochem. J. *409,* 43-52.

Ozkaynak, E., Finley, D., and Varshavsky, A. (1984). The yeast ubiquitin gene: head-to-tail repeats encoding a polyubiquitin precursor protein. Nature *312,* 663-666.

Paiva, S., Vieira, N., Nondier, I., Haguenauer-Tsapis, R., Casal, M., and Urban-Grimal, D. (2009). Glucose-induced ubiquitylation and endocytosis of the yeast Jen1 transporter: role of lysine 63-linked ubiquitin chains. J. Biol. Chem. *284,* 19228-19236.

Papouli, E., Chen, S.H., Davies, A.A., Huttner, D., Krejci, L., Sung, P., and Ulrich, H.D. (2005). Crosstalk between SUMO and ubiquitin on PCNA is mediated by recruitment of the helicase Srs2p. Mol. Cell *19,* 123-133.

Pastushok, L., Moraes, T.F., Ellison, M.J., and Xiao, W. (2005). A single Mms2 "key" residue insertion into a Ubc13 pocket determines the interface specificity of a human Lys63 ubiquitin conjugation complex. J. Biol. Chem. *280,* 17891-17900.

Patterson, C. (2002). A new gun in town: the U box is a ubiquitin ligase domain. Science's STKE *2002,* 1-4.

Petroski, M.D., and Deshaies, R.J. (2005). Function and regulation of Cullin-RING ubiquitin ligases. Nat. Rev. Mol. Cell Biol. *6,* 9-20.

Pfander, B., Moldovan, G.L., Sacher, M., Hoege, C., and Jentsch, S. (2005). SUMO-modified PCNA recruits Srs2 to prevent recombination during S phase. Nature *436,* 428-433.

Pham, A.D., and Sauer, F. (2000). Ubiquitin-activating/conjugating activity of $TAF_{II}250$, a mediator of activation of gene expression in *Drosophila*. Science *289,* 2357-2360.

Pickart, C.M. (2001). Mechanisms underlying ubiquitination. Annu. Rev. Biochem. *70,* 503-533.

Pickart, C.M., and Fushman, D. (2004). Polyubiquitin chains: polymeric protein signals. Curr. Opin. Chem. Biol. *8,* 610-616.

Prasad, B.D., Goel, S., and Krishna, P. (2010). *In silico* identification of carboxylate clamp type tetratricopeptide repeat proteins in Arabidopsis and rice as putative co-chaperones of Hsp90/Hsp70. PloS ONE *5,* e12761.

Raasi, S., Varadan, R., Fushman, D., and Pickart, C.M. (2005). Diverse polyubiquitin interaction properties of ubiquitin-associated domains. Nat. Struct. Mol. Biol. *12,* 708-714.

Reiley, W.W., Jin, W., Lee, A.J., Wright, A., Wu, X., Tewalt, E.F., Leonard, T.O., Norbury, C.C., Fitzpatrick, L., Zhang, M., and Sun, S. (2007). Deubiquitinating enzyme CYLD negatively regulates the ubiquitin-dependent kinase Tak1 and prevents abnormal T cell responses. J. Exp. Med. *204,* 1475-1485.

Renault, L., Kuhlmann, J., Henkel, A., and Wittinghofer, A. (2001). Structural basis for guanine nucleotide exchange on Ran by the regulator of chromosome condensation (RCC1). Cell *105,* 245-255.

Robzyk, K., Recht, L., and Osley, M.A. (2000). Rad6-dependent ubiquitination of histone H2B in yeast. Science *287,* 501-504.

Roest, H.P., van Klaveren, J., de Wit, J., van Gurp, C.G., Koken, M.H.M., Vermey, M., van Roijen, J.H., Hoogerbrugge, J.W., Vreeburg, J.T.M., Baarends, W.M., *et al.* (1996). Inactivation of the HR6B ubiquitin-conjugating DNA repair enzyme in mice causes male sterility associated with chromatin modification. Cell *86,* 799-810.

Rotin, D., Staub, O., and Haguenauer-Tsapis, R. (2000). Ubiquitination and endocytosis of plasma membrane proteins: role of Nedd4/Rsp5p family of ubiquitin-protein ligases. J. Membr. Biol. *176,* 1-17.

Rotin, D., and Kumar, S. (2009). Physiological functions of the HECT family of ubiquitin ligases. Nat. Rev. Mol. Cell Biol. *10,* 398-409.

Ruffner, H., Joazeiro, C.A.P., Hemmati, D., Hunter, T., and Verma, I.M. (2001). Cancer-predisposing mutations within the RING domain of BRCA1: loss of ubiquitin protein ligase activity and protection from radiation hypersensitivity. Proc. Natl. Acad. Sci. USA *98,* 5134-5139.

Saeki, Y., Kudo, T., Sone, T., Kikuchi, Y., Yokosawa, H., Toh-e, A., and Tanaka, K. (2009). Lysine 63-linked polyubiquitin chain may serve as a targeting signal for the 26S proteasome. EMBO J. *28,* 359-371.

Sancho, E., Vila, M.R., Sanchez-Pulido, L., Lozano, J.J., Paciucci, R., Nadal, M., Fox, M., Harvey, C., Bercovich, B., Loukili, N., *et al.* (1998). Role of UEV-1, an inactive variant of the E2 ubiquitin-conjugating enzymes, in in vitro differentiation and cell cycle behavior of HT-29-M6 intestinal mucosecretory cells. Mol. Cell. Biol. *18,* 576-589.

Sato, Y., Yoshikawa, A., Yamagata, A., Mimura, H., Yamashita, M., Ookata, K., Nureki, O., Iwai, K., Komada, M., and Fukai, S. (2008). Structural basis for specific cleavage of Lys 63-linked polyubiquitin chains. Nature *455,* 358-U19.

Sato, Y., Yoshikawa, A., Yamashita, M., Yamagata, A., and Fukai, S. (2009). Structural basis for specific recognition of Lys 63-linked polyubiquitin chains by NZF domains of TAB2 and TAB3. EMBO J. *28,* 3903-3909.

Scheffner, M., and Staub, O. (2007). HECT E3s and human disease. BMC Biochem. *8,* S6.

Schmid, M., Davison, T.S., Henz, S.R., Pape, U.J., Demar, M., Vingron, M., Scholkopf, B., Weigel, D., and Lohmann, J.U. (2005). A gene expression map of Arabidopsis thaliana development. Nat. Genet. *37,* 501-506.

Schwarz, S.E., Rosa, J.L., and Scheffner, M. (1998). Characterization of human hect domain family members and their interaction with UbcH5 and UbcH7. J. Biol. Chem. *273,* 12148-12154.

Semple, C.A.M., RIKEN GER Group, and GSL Members. (2003). The comparative proteomics of ubiquitination in mouse. Genome Res. *6B,* 1389-1394.

Shen, G., Adam, Z., and Zhang, H. (2007a). The E3 ligase AtCHIP ubiquitylates FtsH1, a component of the chloroplast FtsH protease, and affects protein degradation in chloroplasts. Plant J. *52,* 309-321.

Shen, G., Yan, J., Pasapula, V., Luo, J., He, C., Clarke, A.K., and Zhang, H. (2007b). The chloroplast protease subunit ClpP4 is a substrate of the E3 ligase AtCHIP and plays an important role in chloroplast function. Plant J. *49,* 228-237.

Sigismund, S., Woelk, T., Puri, C., Maspero, E., Tacchetti, C., Transidico, P., Di Fiore, P.P., and Polo, S. (2005). Clathrin-independent endocytosis of ubiquitinated cargos. Proc. Natl. Acad. Sci. USA *102,* 2760-2765.

Skaar, J.R., and Pagano, M. (2009). Control of cell growth by the SCF and APC/C ubiquitin ligases. Curr. Opin. Cell Biol. *21,* 816-824.

Smalle, J., and Vierstra, R.D. (2004). The ubiquitin 26S proteasome proteolytic pathway. Annual Review of Plant Biology *55,* 555-590.

Sondheim, E., Tzou, D.S., and Galson, E.C. (1968). Abscisic acid levels and seed dormancy. Plant Physiol. *43,* 1443-&.

Springael, J.Y., Galan, J.M., Haguenauer-Tsapis, R., and Andre, B. (1999). $NH4^{+}$-induced down-regulation of the *Saccharomyces cerevisiae* Gap1p permease involves its ubiquitination with lysine-63-linked chains. J. Cell. Sci. *112,* 1375-1383.

Stelter, P., and Ulrich, H.D. (2003). Control of spontaneous and damage-induced mutagenesis by SUMO and ubiquitin conjugation. Nature *425,* 188-191.

Stone, S.L., Hauksdottir, H., Troy, A., Herschleb, J., Kraft, E., and Callis, J. (2005). Functional analysis of the RING-type ubiquitin ligase family of Arabidopsis. Plant Physiol. *137,* 13-30.

Sugliani, M., Rajjou, L., Clerkx, E.J.M., Koornneef, M., and Soppe, W.J.J. (2009). Natural modifiers of seed longevity in the Arabidopsis mutants *abscisic acid insensitive3-5* (*abi3-5*) and *leafy cotyledon1-3* (*lec1-3*). New Phytol. *184,* 898-908.

Sun, L.J., and Chen, Z.J.J. (2004). The novel functions of ubiquitination in signaling. Curr. Opin. Cell Biol. *16,* 339-340.

Sun, T., Guo, J., Shallow, H., Yang, T., Xu, J., Li, W., Hanson, C., Wu, J.G., Li, X., Massaeli, H., and Zhang, S. (2011). The role of monoubiquitination in endocytic degradation of Human

Ether-a-go-go-Related Gene (hERG) channels under low $K^+$ conditions. J. Biol. Chem. *286*, 6751-6759.

Sy, S.M.H., Huen, M.S.Y., and Chen, J. (2009). PALB2 is an integral component of the BRCA complex required for homologous recombination repair. Proc. Natl. Acad. Sci. USA *106*, 7155-7160.

Tan, X., Calderon-Villalobos, L.I.A., Sharon, M., Zheng, C., Robinson, C.V., Estelle, M., and Zheng, N. (2007). Mechanism of auxin perception by the TIR1 ubiquitin ligase. Nature *446*, 640-645.

Tenno, T., Fujiwara, K., Tochio, H., Iwai, K., Morita, E.H., Hayashi, H., Murata, S., Hiroaki, H., Sato, M., Tanaka, K., and Shirakawa, M. (2004). Structural basis for distinct roles of Lys63- and Lys48-linked polyubiquitin chains. Genes Cells *9*, 865-875.

Terrell, J., Shih, S., Dunn, R., and Hicke, L. (1998). A function for monoubiquitination in the internalization of a G protein-coupled receptor. Mol. Cell *1*, 193-202.

The Arabidopsis Genome Initiative. (2000). Analysis of the genome sequence of the flowering plant *Arabidopsis thaliana*. Nature *408*, 796-815.

Thornton, B.R., and Toczyski, D.P. (2006). Precise destruction: an emerging picture of the APC. Genes Dev. *20*, 3069-3078.

Tsai, Y.C., Fishman, P.S., Thakor, N.V., and Oyler, G.A. (2003). Parkin facilitates the elimination of expanded polyglutamine proteins and leads to preservation of proteasome function. J. Biol. Chem. *278*, 22044-22055.

Ulrich, H.D. (2005). The RAD6 pathway: control of DNA damage bypass and mutagenesis by ubiquitin and SUMO. Chembiochem *6*, 1735-1743.

Ulrich, H.D., and Walden, H. (2010). Ubiquitin signalling in DNA replication and repair. Nat. Rev. Mol. Cell Biol. *11*, 479-489.

Unno, M., Mizushima, T., Morimoto, Y., Tomisugi, Y., Tanaka, K., Yasuoka, N., and Tsukihara, T. (2002). The structure of the mammalian 20S proteasome at 2.75 angstrom resolution. Structure *10*, 609-618.

VanDemark, A.P., Hofmann, R.M., Tsui, C., Pickart, C.M., and Wolberger, C. (2001). Molecular insights into polyubiquitin chain assembly: crystal structure of the Mms2/Ubc13 heterodimer. Cell *105*, 711-720.

Vanlareb, N., Engler, G., Holsters, M., Vandenel, S., Zaenen, I., Schilper, R., and Schell, J. (1974). Large plasmid in *Agrobacterium tumefaciens* essential for crown gall-inducing ability. Nature *252,* 169-170.

Varadan, R., Walker, O., Pickart, C., and Fushman, D. (2002). Structural properties of polyubiquitin chains in solution. J. Mol. Biol. *324,* 637-647.

Verma, R., Aravind, L., Oania, R., McDonald, W.H., Yates, J.R., Koonin, E.V., and Deshaies, R.J. (2002). Role of Rpn11 metalloprotease in deubiquitination and degradation by the 26S proteasome. Science *298,* 611-615.

Vierstra, R.D. (2003). The ubiquitin/26S proteasome pathway, the complex last chapter in the life of many plant proteins. Trends Plant Sci. *8,* 135-142.

Voges, D., Zwickl, P., and Baumeister, W. (1999). The 26S proteasome: a molecular machine designed for controlled proteolysis. Annu. Rev. Biochem. *68,* 1015-1068.

Wang, B., and Elledge, S.J. (2007). Ubc13/Rnf8 ubiquitin ligases control foci formation of the Rap80/Abraxas/Brca1/Brcc36 complex in response to DNA damage. Proc. Natl. Acad. Sci. USA *104,* 20759-20763.

Wang, C., Deng, L., Hong, M., Akkaraju, G.R., Inoue, J., and Chen, Z.J.J. (2001). TAK1 is a ubiquitin-dependent kinase of MKK and IKK. Nature *412,* 346-351.

Wang, H., Zhou, Y., Gilmer, S., Whitwill, S., and Fowke, L.C. (2000). Expression of the plant cyclin-dependent kinase inhibitor ICK1 affects cell division, plant growth and morphology. Plant J. *24,* 613-623.

Wang, W.X., Vinocur, B., Shoseyov, O., and Altman, A. (2004). Role of plant heat-shock proteins and molecular chaperones in the abiotic stress response. Trends Plant Sci. *9,* 244-252.

Weake, V.M., and Workman, J.L. (2008). Histone ubiquitination: triggering gene activity. Mol. Cell *29,* 653-663.

Wen, R., Newton, L., Li, G.Y., Wang, H., and Xiao, W. (2006). Arabidopsis thaliana UBC13: implication of error-free DNA damage tolerance and Lys63-linked polyubiquitylation in plants. Plant Mol. Biol. *61,* 241-253.

Wen, R., Torres-Acosta, J.A., Pastushok, L., Lai, X., Pelzer, L., Wang, H., and Xiao, W. (2008). Arabidopsis UEV1D promotes lysine-63-linked polyubiquitination and is involved in DNA damage response. Plant Cell *20,* 213-227.

Wertz, I.E., O'Rourke, K.M., Zhou, H.L., Eby, M., Aravind, L., Seshagiri, S., Wu, P., Wiesmann, C., Baker, R., Boone, D.L., *et al.* (2004). De-ubiquitination and ubiquitin ligase domains of A20 downregulate NF-kappa B signalling. Nature *430,* 694-699.

Wiborg, J., O'Shea, C., and Skriver, K. (2008). Biochemical function of typical and variant Arabidapsis thaliana U-box E3 ubiquitin-protein ligases. Biochem. J. *413,* 447-457.

Wing, S.S. (2003). Deubiquitinating enzymes - the importance of driving in reverse along the ubiquitin-proteasome pathway. Int. J. Biochem. Cell Biol. *35,* 590-605.

Wobus, U., and Weber, H. (1999). Seed maturation: genetic programmes and control signals. Curr. Opin. Plant Biol. *2,* 33-38.

Wu, L.J.C., Wang, Z.W., Tsan, J.T., Spillman, M.A., Phung, A., Xu, X.L., Yang, M.C.W., Hwang, L.Y., Bowcock, A.M., and Baer, R. (1996). Identification of a RING protein that can interact *in vivo* with the *BRCA1* gene product. Nat. Genet. *14,* 430-440.

Wu, P.Y., Hanlon, M., Eddins, M., Tsui, C., Rogers, R.S., Jensen, J.P., Matunis, M.J., Weissman, A.M., Wolberger, C.P., and Pickart, C.M. (2003). A conserved catalytic residue in the ubiquitin-conjugating enzyme family. EMBO J. *22,* 5241-5250.

Xu, P., Duong, D.M., Seyfried, N.T., Cheng, D., Xie, Y., Robert, J., Rush, J., Hochstrasser, M., Finley, D., and Peng, J. (2009). Quantitative proteomics reveals the function of unconventional ubiquitin chains in proteasomal degradation. Cell *137,* 133-145.

Xu, Z., Kohli, E., Devlin, K.I., Bold, M., Nix, J.C., and Misra, S. (2008). Interactions between the quality control ubiquitin ligase CHIP and ubiquitin conjugating enzymes. BMC Struct. Biol. *8,* 26.

Yan, J.Q., Wang, J., Li, Q.T., Hwang, J.R., Patterson, C., and Zhang, H. (2003). AtCHIP, a U-box-containing E3 ubiquitin ligase, plays a critical role in temperature stress tolerance in Arabidopsis. Plant Physiol. *132,* 861-869.

Yao, T.T., and Cohen, R.E. (2002). A cryptic protease couples deubiquitination and degradation by the proteasome. Nature *419,* 403-407.

Yee, D., and Goring, D.R. (2009). The diversity of plant U-box E3 ubiquitin ligases: from upstream activators to downstream target substrates. J. Exp. Bot. *60,* 1109-1121.

Yin, X., Volk, S., Ljung, K., Mehlmer, N., Dolezal, K., Ditengou, F., Hanano, S., Davis, S.J., Schmelzer, E., Sandberg, G., *et al.* (2007). Ubiquitin lysine 63 chain-forming ligases regulate apical dominance in Arabidopsis. Plant Cell *19,* 1898-1911.

Zeng, L., Park, C.H., Venu, R.C., Gough, J., and Wang, G. (2008). Classification, expression pattern, and E3 ligase activity assay of rice U-box-containing proteins. Mol. Plant *1,* 800-815.

Zhang, M.H., Windheim, M., Roe, S.M., Peggie, M., Cohen, P., Prodromou, C., and Pearl, L.H. (2005). Chaperoned ubiquitylation--crystal structures of the CHIP U box E3 ubiquitin ligase and a CHIP-Ubc13-Uev1a complex. Mol. Cell *20,* 525-538.

Zhang, Y., Gao, J., Chung, K.K.K., Huang, H., Dawson, V.L., and Dawson, T.M. (2000). Parkin functions as an E2-dependent ubiquitin-protein ligase and promotes the degradation of the synaptic vesicle-associated protein, CDCrel-1. Proc. Natl. Acad. Sci. USA *97,* 13354-13359.

Zheng, N., Wang, P., Jeffrey, P.D., and Pavletich, N.P. (2000). Structure of a c-Cbl-UbcH7 complex: RING domain function in ubiquitin-protein ligases. Cell *102,* 533-539.

Zhou, H.L., Wertz, I., O'Rourke, K., Ultsch, M., Seshagiri, S., Eby, M., Xiao, W., and Dixit, V.M. (2004). Bcl10 activates the NF-kappa B pathway through ubiquitination of NEMO. Nature *427,* 167-171.